# AMBIENT AND FORCED VIBRATION TESTING OF A REINFORCED CONCRETE BUILDING

by

Fadıl Fatih Kavarnalı

B.S., Civil Engineering, Trakya University, 2007

Submitted to the Institute for Graduate Studies in
Science and Engineering in partial fulfillment of
the requirements for the degree of
Master of Science

Graduate Program in Civil Engineering

Boğaziçi University

2012

# ACKNOWLEDGEMENTS

I would like to express my sincere thanks to my thesis supervisor, Assist. Prof. Kutay Orakçal for his invaluable guidance, continuous support, and useful suggestions. He has always been very helpful in the preparation of this thesis.

I would like to express my special thanks to my thesis co-supervisor, Assist. Prof. Serdar Soyöz for his guiding suggestions and advice during this study.

I would also like to thank Assoc. Prof. Hilmi Luş, Prof. Uğur Ersoy and Assist. Prof. Çetin Yılmaz for their kind and supportive attitude towards me, and for their valuable recommendations.

I would also like to thank Assoc. Prof. Ertuğrul Taciroğlu and Research Engineer Robert L. Nigbor for their sharing the experimental data obtained during the tests.

I am also grateful to my friend, Research Asistant Ekin Özer for his help in the experimental and theoretical phases of this research.

I am grateful to my parents for the invaluable moral support, advice, and their love, all of which helped prepare my thesis more efficiently.

*To my lovely family…*

# ABSTRACT

## AMBIENT AND FORCED VIBRATION TESTING OF A REINFORCED CONCRETE BUILDING

The seismic performance of reinforced concrete buildings depends on their lateral stiffness and mass distribution, as well as their lateral load capacity and ductility characteristics. In recent decades, seismic strengthening of existing buildings has been commonly employed, for improving their performance under severe earthquake excitation. The results obtained from vibration tests and system identification methods specifically provide valuable information on the influence of seismic strengthening on the lateral stiffness attributes of the building, and help evaluate the effectiveness of the strengthing technique applied, in terms of improving the building's vibration characteristics and seismic performance. In this study, ambient and forced vibration tests were conducted to evaluate the influence of the seismic strengthening on the vibration characteristics of the six-story reinforced concrete ET-B building, located on the Boğaziçi University Campus in Istanbul, Turkey. Modal vibration characteristics of the building were identified at various stages of strengthening. Ambient vibration tests were conducted on the building before and after its seismic strengthening. Forced vibration tests were conducted after seismic retrofit. Results of these tests enabled quantifing the changes, due to strengthening, in the modal characteristics (modal frequencies and mode shapes) of the building, and variation in the modal characteristics of the strenghened building with the intensity of shaking. In addition, simple finite element models of the building were generated, representing its structural configuration before and after seismic strengthening, also considering the impact of the brick-infill partition walls on its stiffness characteristics. The experimentally-identified modal vibration parameters of the building were compared with the results of the finite element model. The experimental and analytical results were found to be consistent in representing the pronounced influence of the structural walls on the lateral stiffness and thus the vibration characteristics of the building, as well as the relatively minor, yet noticeable influence of the brick-infill partition walls on its vibration characteristics.

# ÖZET

## BETONARME BİR BİNANIN ORTAMSAL VE ZORLANMIŞ TİTREŞİM DENEYLERİ

Betonarme bir binanın deprem performansı, binanın yatay yük kapasitesi ve süneklik özelliklerinin yanı sıra, yanal rijitliğine ve kütle dağılımına bağlıdır. Son yıllarda, mevcut binaların şiddetli deprem etkileri altındaki performanslarını iyileştirmek için sismik güçlendirilme yöntemlerine yaygın olarak başvurulmaktadır. Titreşim deneyleri ve sistem tanılama yöntemlerinden elde edilen sonuçlar, uygulanan güçlendirme yönteminin binanın özellikle yanal rijitlik nitelikleri üzerindeki etkisini deneysel olarak gözlemlenebilmesine ve güçlendirilen binanın titreşim özellikleri ve deprem performansındaki iyileşmenin daha gerçekçi bir şekilde değerlendirilmesine olanak sağlar. Bu çalışmada, İstanbul Boğaziçi Üniversitesi Kampüsü içinde yer alan altı katlı betonarme ET-B binası üzerinde uygulanan güçlendirme yönteminin, binanın titreşim özellikleri üzerindeki etkisinin değerlendirilmesi amacıyla, ortamsal ve zorlanmış deneyleri gerçekleştirilmiştir. Binanın modal titreşim özellikleri, güçlendirmenin çeşitli aşamalarında, deneysel olarak tespit edilmiştir. Ortamsal titreşim deneyleri binanın güçlendirilmesi öncesi ve sonrasında yapılmıştır. Zorlanmış titreşim testleri ise güçlendirme sonrasında gerçekleştirilmiştir. Deney sonuçları, binanın modal titreşim özelliklerinin (modal frekanslar ve mod şekilleri) güçlendirme öncesi ve sonrasında ne kadar değişiklik gösterdiğini ve güçlendirilmiş binanın modal titreşim özelliklerinin titreşim etkisinin büyüklüğü ile nasıl değiştiğini gözlemlemeye olanak sağlamıştır. Bu çalışmalara ek olarak, binanın güçlendirme öncesi ve sonrasındaki durumunu temsil eden basit sonlu eleman modelleri oluşturulmuş, modellerde tuğla bölme duvarın binanın yanal rijitlik özelliklerine etkisi dikkate alınmıştır. Binanın titreşim deneylerinden elde edilen modal titreşim özellikleri, sonlu eleman modellerinden elde edilen sonuçlar ile karşılaştırılmıştır. Deneysel ölçümlerin ve analitik model sonuçlarının, hem betonarme perde duvarların binanın yanal rijitlik (dolayısıyla titreşim) özellikleri üzerindeki belirgin etkisinin, hem de tuğla duvarların titreşim özellikleri üzerindeki görece küçük etkisinin yansıtılması açısından tutarlı olduğu gözlemlenmiştir.

# TABLE OF CONTENTS

# LIST OF FIGURES

# LIST OF TABLES

# LIST OF SYMBOLS

| | |
|---|---|
| *Acc* | Acceleration |
| $E_{fe}$ | The Elasticity Modulus of the Concrete in a Frame |
| $E_{me}$ | The Elasticity Modulus of Infill Walls |
| *Freq* | Frequency |
| *g* | Gravitational Acceleration |
| H, $H_{ik}$ | The Frequency Response Function between the Response in a Point 'i' and the Forcing Function Time Signal in a Point 'k' |
| HP | Horse Power |
| Hz | Hertz |
| $h_{col}$ | The Height of the Columns between the Centerlines of Beams |
| $h_{inf}$ | The Clear Height of the Infill Wall |
| *I* | Moment of Inertia |
| $I_{col}$ | The Moment Inertia of Columns |
| *l* | The Length of Beam between Centerlines of Columns |
| $L_{inf}$ | The Clear Length of the Infill Wall |
| min | Minute(s) |
| $M_s$, *Mw* | The Magnitude of Earthquake |
| N | Newton |
| $r_{inf}$ | The Length of a Strut |
| $R_{xf}$ | The Cross-Correlation Function for the Two Signals x(t) and f(t) |
| $R_{xx}$ | The Autocorrelation Function of a Random Signal x(t) |
| $S_{xx}$ | The Power Spectral Density (PSD) of Response |
| $S_{xf}$ | The Cross Spectral Density Defined as the Fourier Transform of $R_{xf}$ |
| $S_{ff}$ | The Power Spectral Density of Input or Driving Force |
| *T* | Period |
| *t* | Time |
| $t_{inf}$ | The Thickness of Infill Walls |
| *w* | The Effective Width of the Infill Wall |

| | |
|---|---|
| $X$ | The Fourier Transform of a Function x |
| $x$ | Signal Function in Time Domain |
| $x_i$ | The Forcing Signal in a Point ‘i’ |
| $y_k$ | The Response in the Point ‘k’ |
| | |
| $\Delta t$ | Time Interval |
| $\theta$ | The Slope of the Infill Diagonal to the Horizontal |
| $\Sigma x$ | The Total Rigidity of Any Floor in the Y Direction |
| $\Sigma y$ | The Total Rigidity of Any Floor in the X Direction |
| $\omega$ | The Radial Frequency |
| Ø | The Diameter of Circular Columns |

# LIST OF ACRONYMS / ABBREVIATIONS

| | |
|---|---|
| 3D | Three Dimensional |
| A/D | Analog-to-Digital |
| ABWR | Advanced Boiling-Water Reactor |
| AVT | The Ambient Vibration Test |
| DFT | Digital Fourier Transform |
| E | The Young's Modulus of Elasticity |
| ET-B | The B Block of the Building of Educational Technologies |
| E-W | East-West |
| FE | Finite Element |
| FEM | Finite Element Model |
| FRF | The Frequency Response Function |
| FVT | Forced Vibration Test |
| GPS | The Global Positioning System |
| N-S | North-South |
| PEER | Pacific Earthquake Engineering Research Center |
| PSD | Power Spectral Density |
| RC | Reinforced Concrete |
| SHM | Structural Health Monitoring |
| SISO | Single-Input, Single Output |
| SSI | Soil Structure Interaction |
| UCLA | University of California, Los Angeles |

# 1. INTRODUCTION

## 1.1. General

Turkey is located in one of the most seismically-active regions of the world. Many reinforced concrete buildings in Turkey have either collapsed or sustained severe damage during past earthquakes; due to the low quality of construction, failure to comply with design code requirements, and lack of inspection during design and construction. Considering the vast vulnerable building stock in Turkey, it becomes very important for residents, property owners, or authorities to assess whether each reinforced concrete building needs to be strengthened or re-constructed, for the purpose of avoiding casualties, injuries, and loss of investment value after a severe earthquake. As part of the process of evaluating the expected structural performance of buildings in their existing configuration, and for making decisions on the necessity of seismic rehabilitation or replacement, experimental vibration tests and system identification techniques have recieved increased attention among civil engineering researchers, as potential performance-assessment tools. Experimental modal analysis and system identification methods have been explored as a recent technology, for identifying vibration characteristics of an existing building, for evaluating its seismic performance (in particular the seismic deformation demand on the building) under expected earthquake excitations.

The natural frequencies and mode shapes are important modal characteristics that influence the dynamic behaviour of a structure under strong ground motion effects, and may have a pronounced impact on the level of the damage experienced by the structure under a severe earthquake. Apart from characteristics of the ground motion, the seismic response of a building within the linear elastic response range (undamaged state) is dominated its natural frequencies and mode shapes of vibration, in addition to its damping characteristics. System identification is a powerful technique to obtain the modal characteristics of a structure. In general, it consists of three basic steps, which are interrelated: (i) the design of an experiment, (ii) the construction of a model, and (iii) the estimation of the modal parameters from the measurements. Proper application of the technique depends on specialized knowledge in the field of study, in terms of deciding on

the approximations and simplifications used in the model, suggesting how to manipulate the system, and revealing the important aspects related to vibration characteristics of a structure [1].

There are mainly two vibration testing methods available for identifing the free vibration (modal) characteristics of a structure; namely Forced Vibration Testing and Ambient Vibration Testing. During Forced Vibration Testing, the structure is excited with a linear or an eccentric mass shaker, creating a time-dependent or harmonic forcing function of single-input type. The vibration (typically acceleration) measurements obtained during the excitation can be directly used to identify the modal parameters of the structure. For relatively small buildings, for which the dynamic response is controlled by only a few modes of vibration, such a single-input type excitation becomes sufficient to identify the governing modal characteristics of the structural system, with relative ease. On the other hand, Ambient Vibration Testing does not require any artifical excitation for identifing the modal characteristics of the structure. Vibrations in the structure as a result of regular use by occupants or excitations created by urban or environmental effects (e.g., vibrations due to wind and nearby traffic) are measured and processed to identify the modal characteristics. This allows the Ambient Vibration Test to be performed without the necessity of presence of testing personnel, and long-term measurement records can be obtained. In this study for example, part of the ambient vibration data was recorded overnight, in the absence of test personnel; and ambient excitations included ongoing construction work on the building, including concrete drilling work and hammering down of the brick infill walls, in addition to wind, traffic, and occupant-induced effects. As such, ambient excitation is multiple-input type, where the structure is excited at various locations simultaneously, under various types of excitation. Ambient Vibration Tests become more feasible for large-scale and relatively sophisticated structural systems, the dynamic responses of which are governed by numerous modes of vibration. Both forced and ambient vibration tests can provide the necessary vibration response data, at different locations of the structure, for identification of the modal parameters.

As mentioned previously, performance evaluation and strengthening of the existing seismically-vulnerable building stock is an important problem for earthquake regions. To date, various strengthening techniques have been applied on existing reinforced concrete

buildings both in Turkey and worldwide, for improving their seismic performance and reducing the expected level of damage under a severe earthquake. Addition of reinforced concrete structural walls is the most commonly-employed strengthening method for improving the lateral stiffness, lateral load capacity, as well as the ductility characteristics of an existing building. In Turkey, this method has been widely used for seismic strengthening of numerous reinforced concrete buildings, especially state-owned public buildings such as schools and hospitals. The alternative to seismic strenghthening of an existing vulnerable building is demolishing and re-construction of the building to comply with design code specifications. Many authorities and property-owners find it difficult to make decisions on whether each particular building needs to be strengthened or replaced, and selection of a suitable and economical strengthening methodology. Considering that the vibration characteristics of a building can be essential in estimating the seismic demand in both linear and nonlinear response ranges, vibration testing methods and system identification techniques for quantifying the modal characteristics of an existing building, before and after its strengthening, can contribute significantly to selection of an appropriate strengthening method, as well as evaluation of the effectiveness of the strengthening method applied.

As well, many reinforced concrete buildings in Turkey include brick-infill non-structural walls, used for architectural partitioning purposes. These infill walls increase the weight of the building, but also contribute to lateral stiffness and strength of the structural system, under earthquake excitation. The impact of the infill walls on the structural response is generally neglected in design calculations; therefore, their influence on the lateral stiffness and modal parameters (natural frequencies, damping ratios and mode shapes) may result in deviation from the expected earthquake response of a multi-storey building. In order to characterize the effects of infill walls analytically, an equivalent diagonal strut method was originally addressed by Polyakov [2], and Mainstone and Weeks [3] proposed empirical relationships to define the properties of the equivalent diagonal strut elements representing the infill walls. Using such analytical modeling approaches allow consideration of the effects of the infill walls on the stiffness and modal characteristics of the building, and also assist in the design process of selecting appropriate locations of the infill walls, so that they do not impose significant irregularities (e.g.,

torsional irregularities and soft story conditions) on the earthquake response of the building.

Recently, Finite Element Model Updating methods have also been widely used for the comparison of the results obtained from the analytical model for the structure, with the instrumentally-measured dynamic response characteristics of the actual constructed structure. Such model updating methods become useful for updating the parameters of the anaytical model (e.g., material modulus of elasticity, cracked section modulus, unit weight, mass distribution, soil stiffness, etc.), for ultimately obtaining better-calibrated modeling parameters and identifying changes in the parameters, which also helps quantify the level of damage on the structure after an earthquake, as part of the structural health monitoring process. As well, commercial structural analysis programs used by design engineers do not always accurately reflect the dynamic characteristics of the modeled structure, due to neglected behavioral characteristics (e.g., cracking of reinforced concrete members, influence of infill walls), as well as possible errors in selection of the model parameters (e.g., elastic modulus, unit weight). The model updating methodology becomes an important tool for verifying the parameters of the structural model, and possible correction of the model parameters for either verifying or identify weaknesses in the design of the structure.

With the research motivations outlined above, in this study, ambient and forced vibration tests were conducted on a six-story reinforced concrete building, before and after the building underwent seismic strengthening, for the purpose of identifying the influence of strengthening on the dynamic characteristics of the building. In addition, finite element structural models of the building were generated, in both original and strengthened configurations, and analytically-obtained dynamic characteristics of the building were compared with the experimentally-measured ones, as an illustration of the finite element model updating process.

## 1.2. Background and Literature Review

### 1.2.1. Overview

Many Structural Health Monitoring studies conducted on bridges and building structures are available on the literature, some of which were conducted during earthquake excitations. Such studies have been conducted for various purposes; including detection of the damage level on the structure after an earthquake, evaluating whether the structure needs to be strengthened or demolished, and assessment of the contribution of the applied strengthening method on the dynamic characteristics of the structure. Through these studies, it was also shown that the interaction between the ground and superstructure reduces the excitation component of an earthquake, possible variation on the building dynamic behaviour is linked to damage spread detected during the seismic excitation. In this context, Structural Health Monitoring is a useful tool which helps in the processes of damage detection, verification of structural performance, and decision making for strengthening applications. System Identification studies have also been conducted under ground acceleration response records obtained during earthquakes, and some system identification procedures have been shown to provide essential estimates of seismic demands on buildings, in both linear and nonlinear response ranges.

Ambient Vibration Tests were typically conducted on historic masonary structures and tall buildings for identification of dynamic structural resonse paremeters as well as damage detection and structural performance assesment. The primary motivation of such tests are to provide some preliminary information about the dynamic behaviour of a structure, as well as the site conditions. Ambient Vibration Tests helped researchers to identify the fundamental modes, as well as and several other vibration modes for structures; the measurement of structural response to ambient levels of vibration has proved to be an effective means for the identification of the dynamic properties of a structure.

Forced Vibration Tests have also been conducted on some reinforced concrete structures and nuclear reactor buildings, for the purpose of investigating their dynamic response characteristics before, after, and during the time they underwent structural

damage, and to identify potential research areas which require further attention. In some of these studies, it was shown that most of the structural displacement of reactor-type buildings corresponding to the first (predominant) mode of vibration, was due to rigid-body motion caused by the soil structure interaction (SSI) effect. In order to achieve a better estimation of the stiffness characteristics of the structural components, the information gathered from Forced Vibration testing were used to calibrate and update the finite element model of such structures.

Model Updating studies were also carried out to identify the damage on laboratory-scale structural systems, and to demonstrate how Output-Only Modal Identification techniques can be effectively used with Model Updating tools to develop reliable finite element models of large-scale civil engineering structures. The results showed that the finite element model updating method can be used to identify damage on a structure, and it is possible to accomplish an effective model updating of a large civil engineering structure using the results from an Output-Only Modal Identification analysis.

Studies on investigating amplitude-dependent frequency change are also available in the literature. Such studies were conducted to evaluate the damage of the a structure through identification of its dynamic characteristics before strenghtening, and to confirm the influence of strengthening on the dynamic characteristics. Results of such studies showed that in a structure with few secondary members, the natural period and the damping ratio became larger, as the amplitude of acceleration increases, and a significant amplitude dependence can be identified.

As well, there are studies presented in the literature on the influence of brick infill partition walls on the dynamic characteristics and seismic performance of multi-story reinforced concrete frame buildings. In some ambient vibration studies, which focused on identifying the fundamental period of vibration for existing reinforced concrete buildings with brick infill walls, it was shown that the presence of infill walls decreases the fundamental period of vibration for the building, and the presence of plaster on the walls influences wall stiffness significantly.

Relevant background information and examples of such studies available in the literature are outlined in the following sub-sections.

### 1.2.2. Structural Health Monitoring

The process of implementing a damage identification strategy of aerospace, civil and mechanical engineering infrastructure is referred to as Structural Health Monitoring (SHM) [4]. This process involves the observation of a structure or mechanical system over time using periodically spaced measurements, the extraction of damage-sensitive features from these measurements and the statistical analysis of these features to determine the current state of system health. The SHM problem can be addressed in the context of a statistical pattern recognition procedure. This procedure can be broken down into four parts: (i) operational evaluation, (ii) data acquisition, normalization and cleansing, (iii) feature selection and information condensation, and (iv) statistical model development for feature discrimination. When one attempts to apply this paradigm to data from real world structures, it quickly becomes apparent that the ability to cleanse, compress, normalize and fuse data to account for operational and enviromental variability is a key implementation issue when addressing parts 2-4 of this paradigm. These processes can be implemented through hardware or software and, in general, some combination of these two approaches need to be used.

Nishimura [5] conducted tests on the application of structural health monitoring for improving the performance of building structures. The initial test structure was a newly constructed building on the campus of Tokyo City University. The structure was a complex building consisting of a newly constructed building and an existing faculty office building. The main purpose of the structural health monitoring in this study was to check the performance of the damping devices installed between the newly constructed structure and the existing faculty office building. This observation showed that the interaction between the ground and the superstructure might reduce the excitation component of the earthquakes. Two application projects showed the information available from the structural monitoring technology. The expansion of low cost data acquision would enhance the common recognition among the engineers and scientists about the intensity and behaviour of earthquakes that will happen in the future.

Picozzi *et al.* [6] conducted a study on structural health monitoring of a damaged reinforced concrete building after the 2009 *Mw* 6.3 Central Italy Earthquake, which caused death of approximately 300 people. In this study, possible variation of the building dynamic behaviour during the seismic sequence linked to damage evolution was detected, and the velocity fluctuations were interpreted as evidence of recoverable nonlinear behaviour related to the opening of existing cracks in concrete during the occurance of shaking.

As well, organized Structural Health Monitoring (SHM) applications on bridges in Sweden have commenced in recent years [7], together with construction of innovative bridge systems with complicated designs. Several old or deteriorated bridges subject to classification and strengthening benefited from these SHM applications.

### 1.2.3. Field Testing

1.2.3.1. Ambient Vibration Testing (AVT). In the dynamic analysis of structures, idealizations are used to model the real structure in order to represent its response to various dynamic loads for strong earthquake, strong winds, explosions, etc. Identification of these structural parameters can best be represented by a particular structure subjected to an earthquake, and being able to record strong motions of the input shaking and structural response, through instrumentation.

There are experimental procedures available to excite the structure artificially, and thereby measure the input shaking. These methods vary depending on the type of input forces used, whether they be drop weights or a vibration generator (shaker). The concept is to apply sufficient magnitude of force to the structure in order to produce useful response amplitudes and lead to more prominent excitation of the modes of vibration. However, large engineering structures are not easily excited. In applying identification experiments to large, heavy and actual structures, some problems typically occur because of the complexity and extent of the system (as in the case of tall buildings, towers, bridges etc.), difficulties may arise in exciting large scale structures in a controlled manner. The difficult task of measuring the load acting on a structure or in exciting the structure artificially can be avoided by using methods that identify the structure exclusively on the basis of

measurements of the output caused by ambient vibration. This kind of experiment is referred to as ambient vibration testing.

Large civil engineering structures are often loaded by natural (ambient) loads that cannot easily be controlled as, for instance, wave loads (for offshore structures), wind loads (for buildings) or traffic loads (for bridges). Every building therefore is in continuous motion and vibrates constantly, at a rate that is seldom perceptible to the human senses because of the small amplitude caused by this ambient vibration. Indeed a building deforms and vibrates because it is not infinitely rigid. The vibration is uniquely defined by the building's stiffness and weight. Again, these vibrations are hardly felt by human senses, since their amplitudes are very small. Ambient vibration testing therefore aims to capture and record these vibrations. Instead of exciting the structure artifically, it offers the advantage to measure the natural (or ambient) vibration response of the structure, and then estimate the modal parameters by performing and output-only modal identification.

Whenever the technique of output-only modal identification is used in civil applications, the basic idea is that instead of loading the strucutre artificially, and dealing with the natural loading as an unwanted noise source, the natural loading is used as the loading source. The main advantages of this kind of testing are that testing is cheap and fast; since equipment for excitation is not needed, less time is spent on testing. As well, testing does not interfere with the operation of the structure, and the measured response is representative of the real operating conditions of the structure. The underlying principle used to evaluate the modal parameters of a building using ambient vibration testing is that the prevailing ground-borne and wind-induced excitations to the building are composed of an almost infinite number of harmonics with different periods of vibration. The harmonic component whose period corresponds to a natural period of the building is amplified in the building response due to resonance [8].

Gentile and Saisi [9] conducted ambient vibration tests on historic masonary towers for structural identification and damage assesment. The dynamic tests were carried out to complement an extensive research program planned to evaluate the structural condition of the tower, characterised by the presence of major cracks, especially on the load-bearing walls. As a result, the measurement of structural response to the ambient levels of vibration

has proved to be an effective means for the identification of the dynamic properties of masonry towers. Due to the good correlation between experimental and theoretical modal behaviour, the updated models were found to be adequate for providing reliable predictions of the structural response under the loading conditions, for assessing the structural safety of the towers.

Brownjohn [10] conducted ambient vibration studies for system identification of tall buildings. In the study, various modal analysis procedures were used to obtain modal parameters. The performance of two 'response only' modal analysis procedures, natural excitation technique, eigensystem realisation algorithm, and frequency domain decomposition were investigated via case studies on two tall office buildings. It was shown that provided all sensors calibrations and locations are known, it is possible to examine how the mode shapes improve as more measurements are made. In paralel, the simpler frequency domain decomposition procedure allows identify a convincing set of lower frequency modes.

Turek et al. [11] conducted a study on ambient vibration testing of three unreinforced brick masonry buildings. A series of ambient vibration tests were carried out on three buildings, as well as two sets of microtremor measurements to characterize the site dynamics. The intention of the tests was to provide some preliminary information about the dynamic behaviour and the dynamic site conditions for three buildings. The ambient vibration tests of the buildings allowed identifying the fundamental modes and several higher modes for each building.

1.2.3.2. Forced Vibration Testing (FVT). With forced vibration testing, the structure to be identified is artificially-excited with a forcing function at a location *i*, and its response $y_k(t)$ to this excitation is measured together with the forcing signal $x_i(t)$ (Figure 1.1). Transformation of these time signals into the frequency domain and calculation of all Frequency Response Functions (FRF's) $H_{ik}$ between the response and the forcing function time signals yields the Frequency Response Matrix, which is also referred to as Transfer Matrix, $H(i\omega)$ (Figure 1.2 and 1.3).

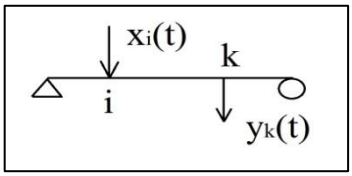


Figure 1.1. Forced Vibration Testing Scheme [12].

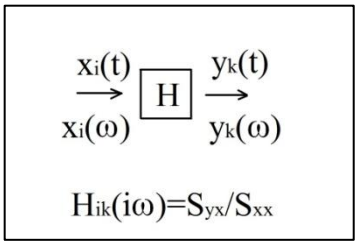


Figure 1.2. Calculation of the Frequency Response Function $H_{ik}$ [12].

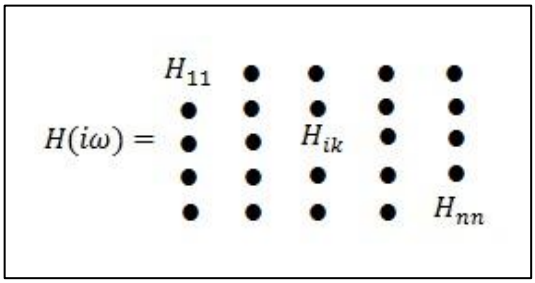


Figure 1.3. The Frequency Response Matrix [12].

For linear systems, the Frequency Response Matrix is diagonal. This means that it sufficies to either determine one row or one column of this matrix (Figure 1.3). The choice is to either keep the excitation point constant and rove the response points over the structure, or vice versa. The Frequency Response Matrix contains all the information necessary to determine the dynamic natural properties of the structure under investigation (natural frequencies and the associated mode shapes and damping coefficients). Generally speaking, the means of excitation has to be chosen such as to excite all natural frequencies of interest, and to be significantly larger in effect than any other unwanted excitation, since the processing procedures are based on the assumption that the measured artificial excitation is the only source of excitation during the test. It can be seen from many experiments that the number of measurement points can be as high as 200 to 300. The number of degrees-of-freedom to be measured is even higher in case where it is necessary to measure in two or three directions per point. As the forcing signal is always measured,

there is no problem for the processing of the information gathered from the different setups [12].

Chen et al. [13] conducted a study on vibration testing of a four-story reinforced concrete building to investigate its dynamic response before, after, and during the time it underwent structural damage. Results of nondestructive and post-destructive tests on this concrete structure indicated that its response at small amplitudes was that of a slightly nonlinear softening system. The response properties of the damaged structure differed from those of the undamaged structure, with a longer period, higher damping, and some mode shape discontinuity. As the input force was further increased, major damage to the structure occured, resulting in a permanent change in its damping and stiffness characteristics.

Onouchi et al. [14] carried out forced vibration testing of a Nuclear Reactor Building. The test was conducted on Hamoaka Unit 5 ABWR-type reactor building during May and June 2003. The investigated building is a reinforced concrete building with steel framing at the roof. As a result, it was shown that most of the displacement of the reactor building at the first mode (predominant peak) was due to rigid-body motion caused by the soil structure interaction (SSI) effects.

Karim et al. [15] conducted a study on the forced vibration response of a small scale unreinforced masonry building. The primary purpose of this research was to investigate the system level response of unreinforced masonary buildings. A 4m by 4m unreinforced masonary house structure consisting of a flexible timber diaphragm was constructed and tested to identify the possible mode shapes. This results indicated that in order to achieve a better estimation of the mechanical properties of the structural elements, the information gathered from the modal testing would be useful to update the finite element model of the building.

### 1.2.4. System Identification

Çelebi and Şafak [16, 17] conducted a study on seismic response of TransAmerica Building. The objective of the study was to present preliminary analyses of a set of

acceleration response records obtained during the 1989 Loma Prieta Earthquake ($M_s$ = 7.1), from the sixty-story vertically tapered, a pyramid shaped building. The results showed that the building's motion was dominated by a coupled mode in the southwest-northeast direction, almost parallel to one of the diagonals in the building's square cross section. The reason for this behaviour is the symmetry of the building's structural characteristics, as well as the strong polarization of the S-waves of the earthquake.

Conte et al. [18] conducted a study on system and damage identification of a seven-story reinforced concrete building structure tested on the UCSD-NEES shake table. The objective of this test program was to verify the seismic performance of a reinforced concrete wall system designed for lateral forces obtained from a displacement-based design methodology, which are significantly smaller than those dictated by current seismic design provisions. As a result, the natural frequencies identified using different methods were reasonably consistent within each damage state, while the identified damping ratios exhibit much larger variability across system identification methods. The first longitudinal modal frequencies identified from white noise base excitation test data were systematically lower than their counterparts identified using ambient vibration data at all damage states considered. This was found to be most likely due to the fact that the test structure is nonlinear with effective modal parameters depending strongly on the amplitude of the excitation.

Liu et al. [19] carried out a study on system identification, modelling and performance prediction of a twenty-story office building. In this study, a three-dimensional Finite Element (FE) model was calibrated in two horizontal directions by matching the natural periods from FE analysis with those from system identification applied to ambient vibration data. The results showed that, the Incremental Dynamic Analysis and Modal Pushover Analysis procedures can both provide essential estimates of seismic demands of the building in both linear and nonlinear ranges.

Şafak [20] conducted a study on the principles of stochastic-adaptive modeling, identification, and control of single-input, single output (SISO) dynamic systems. The contents of this study included discrete-time models for noisy SISO systems, the concept of stochastic approximation, the recursive prediction error method, and stochastic-adaptive

control. The objective was to present a concise review of stochastic filtering, estimation, and control theories. Şafak [21] also carried out a study on a discrete-time method for system identification based on linear filtering theory and least-squares estimation. The objective of this study was to present the method by emphasising the close relationship between the well-known modal-analysis technique in structural engineering and the discrete-time linear systems theory in systems engineering. As a result of the study, the method was found to be valid for linear elastic responses, and recordings with wide-band measurement noise, which is usually the case in real life.

In the study of Ghanem and Shinozuka [22, 23], a number of structural-identification algorithms were reviewed and applied to the identification of structural systems subjected to earthquake excitations. The algorithms were applied to experimental data obtained in controlled laboratory conditions. The aim of this study was a comprehensive treatment of system-identification techniques in structural-engineering applications, with a special focus on civil-engineering structures. As a result of this study, the importance of robustness and simplicity in the identification algorithms were emphasized.

Doebling et al. [24] conducted a study on the global methods that were used to infer damage from changes in vibration characteristics of the structure. The scope was to present the methods that use changes in modal properties to infer changes in mechanical properties, and the application of these methods to engineering problems. In this study, the, researchers focused on the issues that must be addressed by future research to make the identification of damage using vibration measurements a viable, practical, and commonly implemented technology. According to the researchers, sufficient evidence existed to promote the use of measured vibration data for the detection of damage in structures, using both forced-response testing and long-term monitoring of ambient signals and research should be focused more on testing of real structures in their operating environment, rather than laboratory tests of representative structures.

### 1.2.5. Model Updating

Updating by improving the physical meaning of the models always requires the application of considerable physical insight in the choice of parameters to update and the

arrangement of constraints, force inputs and response measurements in the vibration test. Model updating brings together the skills of the numerical analyst and the vibration test engineer, and requires the application of modern estimation techniques to produce the desired improvement [25].

Fang et al. [26] conducted a study on damage identification of a reinforced concrete frame specimen by finite element model updating, using damage parameterization. A sensivity-based finite element model updating method was developed to identify the damage on a laboratory-scale reinforced concrete frame. The updating method in this study aimed to adjust the finite element model of the reinforced concrete frame, as closely as possible to the experimental results, by updating (calibrating) the Young's Modulus for concrete. The results revealed that the finite element model updating method can identify the damage observed on the specimen.

Ventura et al. [27] conducted a study on finite element model updating of a historical court building structure. The aim of this study was to demonstrate how Output-Only Modal Identification techniques can be effectively used with model updating tools to develop reliable finite element models of large-scale civil engineering structures. This case study showed that it is possible to accomplish an effective model updating of a large structures using the results from an Output-Only Modal Identification analysis.

Skolnik et al. [28] carried out a study on identification and model updating of the UCLA Louis Factor Building. The building was instrumented by the U.S. Geological Survey with an embedded 72 channel accelerometer network, after the 1994 Northridge earthquake. At the end of the study, a reliable baseline linear elastic finite element model of the UCLA Louis Factor building was established, which is to be used use in the event of future local strong ground motions.

### 1.2.6. Influence of Brick Infill Walls on the Seismic Behaviour of Reinforced Concrete Frames

The structural response of infilled wall frames depends on the frame and infill wall geometry as well as the constituent materials of infill walls and workmanship quality. The

behaviour of infilled wall frames may generally be categorized in two distinct conditions. In the first, infill walls are highly lightweight and flexible, or fragile enough to crack or crush under weak and medium levels of earthquake excitation. Or, the infill walls may be isolated (separated) from the structural frame system. In such cases, the infill walls do not have significant impact on the structural response, and their design only considers the possible risk of infill wall collapse on the residents and equipment. In the second condition, the infill walls (e.g., brick or masonry infill walls) may contribute to structural response (e.g., stiffness) of the frame, but their behavior is essentially linear elastic prior to failure (e.g., crushing), due to the brittle nature of the infill material. In other cases, the infill walls may influence the structural behavior in the nonlinear response range.

The first and simpliest method of masonry infill wall modelling is the equivalent strut method, addressed and discussed initially by Polyakov [2]. Smith [29] demonstrated that the equivalent diagonal element width depends on the common length between frame and masonry infill wall. Mainstone [30] proposed a method to calculate the equivalent diagonal element specifications. Saneinejad [31] suggested empirical equations for calculation of masonry infill wall strength. Mehrabi [32] and Dawe [33] also suggested new methods for modeling of compound infilled frames using the finite element modeling approach. Stavridis and Shing [34] also developed a complex nonlinear finite elements modeling methodology for RC frames with masonry infills.

Davis et al. [35] conducted a study on effect of infill stiffness on seismic performance of multi-story reinforced concrete infill-framed buildings. The buildings investigated were four and seven stories tall, and were composed of reinforced concrete ordinary moment resisting frames. The results of this study indicated that infilled frames behaved similarly to braced frames, following a truss mechanism formed by the compression strut in the masonry infill walls, together with tension in the columns.

Öztürk [36] prepared a thesis on the effects of brick infill walls on the seismic performance of reinforced concrete buildings. In the study, the contribution of the hollow brick infill walls to the lateral stiffness of reinforced concrete buildings was investigated. For this purpose, two different buildings were chosen as case studies. The three and six story buildings with symmetric plans were modeled as bare and infilled frames, and

subjected to seismic loads acting on each story. The results of this study showed that the differences in the global drift ratios for three different symmetric wall arrangements were within 5%.

Güler et al. [37] carried out a study on the estimation of the fundamental vibration period of existing reinforced concrete buildings in Turkey, utilizing ambient vibration records. The building tested had twelve stories, and the ambient vibration tests were conducted during three different construction stages. As expected, the presence of infill walls had the effect of increasing the mass and lateral stiffness of the system. The former effect caused the fundamental period of the building to increase, whereas the latter effect reduced the fundamental period. The experimental results indicated that the effect of infill walls on the lateral stiffness of the building was much more pronounced than that of the increase in building mass. As well, the presence of plaster on the infill walls influenced the wall stiffness, significantly.

### 1.2.7. Amplitude-Dependent Frequency Change

It is well known today that the damping ratio and natural vibration periods of a building depend on the vibration amplitude. Research studies have been conducted on this amplitude dependency. Most of these studies only compare the damping ratio and fundamental natural period under microtremors, with their respective values of responses during earthquakes or strong winds. There are only a few studies on amplitude dependence, for which the amplitude of vibration is changed gradually. Although some models for the damping have been proposed in the literature, it is difficult to discuss their appropriateness because of the complexities in the building structural system, such as the existance of secondary (e.g., partition) members.

Morita and Kanda [38] conducted a study on the experimental evaluation of amplitude dependent natural period and damping ratio of a multi-story structure. It was demonstrated in this study that in a structure with few secondary members, the natural period and the damping ratio increase, as the amplitude of acceleration increases and a significant amplitude dependence can be identified in the modal vibration characteristics.

Motosaka et al. [39] carried out a study on the amplitude dependent dynamic characteristics of an existing building before and after its seismic retrofit. Different types of observations and vibration tests were performed on an existing nine-story reinforced concrete building, for 35 years since its completion in 1969, up to date. As a result, it was possible to discuss the amplitude dependency of dynamic characteristics and also to evaluate the damage degree before the retrofit work, as well as the effects of the retrofit on the dynamic characteristics. A damage detection technique was also addressed in this study, via comparison of the measured vibration characteristics with those estimated using the structural model of the building.

### 1.3. Objectives and Scope

The primary objective of this study is to investigate the effects of seismic strengthening on the modal characteristics of a six-story reinforced concrete building (the Educational Technologies Building Block B, a.k.a. the ET-B Building) located in Bogazici University North Campus in Istanbul, Turkey. Ambient vibration tests were conducted before, during, and after the strengthening work, between June and December 2010. The building was strenghthened via jacketing of columns, addition of structural walls, and construction of a mat foundation. These ambient vibration test results were complemented with data from forced vibration tests, which were performed using an eccentric mass shaker, after strengthening was completed. During forced vibration testing, it was also found that the modal frequencies slightly decreased with the amplitude of the excitation force. These experimental results enabled quantifying the influence of seismic strengthening on selected modal characteristics (modal frequencies and mode shapes) of the building, and variation in modal frequencies due to intensity of shaking. As well, a linear elastic finite element model of the building was generated, for comparison of the modal parameters obtained from system identification with those predicted by the model. The main objectives of finite element modeling were to verify the basic modeling assumptions, and to illustrate the level of consistency, among the system identification results with the results of a “baseline” model, which may be further improved via model updating. The finite element model results allowed investigating the influence of brick infills on the modal frequencies of the building.

## 1.4. Thesis Outline

The description and results of the ambient and forced vibration tests, as well as the finite element modeling studies conducted on the ET-B building, are presented in this thesis. In the first Chapter, an introduction and a literature review were presented, together with objectives and scope of this study. The system identification methodology used for processing of the vibration test data is presented in Chapter 2. A description of the building investigated, before and after its strengthening, is provided in Chapter 3. Details of the ambient and forced vibration tests conducted on the building are described in Chapter 4, where the processed test results are also presented. The finite element model of the building is presented in Chapter 5, where comparison of the results of the vibration tests and the finite element model is also provided. Conclusions of this study are presented in Chapter 6.

# 2. SYSTEM IDENTIFICATION PROCEDURE FOR THE VIBRATION TESTS

The system identification methodology used for processing the measured acceleration data obtained during the vibration tests conducted on the ET-B Building, is presented in this Chapter. The digital signal processing, random signal analysis, and peak amplitude selection procedures used in this study for modal data extraction are described in the following sections.

## 2.1. Digital Signal Processing

Much of the analysis done in modal testing is performed in the frequency domain. The aim is to convert analog time-domain signals into digital frequency-domain information compatible with digital computing and then to perform the required computations with these signals. The method used to change an analog signal, *x(t)*, into frequency-domain information is the Fourier Transform (defined by Equation 2.1 and 2.2, or a Fourier series as defined by Equation 2.3-6. The Fourier series is used to introduce the Digital Fourier Transform (DFT). The Fourier Transform of a function *x(t)* is denoted by *X(ω)* and is defined by :

$$X(\omega) = \frac{1}{\sqrt{2\pi}} \int_{-\infty}^{\infty} x(t) e^{-j\omega t} dt \tag{2.1}$$

which transforms the variable *x(t)* from a function of time into a function of frequency *ω*. The inversion of this transform is performed by the integral

$$x(t) = \frac{1}{\sqrt{2\pi}} \int_{-\infty}^{\infty} X(\omega) e^{j\omega t} d\omega \tag{2.2}$$

A periodic time signal of period *T* can be represented by a Fourier Series in time of the form given by Equation 2.3 with Fourier coefficients, or spectral coefficients as defined

by Equation 2.3-6. These spectral coefficients represent frequency-domain information about a given time signal. These equations are repeated below :

$$F(t) = \frac{a_0}{2} + \sum_{n=1}^{\infty} (a_n cos(n\omega_T t) + b_n \sin(n\,\omega_T t)) \tag{2.3}$$

where

$$\omega_T = \frac{2\pi}{T}$$

$$a_0 = \frac{2\pi}{T}\int_0^T F(t)dt \tag{2.4}$$

$$a_n = \frac{2}{T}\int_0^T F(t)\cos\,(n\omega_T t)dt \quad n = 1, 2, \ldots \tag{2.5}$$

$$b_n = \frac{2}{T}\int_0^T F(t)\sin\,(n\omega_T t)dt \quad n = 1, 2, \ldots \tag{2.6}$$

The Fourier coefficients $a_n$ and $b_n$ given by Equation 2.3-6 also represent the connection between Fourier analysis and vibration experiments. The analog output signals of force balance accelerometers, represented by $x(t)$, are inputs to the analyzer. The analyzer, in turn, calculates the spectral coefficients of these signals, thus setting the stage for a frequency-domain analysis of the signals. The digital recorders first convert the analog signals into digital records. They sample the signals $x(t)$ at many different equally spaced values and produces a digital record, or version, of the signal in the form of a set of numbers $\{ x(t_k) \}$. Here $k = 1, 2, \ldots, N$, where the digit $N$ denotes the number of samples and $t_k$ indicates a discrete value of the time.

This process is performed by an analog-to-digital (A/D) converter (or recorder) as mentioned above. This conversion from an analog to a digital signal can be thought of in two ways. First, one can imagine a gate that samples the signal every $\Delta t$ seconds and passes through the signal $x(t_k)$. The process of A/D conversion can also be considered as

multiplying the signal *x(t)* by a square-wave-function, which is zero over alternate values of $t_k$ and has the value of 1 at each $t_k$ for a short time.

## 2.2. Random Signal Analysis in Testing

The digital signal recorded to measure the output during a vibration test usually contains noise. Additionally, confidence in a measured quantity is increased by performing a number of identical tests and averaging the results. The stiffness of a single structure is determined by multiple measurements. Thus, it is important to consider the random input vibration response.

The definiton of the autocorrelation function of a signal and the associated power spectral density (PSD) are reviewed by Equation 2.8 and 2.9. The PSD of the input or driving force can be related to the PSD of the response and the frequency response function of the system by

$$S_{xx}(\omega) = |H(\omega)|^2 S_{ff}(\omega) \tag{2.7}$$

The autocorrelation function of the random signal *x(t)* is given by

$$R_{xx}(\tau) = \lim_{T\to\infty} \frac{1}{T} \int_0^T x(t)x(t+\tau)dt \tag{2.8}$$

The power spectral density (PSD) of a signal is the Fourier Transform of the signal's autocorrelation:

$$S_{xx}(\omega) = \frac{1}{2\pi} \int_{-\infty}^{\infty} R_{xx}(\tau)e^{-j\omega\tau}d\tau \tag{2.9}$$

Equation 2.7 relates the dynamics of the test structure contained in H(ω) to measurable quantities (i.e., the PSDs). The common approach to measuring the frequency response function is to average several matched sets of input force time histories and

output response time histories. These averages are used to produce correlation functions that are transformed to yield the corresponding PSDs. Equation 2.7 is then used to calculate the magnitude of the frequency response function $|H(\omega)|$. The experimental vibration data are then picked from the plot of $|H(\omega)|$.

The frequency response function can also be related to the cross-correlation between the two signals *x(t)* and *f(t)*. The cross-correlation function, denoted $R_{xf}(\tau)$, for the two signals *x(t)* and *f(t)*, is defined by:

$$R_{xf}(\tau) = \lim_{T\to\infty} \frac{1}{T} \int_0^T x(t) f(t+\tau) dt \tag{2.10}$$

Here *x(t)* is considered to be the response of the structure to the driving force *f(t)*. Similarly, the cross-spectral density is defined as the Fourier Transform of the cross-correlation:

$$S_{xf}(\omega) = \frac{1}{2\pi} \int_{-\infty}^{\infty} R_{xf}(\tau) e^{-j\omega\tau} d\tau \tag{2.11}$$

These correlation and density functions also allow calculation of the transfer functions of test structures. The frequency response function, $H(j\omega)$, can be shown to be related to the spectral density functions by the two equations

$$S_{fx}(\omega) = H(j\omega) S_{ff}(\omega) \tag{2.12}$$

and

$$S_{xx}(\omega) = H(j\omega) S_{xf}(\omega) \tag{2.13}$$

These hold if the structure is excited by a random input *f(t)* resulting in the response *x(t)*. The cross-correlation functions include information about the phase and magnitude of the structure's transfer function and not just the magnitude, as in the case of the correlation function of equation 2.7, repeated below:

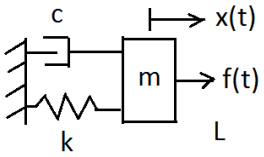


$$transfer\ function: G(s) = \frac{1}{ms^2 + cs + k}$$

$$Frequency\ Response\ Function: G(j\omega) = H(\omega) = \frac{1}{k - m\omega^2 + c\omega j}$$

$$Impulse\ Response\ Function: h(t) = \frac{1}{m\omega_d} e^{-\zeta\omega_n t} sin\omega_d t$$

$$which\ has\ Laplace\ Transform\ \ L[h(t)] = \frac{1}{ms^2 + cs + k} = G(s)$$

and the Fourier Transform of the Impulse Response Function is just the frequency response function *H(ω)*. These quantities relate to the input and response by:

| For deterministic *f*(*t*) | For random *f*(*t*) |
|---|---|
| $X(s) = G(s)F(s)$ | $S_{xx}(\omega) = \lvert H(\omega)\rvert^2 S_{ff}(\omega)$ |
| $x(t) = \int_0^t h(t-\tau)f(\tau)d\tau$ | $E[\hat{x}^2] = \int_{-\infty}^{\infty} \lvert H(\omega)\rvert^2 S_{ff}(\omega)d\omega$ |

In the spectrum analysis, various spectral density functions are calculated (or estimated) from the sensor outputs. Then, using the above Equation 2.12 or 2.13, the frequency response function *H*(*jω*) can be calculated. In ambient vibration tests, the input due to the existance of people and passing-by traffic can be considered as white noise and its PSD wil be a constant value. Therefore, PSD of the output signals will directly represent the frequency response function of the structure.

## 2.3. Peak-Amplitude (Peak-Picking) Method

In this study, the so-called Peak-Picking method was used to obtain the modal parameters from the vibration test data. Once the frequency response of the test structure is calculated from Equation 2.12 or 2.13, the analyzer is used to construct various vibration parameter information from the processed measurements. This is what is referred to as experimental modal analysis. In what follows, it is assumed that the frequency response function $H(j\omega)$ has been measured via Equation 2.12 or 2.13 or their equivalents.

The task of interest in this study is to compute the natural frequencies and mode shapes (modal amplitudes) associated with each resonant peak of the measured Frequency Response Function. There are several ways to examine the measured

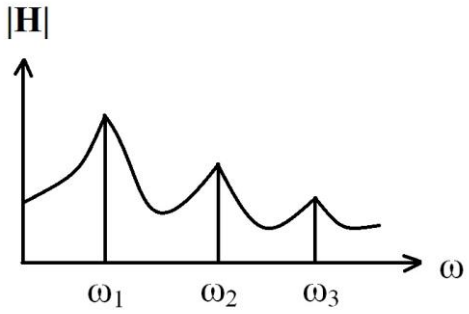


Figure 2.1. Sample Magnitude Plot of the Frequency Response Function from a Test Article Excited at One Point and Measured at Another Point [40].

Frequency Response Function to extract these data. To illustrate the basic method, the somewhat idealized (compliance) Frequency Response Function record of Figure 2.1, resulting from measurements taken between two points on a simple structure, can be considered. Here, it is assumed that a sinusoidal force of adjustable frequency is applied to one point on the structure and that the displacement response is measured at a second point. The response is measured for many values of the driving frequency to produce the plot of Figure 2.1 [40].

To obtain the mode shapes of the structure, the amplitudes of the natural frequencies on the Frequency Response Function plots of the points are taken into account. Also, the

phase plots of the Frequency Respons Functions of these points are considered in order to obtain the signs of the displacements (Figure 2.2).

Both the natural frequency and the mode shape can be determined directly from the accelerometer measurements and force input measurements, by plotting the magnitude of the inertance Frequency Response Function, and applying the method shown in Figure 2.2.

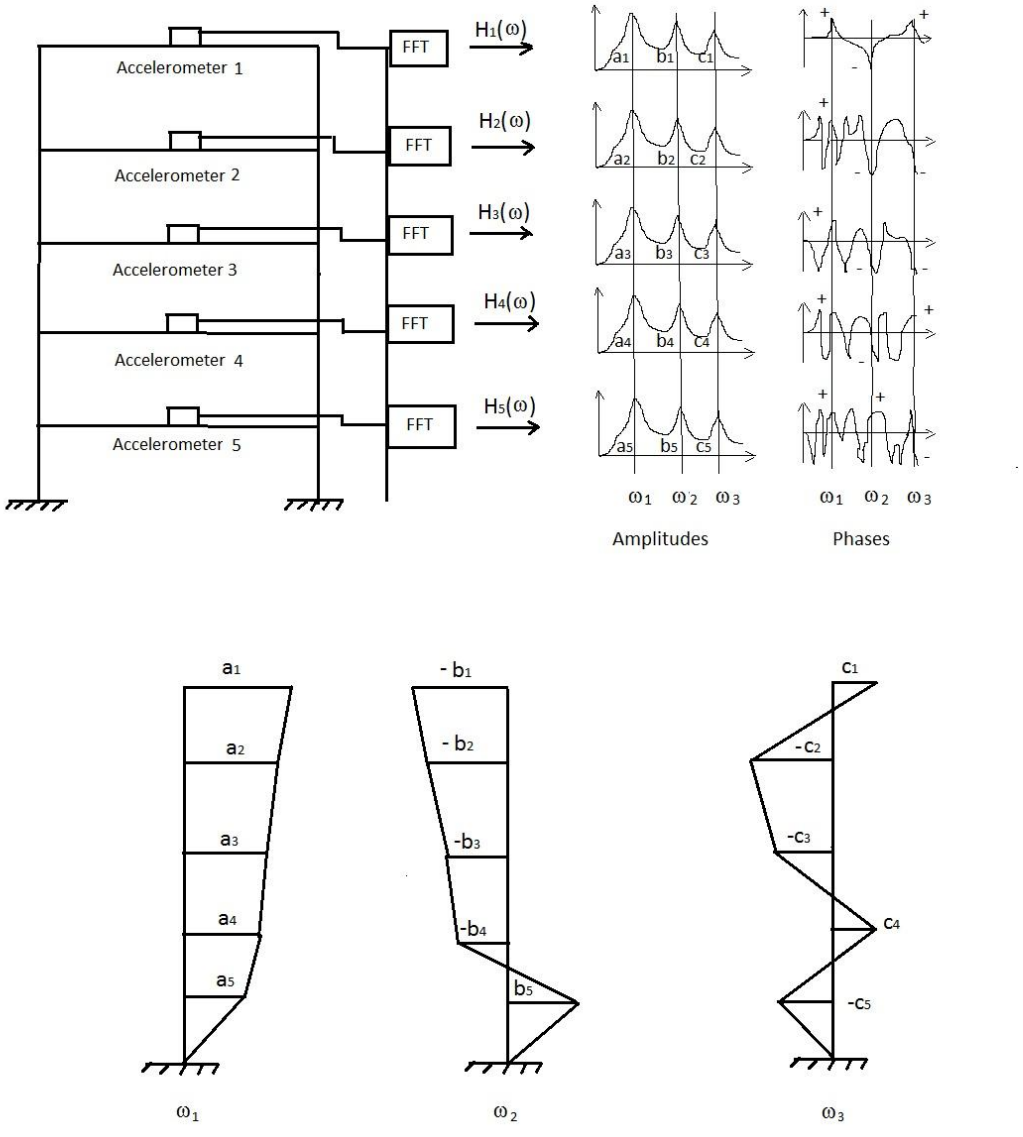


Figure 2.2. Obtaining the Mode Shapes from the Frequency Response Functions ($H_1(\omega)$, $H_2(\omega)$, $H_3(\omega)$, $H_4(\omega)$, and $H_5(\omega)$).

Processing of the data obtained during the vibration tests of the building also includes the following steps. First, the raw data values (acceleration recordings) are converted into

fractions of the gravitational acceleration constant, "g". Next, the mean value of the data is removed from each recording, to eliminate the electronic offset in the sensors. The data also incorporated a drift from the zero acceleration axis, as shown in Figure 2.3; therefore a high-pass filter was applied on the data to remove this drift. An example of the filtered data is shown in Figure 2.4. Finally, the power spectral density (PSD) of the processed data is calculated for obtaining the natural frequencies and mode shapes using the peak picking method described above. The results are presented in Chapter 4. The mode shapes corresponding to each modal frequency are obtained using the amplitudes at the natural frequency value on the PSD graphs.

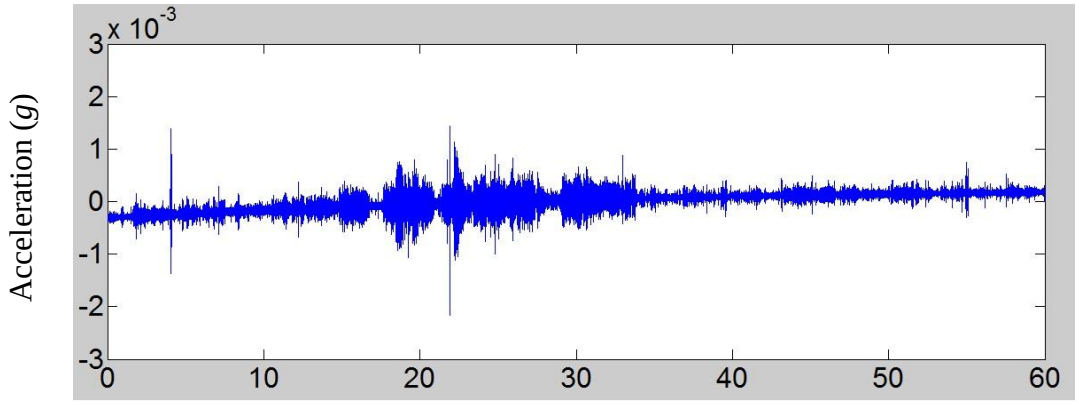


Figure 2.3. Drift from the Zero Acceleration Axis in Raw Data.

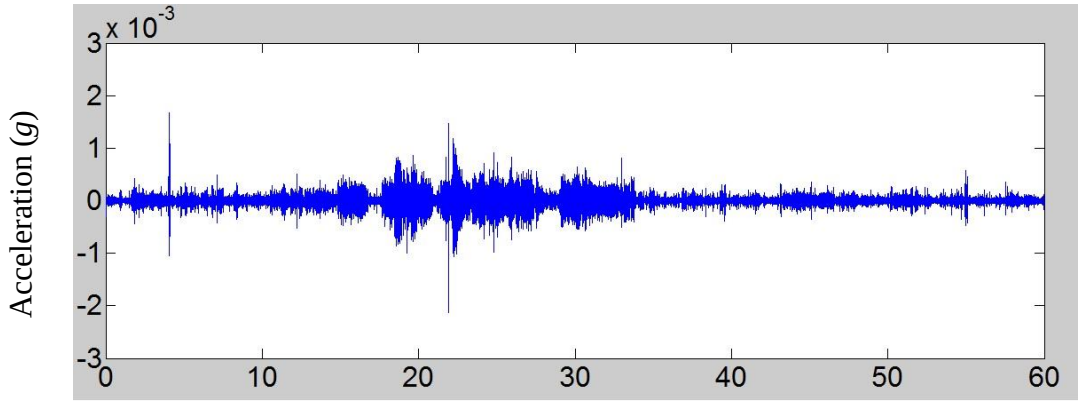


Figure 2.4. Filtered Acceleration Data.

# 3. DESCRIPTION OF THE BUILDING INVESTIGATED

## 3.1. General Description

The building investigated in this study is the Educational Technologies Building, Block-B (a.k.a., the ET-B Building) of Bogazici University (Figure 3.1). This six-story reinforced concrete structure is located on the North Campus of Bogazici University in Istanbul, Turkey (Lat. 41°5'10.5"N, Long. 29°2'38.8"E). The building was constructed in 1988 for educational and research purposes; and comprises several offices, classrooms, and laboratories. The plan view of a typical story of a building shown in Figure 3.2, and the building's elevation view is illustrated in Figure 3.3. Results of performance assessment studies indicated that the building did not satisfy the performance criteria set forth in the 2007 Turkish Seismic Code [41] for existing buildings. As a result, the building underwent a government-funded seismic strengthening program. The description of the structural system of the building, before and after seismic strengthening, as well as details of the strengthening method applied, is presented in the following sections.

Figure 3.1. Overall View of the ET-B Building from the North-East Direction.

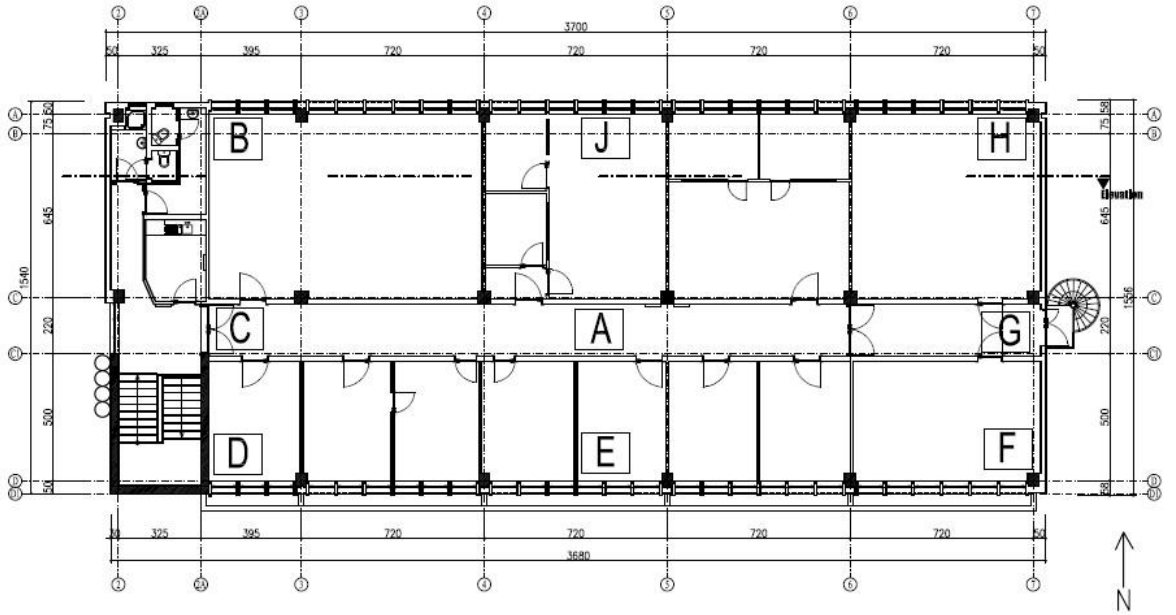


Figure 3.2. Plan View of a Typical Floor.

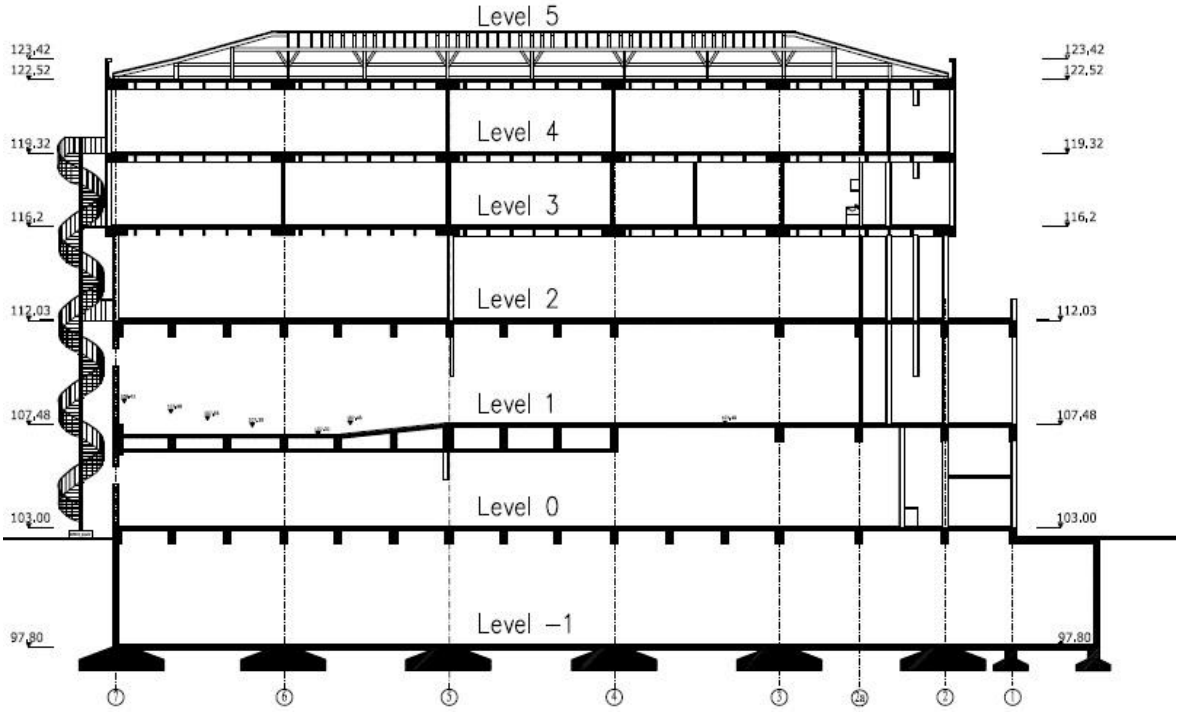


Figure 3.3. Elevation of the Building from South.

### 3.2. Structural Configuration before Strenghtening

The Educational Technologies Building Block B (the ET-B Building) is a reinforced concrete frame structure. The building consists of six stories, including three basement stories, one ground story, and two typical (normal) stories. The total height of the building is 24.7 meters. The normal story and roof floors incorporate two-way joist slabs (waffle slabs), whereas one-way joist slabs (with joists in the N-S) direction are used in the ground and basement story floors. The lowermost basement floor includes peripheral structural walls for resisting lateral soil pressure, which also contribute in the overall lateral stiffness of the building. The structural system also incorporates a stairway-peripheral U-shaped structural wall, located at the SouthWest corner of the building plan (Figure 3.2). The foundation system of the building consist of individual footings, connected with coupling beams. Hollow-clay tile brick infills are used in the building for partitioning purposes. Figure 3.2 depicts a view of the West side of the building, during the early stages of strengthening.

Figure 3.4. View of the Building during Strengthening, from East.

### 3.3. Structural Configuration after Strengthening

Results of code-compliant performance assessment studies indicated that the ET-B building did not satisfy the performance criteria set forth in the 2007 Turkish Seismic Code [41] for existing buildings. The building lacked adequate lateral stiffness and ductility attributes necessary to conform with the immediate occupancy and life safety performance objectives specified in the seismic code. As a result, between July and December 2010, the building underwent a comprehensive government-funded seismic retrofit program; during which the columns of the building were strengthened via reinforced concrete jacketing, several structural walls were added to the building, and a mat foundation was constructed underneath the building. Figure 3.5 shows the view of the East side of the building, after addition of the structural walls for strengthening.

Figure 3.5. View of the Building after Strengthening, from East.

Addition of structural walls served towards improving the lateral stiffness, as well as the lateral ductility of the overall structural system, whereas the motivation behind

jacketing of the columns was to increase column capacity (both axial and flexural) and to improve ductility (through added confinement). Incorporation of structural walls brought together the necessity to construct a mat foundation underneath the building, to prevent wall rocking and to reduce bearing stresses in the underlying soil under earthquake excitation. The locations of the jacketed columns and add-on structural walls on the building floor plan are shown in Figure 3.6, whereas Table 3.1 lists the cross-sectional dimensions of the columns and structural walls in the building before and after seismic strengthening.

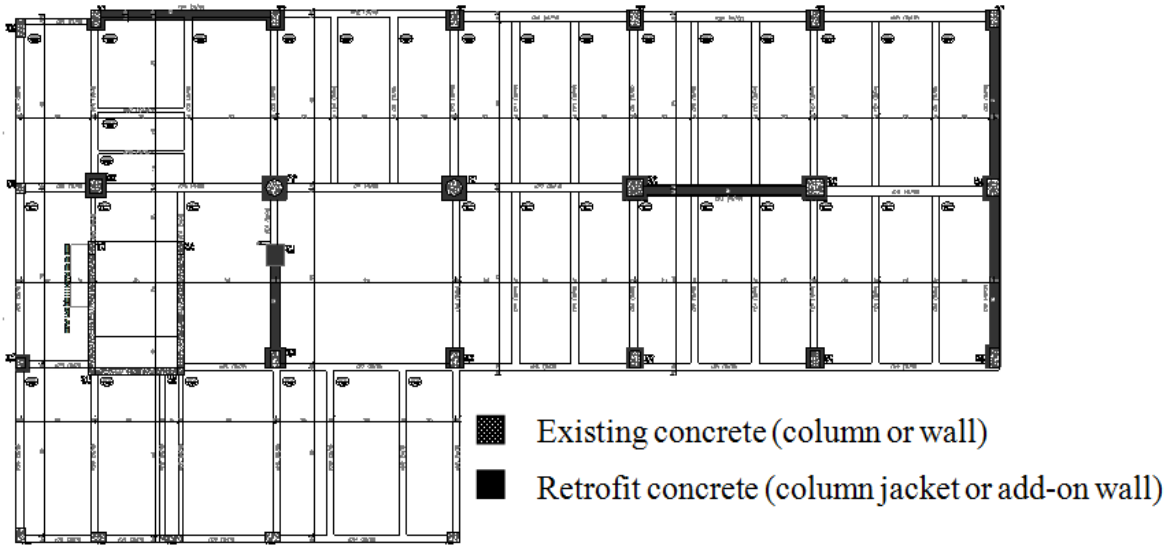


Figure 3.6. Location of Jacketed Columns and Added Structural Walls on Floor Plan.

The process of strengthening of columns via reinforced concrete jacketing included cover-breaking and surface roughening of the existing columns, addition of longitudinal reinforcement, addition of transverse reinforcement, and concrete jacketing. Figure 3.7 shows an existing column in preperation for jacketing, with the cover concrete broken off. Continuity in the longitudinal reinforcement within the jacket was maintained via continuation of the reinforcing bars through holes drilled in the floor slabs, as shown in Figure 3.8. The longitudinal bars were lap-spliced at column mid-height. Additional transverse reinforcement consisting of recrtangular ties was provided within the jacket, for confinement purposes, as well as increase of column shear capacity. Details of the completed jacket reinforcement are shown in Figure 3.9.

Table 3.1. Dimensions of Columns and Structural Walls before and after Strenghtnening.

| Before Strenghtening | | After Strengthening | |
|---|---|---|---|
| Columns | | | |
| Dimensions (mm) | Quantity | Dimensions (mm) | Quantity |
| 400 x 600 | 13 | 700 x 750 | 9 |
| | | 550 x 750 | 2 |
| | | 700 x 900 | 1 |
| | | 650 x 900 | 1 |
| Ø600 | 2 | 900 x 900 | 2 |
| 600 x 500 | 1 | 900 x 800 | 1 |
| 500 x 600 | 1 | 800 x 900 | 1 |
| 300 x 300 | 2 | 300 x 300 | 2 |
| 300 x 500 | 2 | 300 x 500 | 2 |
| Additional Column (after strengthening) | | | |
| | | 700 x 900 | 1 |
| Additional Structural Walls (after strengthening) | | | |
| Dimensions (mm) | Number | Direction | |
| 6500 x 450 | 1 | E-W | |
| 6350 x 400 | 1 | E-W | |
| 400 x 3450 | 1 | N-S | |
| 400 x 6200 | 2 | N-S | |
| Stairway-Peripheral Structural Walls (Before and After Retrofit) | | | |
| Dimensions (mm) | Number | Direction | |
| 3250 x 300 | 1 | E-W | |
| 300 x 4700 | 2 | N-S | |

Figure 3.7. Existing Column with Cover Concrete Removed.

Figure 3.8. Holes Drilled in Slab for Continuation of Longitudinal Reinforcement.

Figure 3.9. Reinforcement Details of the Column Jacket.

The process of addition of structural walls between existing columns comprised of jacketing of the boundary columns with both longitudinal and transverse reinforcement, addition of distributed web reinforcement between the boundary columns in both vertical and horizontal directions. Reinforcement details in the boundary column jackets resembled that of the individual jacketed columns. Figure 3.10 shows an existing boundary column in preperation for jacketing, with the cover concrete removed and the holes drilled in the floor slab for continuation of longitudinal reinforcement. The vertical web bars of the walls were not continuous; instead, they were lap-spliced with anchor bars epoxied into holes drilled in the beams (Figure 3.11). Details of the reinforcement for the additional structural walls are shown in Figure 3.12.

Figure 3.10. Preparation of the Wall Boundary Column.

Figures 3.11. Vertical Anchor Bars Epoxied into Holes Drilled in Beams.

Figure 3.12. Reinforcement Details for Additional Structural Walls.

# 4. AMBIENT AND FORCED VIBRATION TESTS CONDUCTED ON THE BUILDING

Both ambient and forced vibration tests were conducted for experimental identification of selected vibration characteristics (modal frequencies and mode shapes) of the ET-B building. Ambient vibration tests were carried out both before and after seismic strengthening of the building, whereas the forced vibration test was conducted only in the strengthened configuration. In the following sections, the instrumentation and testing procedures are described, and processed results of the test data are presented.

## 4.1. Instrumentation of Building

The building was instrumented with accelerometers during the vibration tests. The sensors used were Kinemetrics "Episensor ES-T" type tri-axial accelerometers, whereas "Quanterra Q330" data-loggers were used for data acquisition. Acceleration data were collected through 24 channels (with 8 tri-axial accelerometers). The Episensor force-balance accelerometers have a wide frequency and acceleration range (0 to 200 Hz and ±4*g*, respectively) and capture vibrations as low as $10^{-8}$ *g*. Q330 data loggers provide signal conditioning, 24-bit A/D conversion, and GPS time stamping for synchronization across multiple nodes. The data loggers were connected to a computer to monitor the data real-time, and to save the data in a hard drive. Data from each sensor were saved as one-hour records.

Figure 4.1 shows the sensor layout plan on a typical floor, and Figure 4.2 shows the elevation view of the building with the instrumentation levels. The sensors at location A (Figure 4.1) existed on each floor of the building. At the top floor (Level 5 in Figure 4.3), sensors were also deployed at locations B, D, F, and H, to be able to capture the torsional characteristics of each vibration mode. Figure 4.3 displays the photographs of two of the sensors deployed. The sensors were affixed to the slabs, at locations close to the columns.

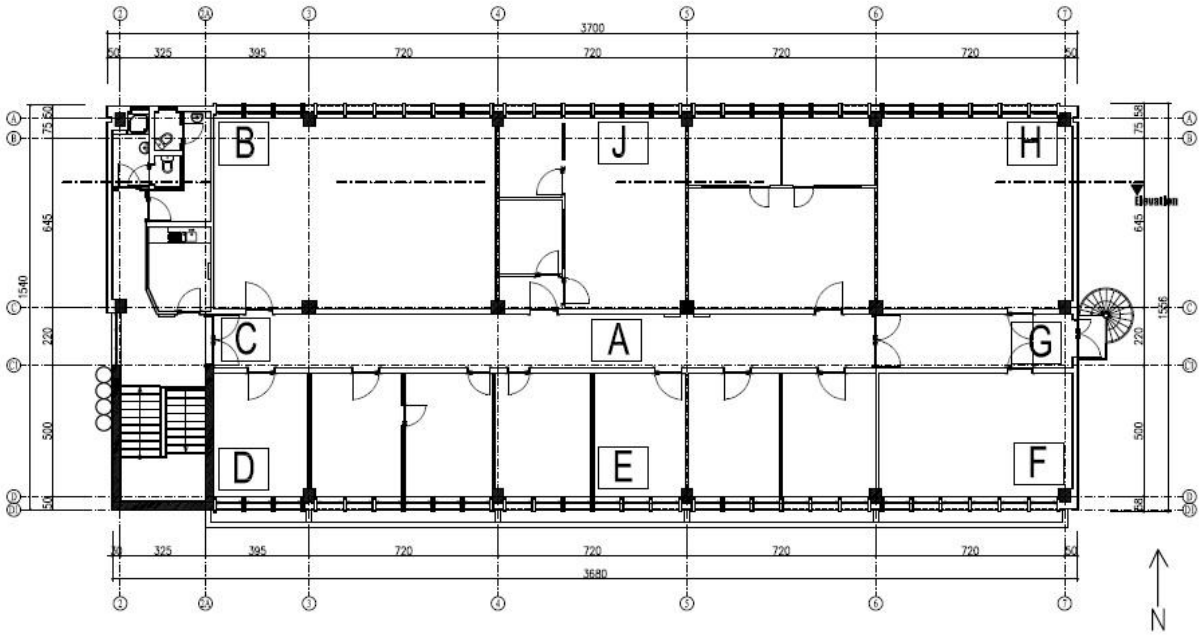


Figure 4.1. Instrumentation Plan of the Building on a Typical Floor.

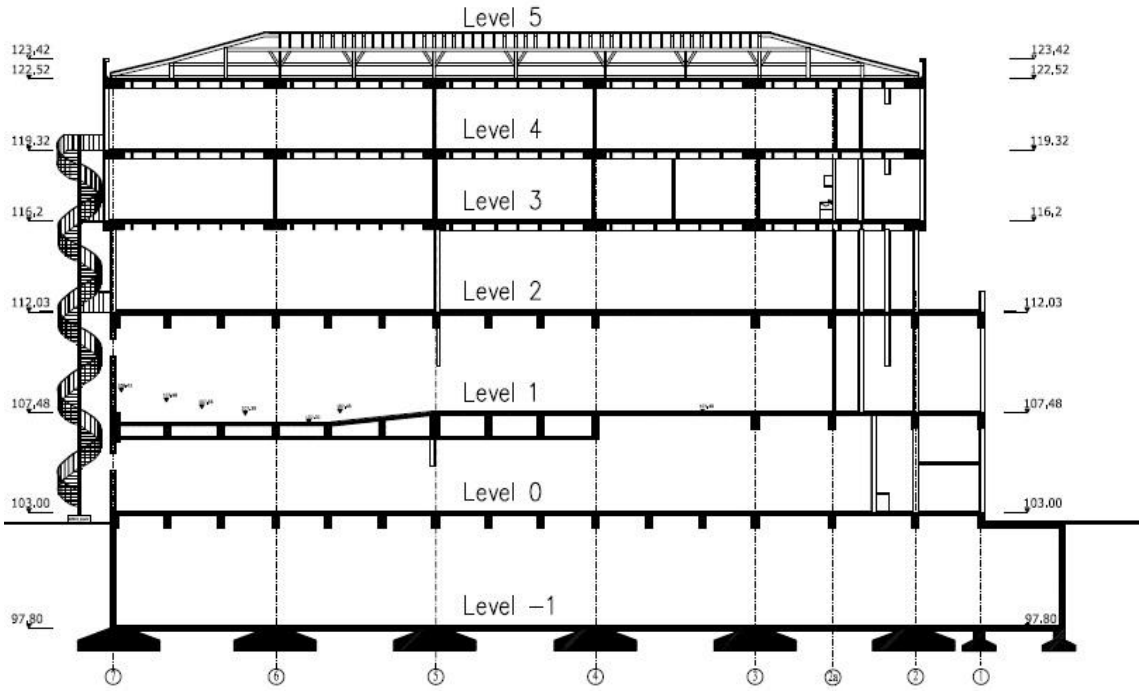


Figure 4.2. Instrumentation Levels.

Figure 4.3. Accelerometers Affixed on the Slabs Near Columns.

## 4.2. Ambient Vibration Tests

Two set of ambient vibration tests were conducted on the building. The first test was performed in July 2010 before the building was strengthened, and the second test was performed in November 2010, after strengthening was completed. The data obtained from ambient vibration tests clearly demonstrated the influence of strengthening on the modal frequencies and mode shapes of the building, and also allowed comparison of the findings with the results of the forced vibration test and the modal analysis of the finite element model of the building.

As part of the seismic retrofit process, the building was cleared out while it underwent ambient vibration testing. All non-structural components (partition walls, ceilings, plumbing, etc.) were removed; the cover concrete on the columns was broken off, and holes were drilled through the slabs to accommodate the extra reinforcing bars in the column jackets. Building traffic was limited to construction activity, which was concentrated mostly in the lower levels of the building. No machinery was running in the building regularly, but the construction workers were using jackhammers to remove floor coverings and the concrete cover on the columns.

### 4.2.1. Ambient Vibration Test Results Before Strengthening

During the tests, the sensors at location A (Figure 4.1) were present on all 7 levels (Figure 4.2) of the building. On level 5 (top floor), sensors were also deployed at locations

B, D, F, and H, in order to identify torsional modes of vibration. The amplitude (power spectral density) spectra of the acceleration records at different instrumentation locations, and in the North-South (N-S) and East-West (E-W) directions of the building are presented in Figure 4.4-23. Modal frequencies at each location and in each direction (N-S or E-W) were identified from the peaks of the power spectral density, as described in Chapter 2.

As shown in Figure 4.4, for Level 5 Location A, the acceleration response in the East-West direction is dominated by the third mode of vibration. The amplitudes (power spectral densities) of the first and second modes are close to each other. The first, second and third-mode natural frequencies can be identified as 2.6 Hz, 3.1 Hz, and 3.4 Hz, respectively.

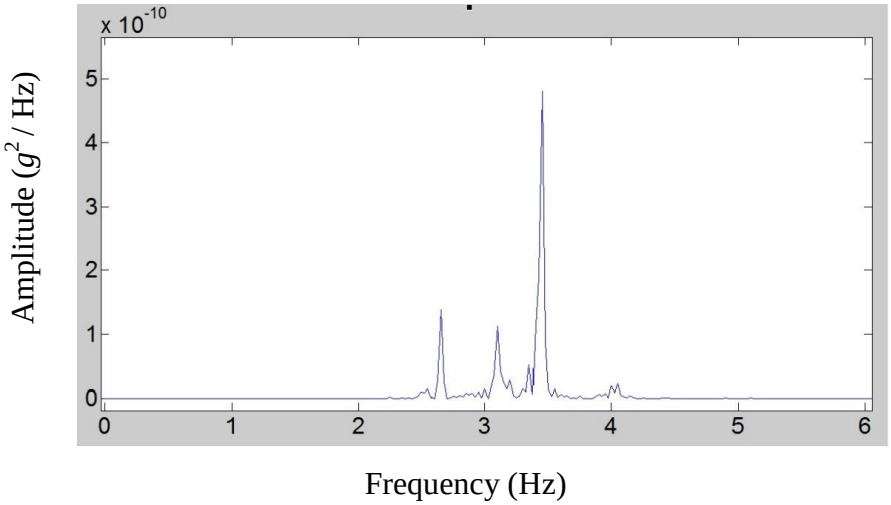


Figure 4.4. Power Spectral Density for Level 5, Location A, E-W Direction.

For Level 5 Location A, the acceleration response in the North-South direction is dominated by the first mode of vibration. The first and third-mode natural frequencies can be identified as 2.6 Hz and 3.4 Hz, respectively (Figure 4.5).

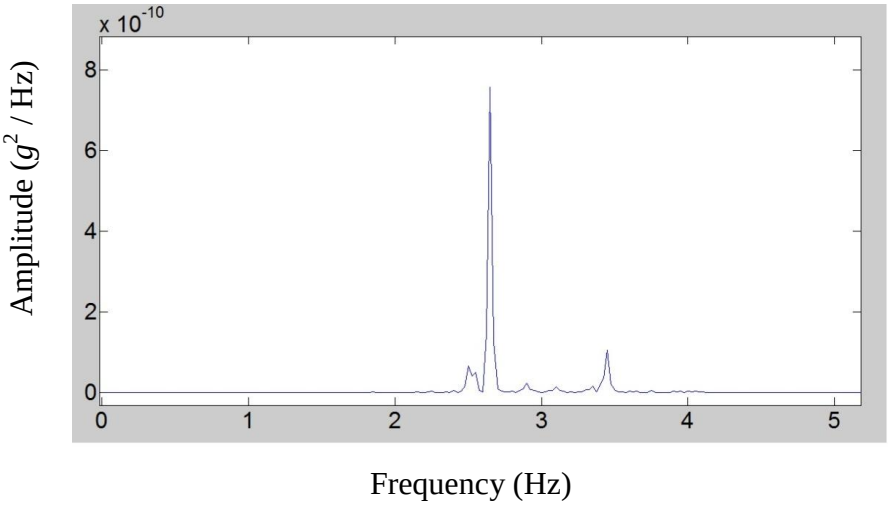


Figure 4.5. Power Spectral Density for Level 5, Location A, N-S Direction.

For Level 4 Location A, the acceleration response in the East-West direction is dominated by the first and third modes of vibration. The first, second and third-mode natural frequencies can be identified as 2.6 Hz, 3.1 Hz, and 3.4 Hz, respectively (Figure 4.6).

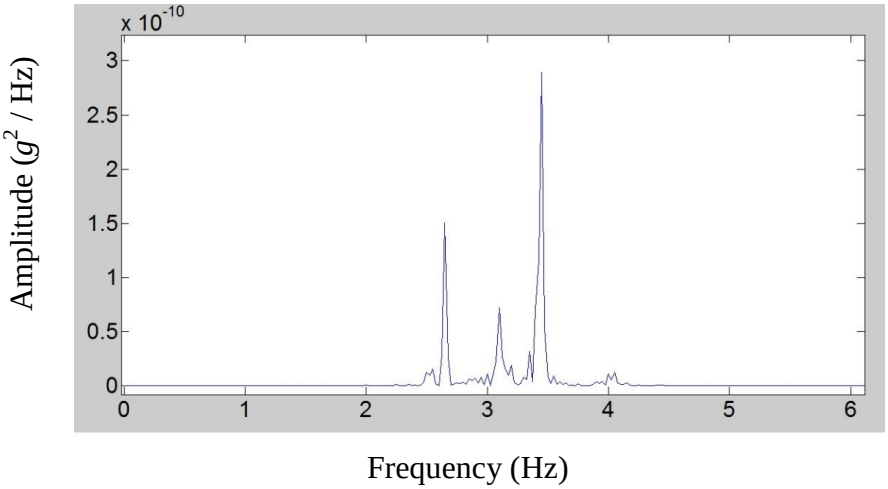


Figure 4.6. Power Spectral Density for Level 4, Location A, E-W Direction.

For Level 4 Location A, the acceleration response in the North-South direction is dominated by the first mode of vibration. The first and third-mode natural frequencies can be identified as 2.6 Hz and 3.4 Hz, respectively (Figure 4.7).

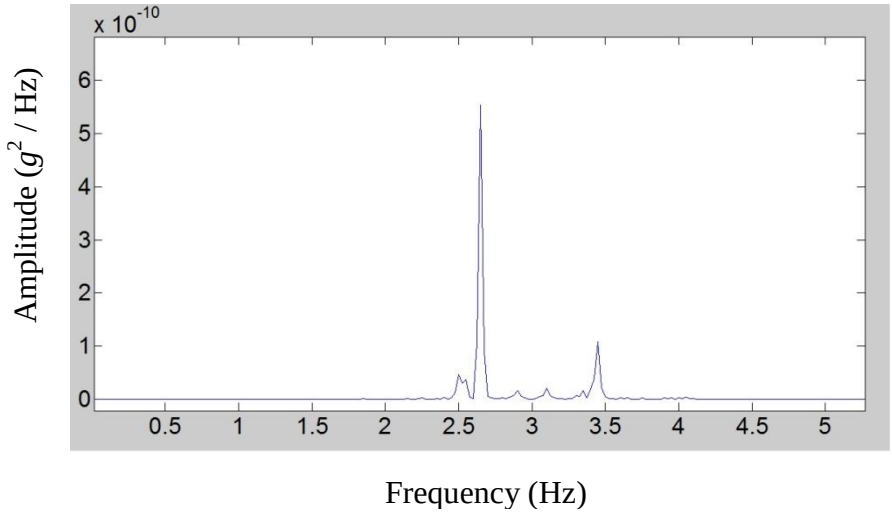


Figure 4.7. Power Spectral Density for Level 4, Location A, N-S Direction.

For Level 3 Location A, the acceleration response in the East-West direction is dominated by the first and third modes of vibration. The first, second and third-mode natural frequencies can be identified as 2.6 Hz, 3.1 Hz, and 3.4 Hz, respectively (Figure 4.8).

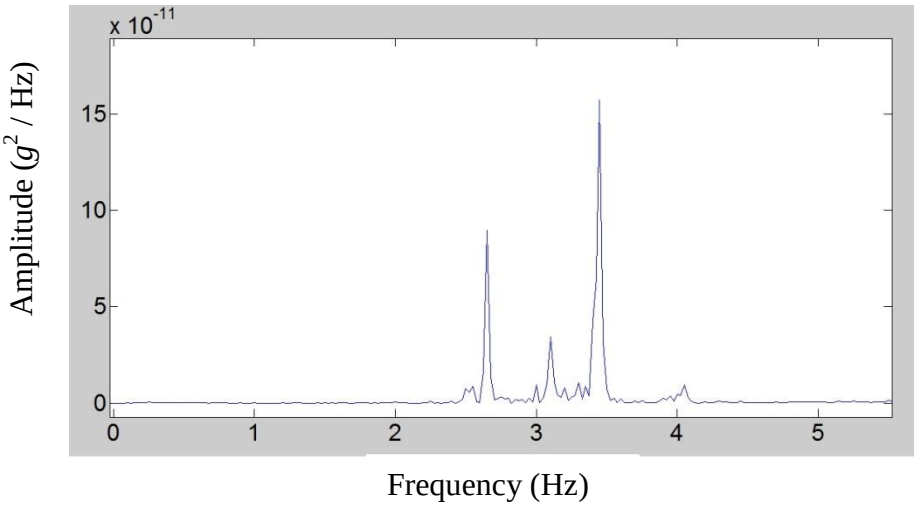


Figure 4.8. Power Spectral Density for Level 3, Location A, E-W Direction

For Level 3 Location A, the acceleration response in the North-South direction is dominated by the first mode of vibration. Again, the first, second and third-mode natural frequencies can be identified as 2.6 Hz, 3.1 Hz, and 3.4 Hz, respectively (Figure 4.9).

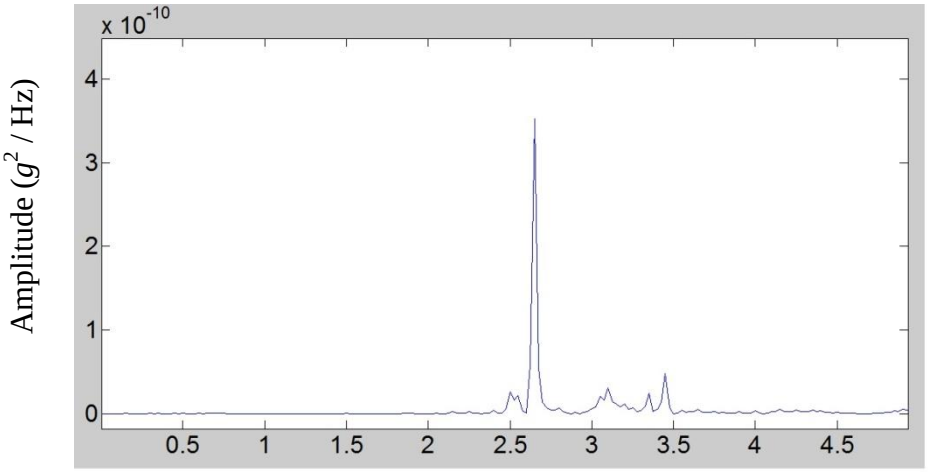


Figure 4.9. Power Spectral Density for Level 3, Location A, N-S Direction.

For Level 2 Location A, the acceleration response in the East-West direction is dominated by the first and third modes of vibration. The first, second and third-mode natural frequencies can be identified also at this location as 2.6 Hz, 3.1 Hz, and 3.4 Hz, respectively (Figure 4.10).

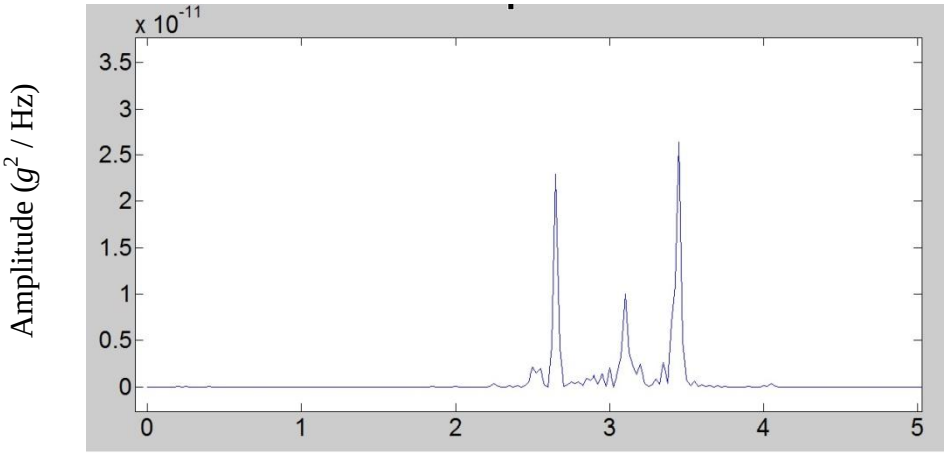


Figure 4.10. Power Spectral Density for Level 2, Location A, E-W Direction.

For Level 2 Location A, the acceleration response in the North-South direction is dominated by the first mode of vibration. The first and third-mode natural frequencies can be identified as 2.6 Hz and 3.4 Hz, respectively (Figure 4.11).

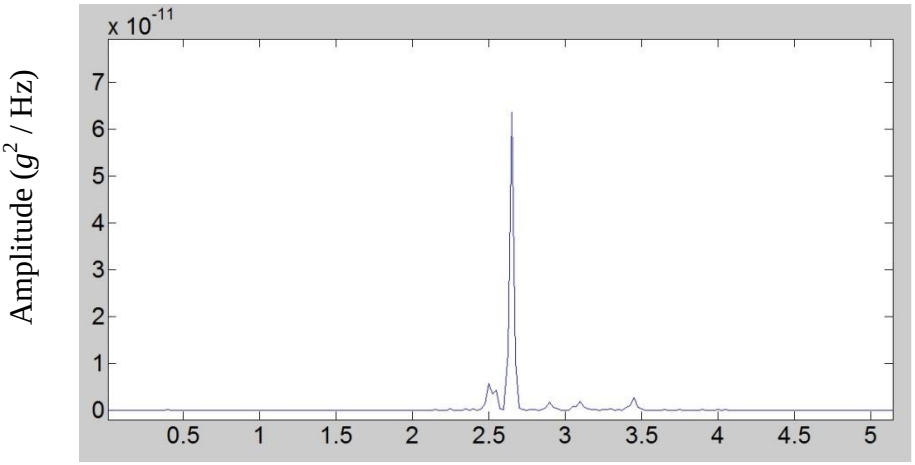


Figure 4.11. Power Spectral Density for Level 2, Location A, N-S Direction.

For Level 1 Location A, the acceleration response in the East-West direction is dominated by the first and third modes of vibration. The first, second and third-mode natural frequencies can all be identified as 2.6 Hz, 3.1 Hz, and 3.4 Hz, respectively (Figure 4.12).

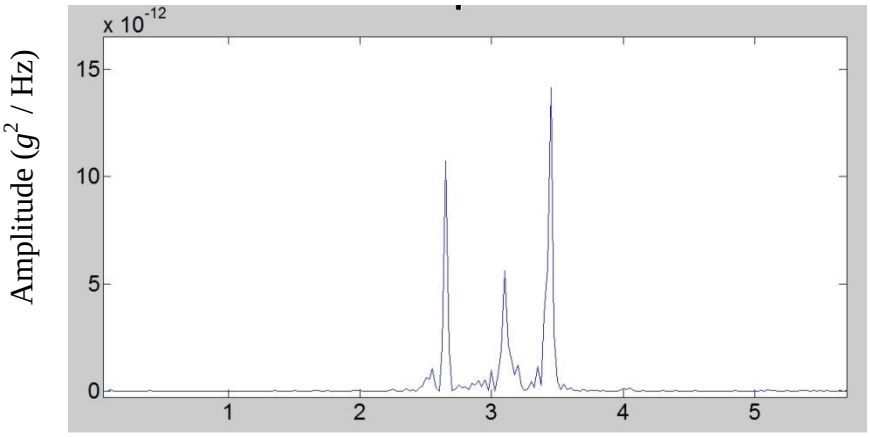


Figure 4.12. Power Spectral Density for Level 1, Location A, E-W Direction.

For Level 1 Location A, the acceleration response in the North-South direction is dominated by the first mode of vibration. At this location, the first-mode natural frequency can be identified as 2.6 Hz (Figure 4.13).

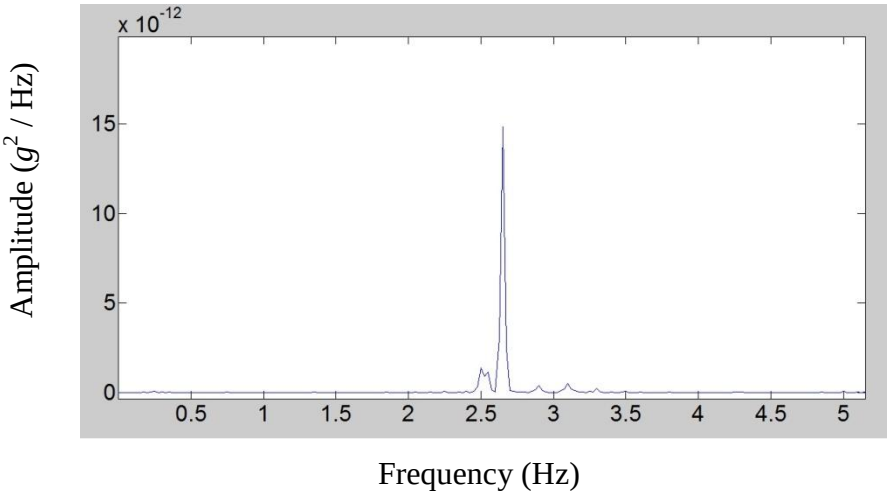


Figure 4.13. Power Spectral Density for Level 1, Location A, N-S Direction.

For Level 0 Location A, the acceleration response in the East-West direction is dominated by the third mode of vibration. The first, second and third-mode natural frequencies can all be identified as 2.6 Hz, 3.1 Hz, and 3.4 Hz, respectively (Figure 4.14).

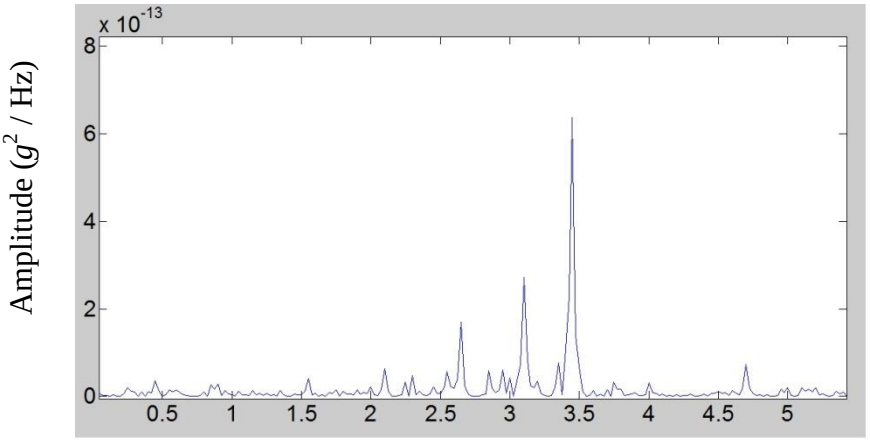


Figure 4.14. Power Spectral Density for Level 0, Location A, E-W Direction.

For Level 0 Location A, the acceleration response in the North-South direction is dominated by the first mode of vibration. Here, the first-mode,natural frequency can be identified as 2.6 Hz (Figure 4.15).

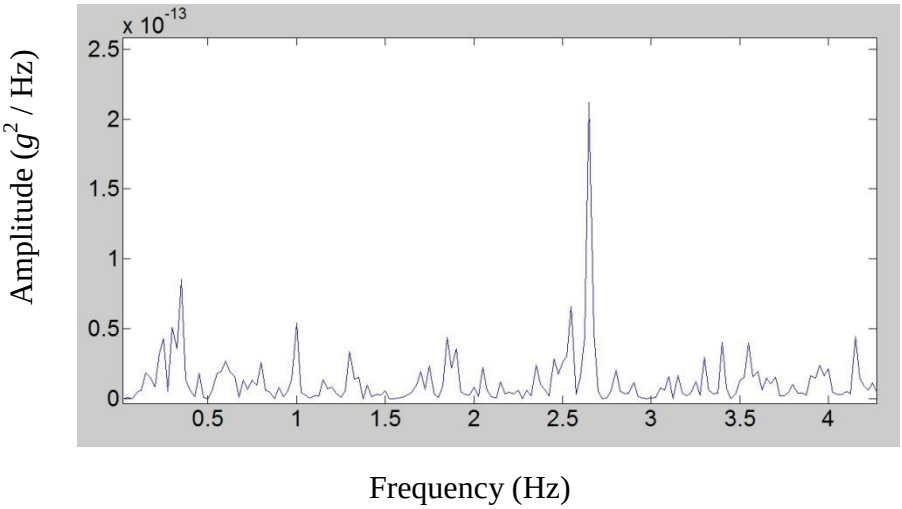


Figure 4.15. Power Spectral Density for Level 0, Location A, N-S Direction.

For Level 5 Location B, the acceleration response in the East-West direction is dominated by the first mode of vibration. At this location, the first, second and third-mode natural frequencies can be identified as 2.6 Hz, 3.1 Hz, and 3.4 Hz, respectively (Figure 4.16).

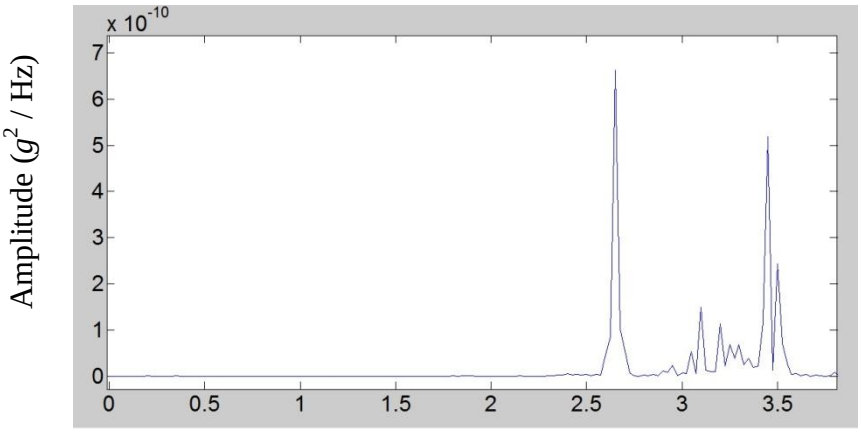


Figure 4.16. Power Spectral Density for Level 5, Location B, E-W Direction.

For Level 5 Location B, the acceleration response in the North-South direction is dominated by the first mode of vibration. At this location, the first and third-mode natural frequencies can be identified as 2.6 Hz and 3.4 Hz, respectively (Figure 4.17).

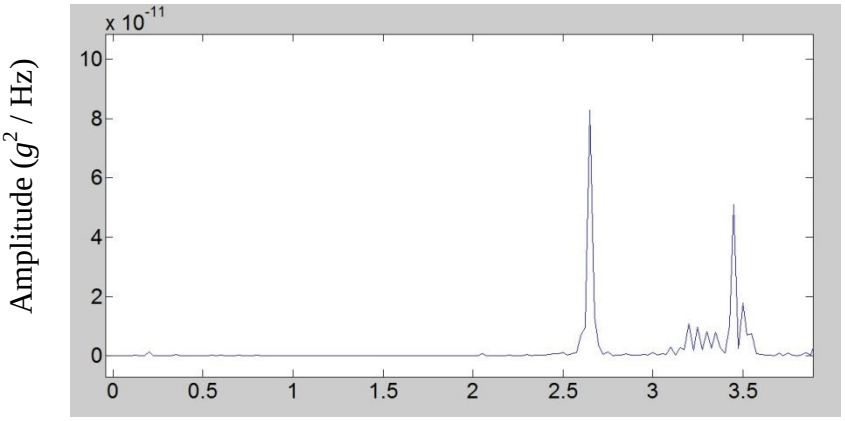


Figure 4.17. Power Spectral Density for Level 5, Location B, N-S Direction.

For Level 5 Location D, the acceleration response in the East-West direction is dominated by the third mode of vibration. The first, second and third-mode natural frequencies can be identified as 2.6 Hz, 3.1 Hz, and 3.4 Hz, respectively (Figure 4.18).

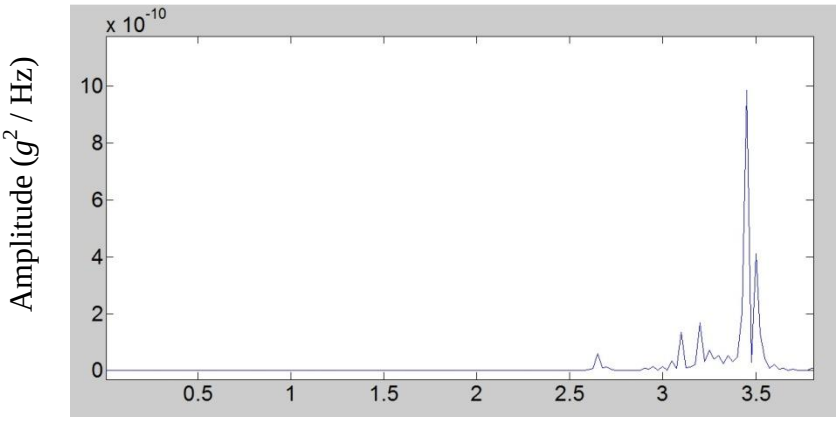


Figure 4.18. Power Spectral Density for Level 5, Location A, E-W Direction.

For Level 5 Location D, the acceleration response in the North-South direction is dominated by the third mode of vibration. The first,and third-mode natural frequencies can be identified as 2.6 Hz and 3.4 Hz, respectively (Figure 4.19).

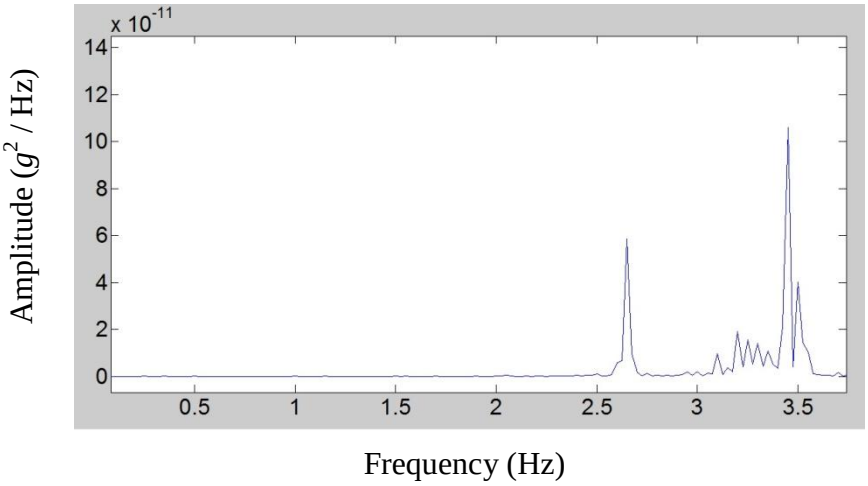


Figure 4.19. Power Spectral Density for Level 5, Location D, N-S Direction.

For Level 5 Location F, the acceleration response in the East-West direction is dominated by the third mode of vibration. Here, the third-mode natural frequency can be identified as 3.4 Hz (Figure 4.20).

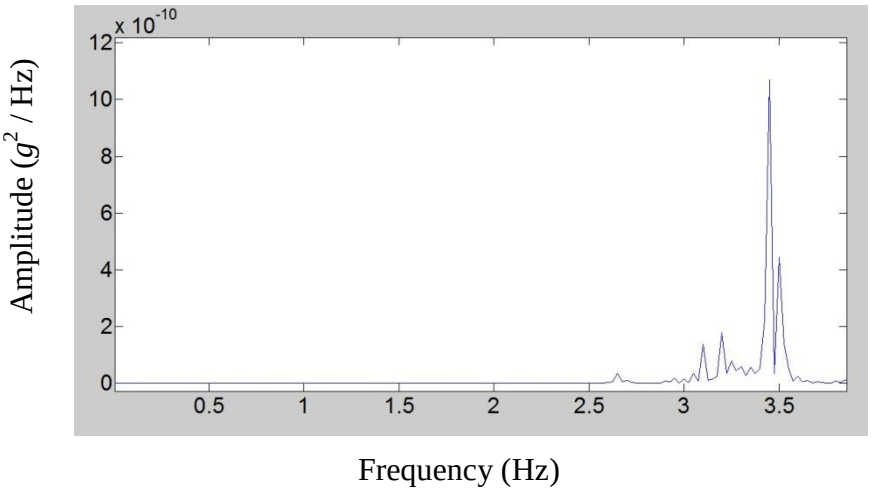


Figure 4.20. Power Spectral Density for Level 5, Location F, E-W Direction.

For Level 5 Location F, the acceleration response in the North-South direction is dominated by the first mode of vibration. Here, the first and third-mode natural frequencies can be identified as 2.6 Hz and 3.4 Hz, respectively (Figure 4.21).

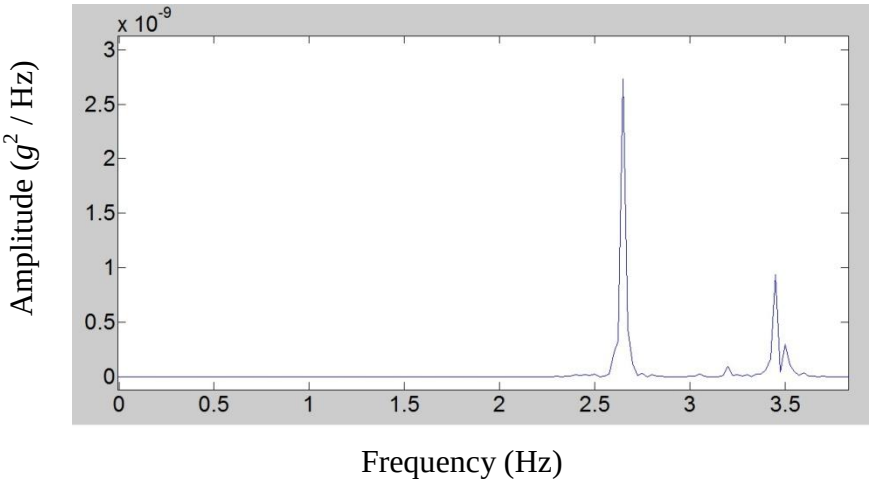


Figure 4.21. Power Spectral Density for Level 5, Location F, N-S Direction.

For Level 5 Location H, the acceleration response in the East-West direction is dominated by the first mode of vibration. The first, second and third-mode natural frequencies can all be identified as 2.6 Hz, 3.1 Hz, and 3.4 Hz, respectively (Figure 4.22).

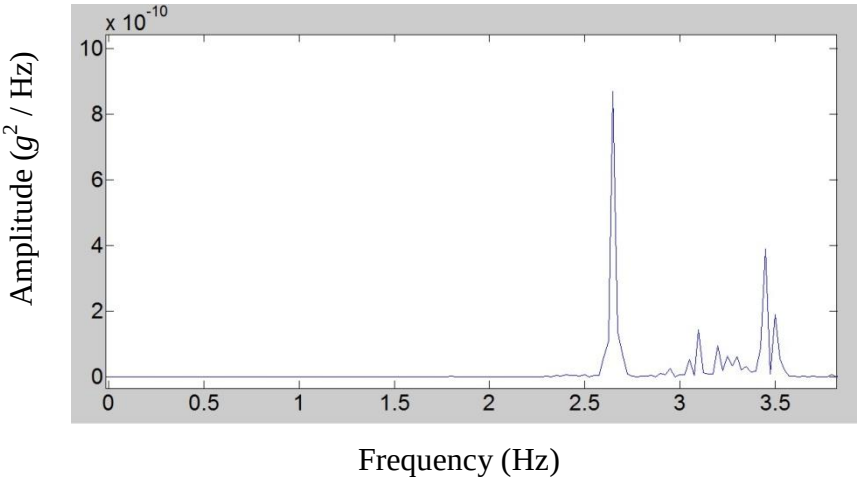


Figure 4.22. Power Spectral Density for Level 5, Location H, E-W Direction.

For Level 5 Location H, the acceleration response in the North-South direction is dominated by the first mode of vibration. The first and third-mode natural frequencies can be identified as 2.6 Hz and 3.4 Hz, respectively (Figure 4.23).

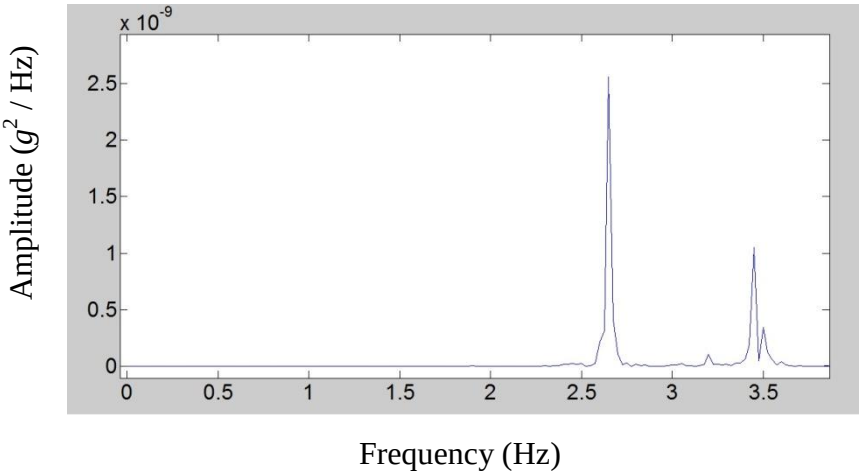


Figure 4.23. Power Spectral Density for Level 5, Location H, N-S Direction.

Results presented in Figure 4.4-23 show that the natural frequencies of the building for the first, second and third modes of vibration are 2.6 Hz,, 3.1 Hz, and 3.4 Hz, respectively. The first mode of vibration is in the diagonal North-West – South-East direction of the building and the second and third modes are in the diagonal North-East - South-West direction. The East-West and North-South amplitudes of the first, second and third modes of vibration are very close to each other, indicating that these modes are in a diagonal direction. In order to determine the modal directions of vibration, the acceleration data at locations B, H, D and F on Level 5 was processed (Figure 4.24, 4.25 and 4.26). The directions of vibrational motion were obtained from the phase signs of the modes of the spectra generated for the acceleration data (Table 4.1). The modal frequencies obtained from the data recorded at these locations are also 2.6 Hz, 3.1 Hz, and 3.4 Hz, and the phase signs of the data are listed in Table 4.1.

Table 4.1. The Natural Frequencies and Phase Signs of the Spectra Obtained from Sensors at Locations B, D, F and H on Level 5.

| Modal Freq. (Hz) | Locations | | | | | | | |
|---|---|---|---|---|---|---|---|---|
| | B | | H | | D | | F | |
| | X | Y | X | Y | X | Y | X | Y |
| 2.6 | + | - | + | - | + | - | + | - |
| 3.1 | - | - | - | - | - | - | - | - |
| 3.4 | + | + | + | + | + | + | + | + |

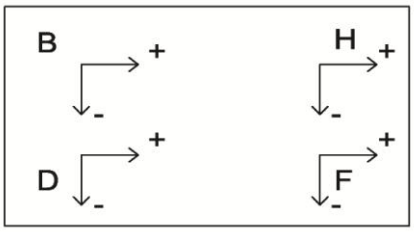


Figure 4.24. First Mode Phase Signs at Sensor Locations B, D, H, and F on Level 5.

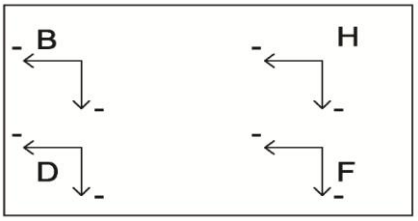


Figure 4.25. Second Mode Phase Signs at Sensor Locations B, D, H, and F on Level 5.

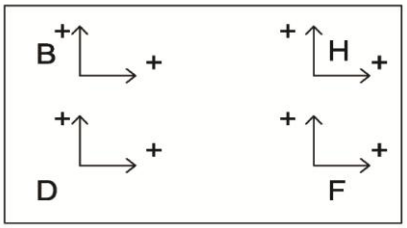


Figure 4.26. Third Mode Phase Signs at Sensor Locations B, D, H, and F on Level 5.

Accordingly, the mode shapes obtained first three modes of vibration are shown in Figure 4.27-29. The mode shapes were obtained based on the relative amplitudes corresponding to the first three natural frequencies on the amplitude spectra of the acceleration records (Figure 4.4-23) at sensor location A, on all seven floors of the building (Figure 4.1 and 4.2).

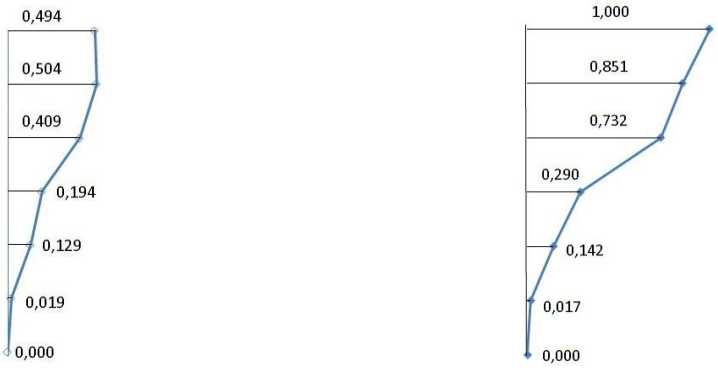


(a) (b)

Figure 4.27. First Mode Shape Amplitudes Before Strengthening: (a) E-W Direction, (b) N-S Direction.

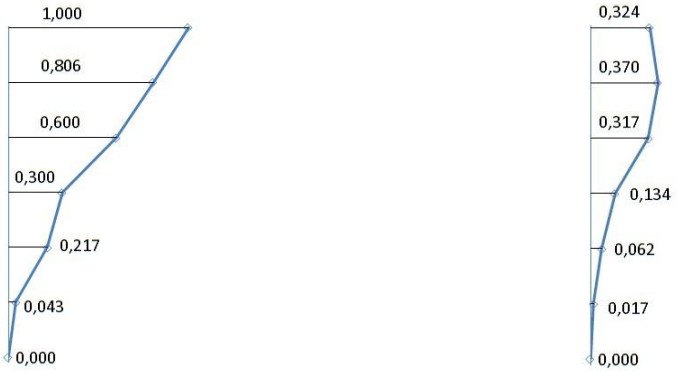


(a) (b)

Figure 4.28. Second Mode Shape Amplitudes Before Strengthening: (a) E-W Direction, (b) N-S Direction.


(a) (b)

Figure 4.29. Third Mode Shape Amplitudes Before Strengthening: (a) E-W Direction, (b) N-S Direction.

### 4.2.2. Ambient Vibration Test Results After Strengthening

During the tests, the sensors at location A (Figure 4.1) were present on all 7 levels (Figure 4.2) of the building. On level 5 (top floor), sensors were also deployed at locations A and H in order to identify torsional modes of vibration. The amplitude (power spectral density) spectra of the acceleration records at different instrumentation locations, and in the North-South (N-S) and East-West (E-W) directions of the building are presented in Figure 4.30-45. Modal frequencies at each location and in each direction (N-S or E-W) were identified from the peaks of the power spectral density, as described in Chapter 2.

As shown in Figure 4.30, for Level 5 Location A, the acceleration response in the East-West direction is dominated by the first mode of vibration. From this data, the first-mode natural frequency of the building can be identified as 4.7 Hz.

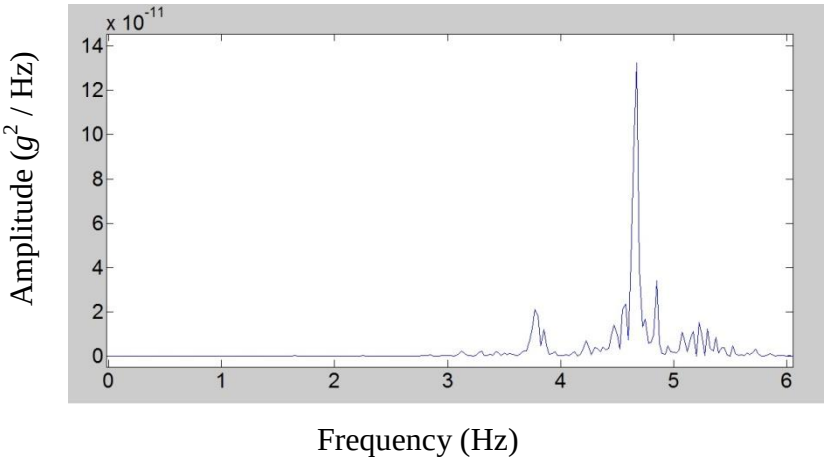


Figure 4.30. Power Spectral Density for Level 5, Location A, E-W Direction.

For Level 5 Location A, the acceleration response in the North-South direction is dominated by the second mode of vibration. From the data measured at this location, the first and second-mode natural frequencies can be identified as 4.7 Hz and 5.2 Hz, respectively (Figure 4.31).

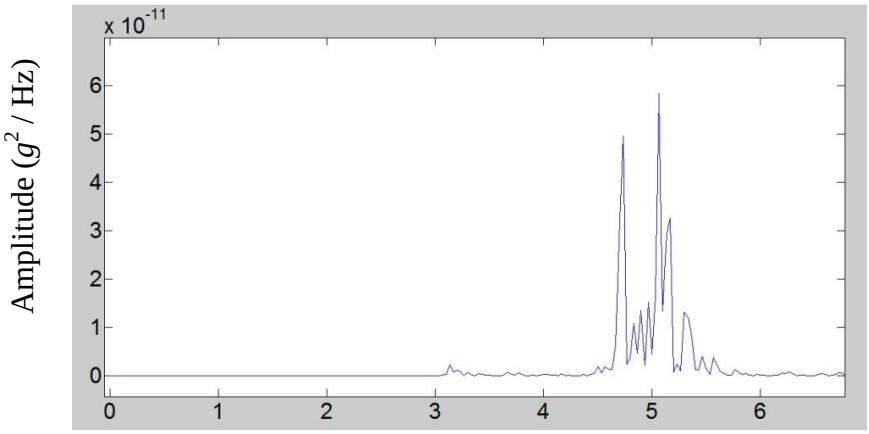


Figure 4.31. Power Spectral Density for Level 5, Location A, N-S Direction.

For Level 4 Location A, the acceleration response in the East-West direction is dominated by the first mode of vibration. Here, the first-mode natural frequency can be identified as 4.7 Hz (Figure 4.32).

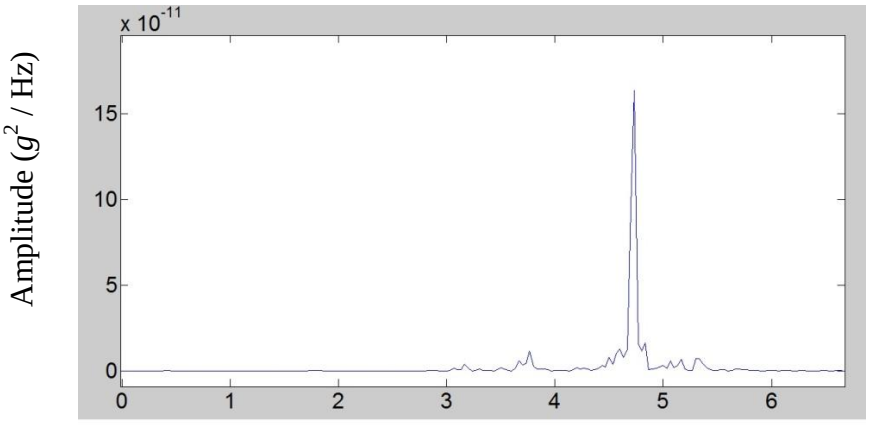


Figure 4.32. Power Spectral Density for Level 4, Location A, E-W Direction.

For Level 4 Location A, the acceleration response in the North-South direction is dominated by the second mode of vibration. At this location, the first and second-mode natural frequencies can be identified as 4.7 Hz and 5.2 Hz, respectively (Figure 4.33).

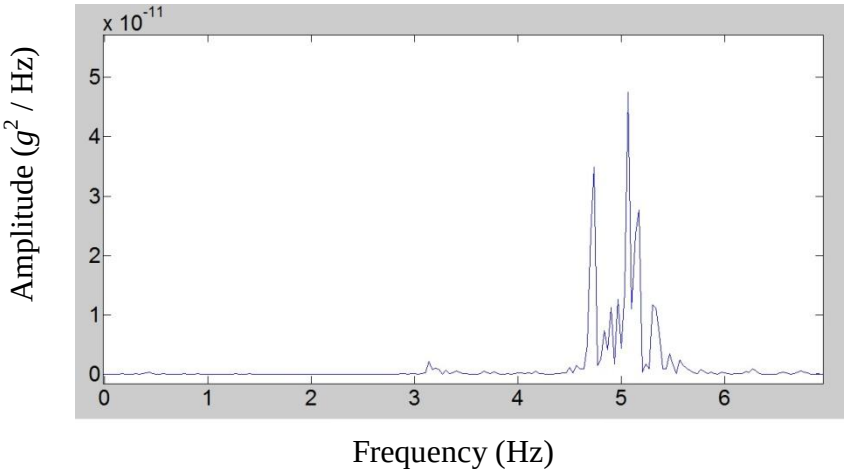


Figure 4.33. Power Spectral Density for Level 4, Location A, N-S Direction.

For Level 3 Location A, the acceleration response in the East-West direction is dominated by the first mode of vibration. Here, the first-mode natural frequency can be identified as 4.7 Hz (Figure 4.34).

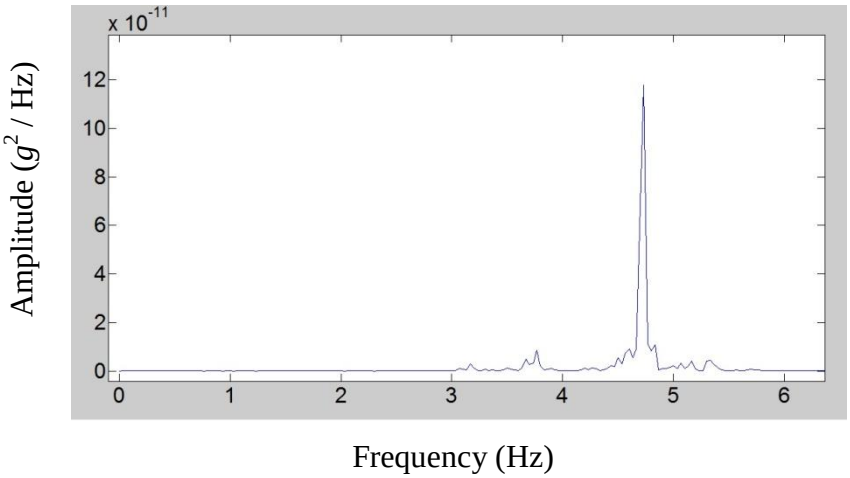


Figure 4.34. Power Spectral Density for Level 3, Location A, E-W Direction.

For Level 3 Location A, the acceleration response in the North-South direction is dominated by the second mode of vibration. At this location, the first and second-mode natural frequencies can be identified as 4.7 Hz and 5.2 Hz, respectively (Figure 4.35).

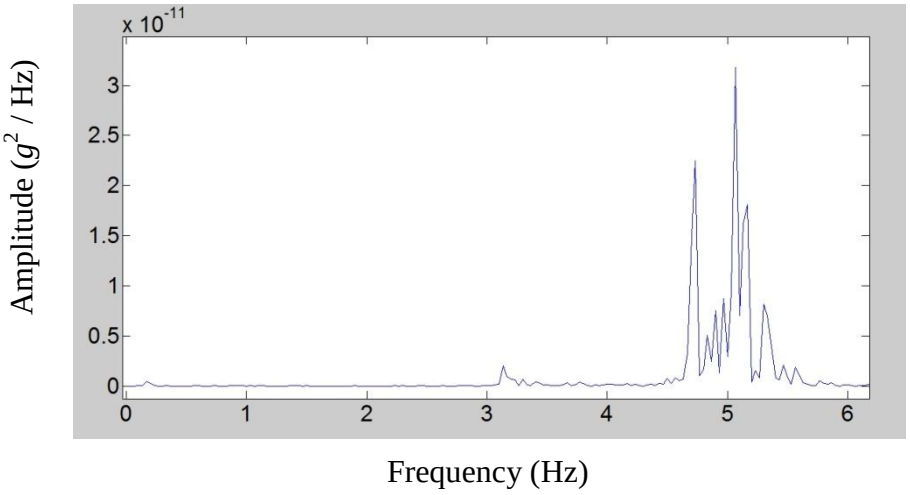


Figure 4.35. Power Spectral Density for Level 3, Location A, N-S Direction.

For Level 2 Location A, the acceleration response in the East-West direction is dominated by the first mode of vibration. The first-mode natural frequency can again be identified as 4.7 Hz (Figure 4.36).

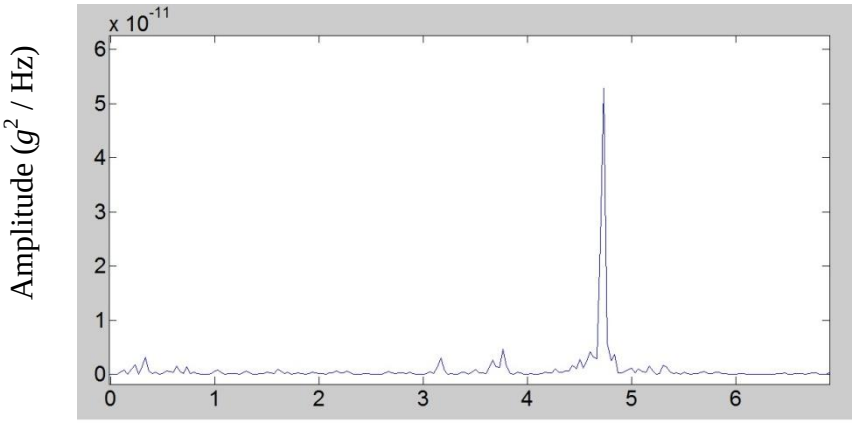


Figure 4.36. Power Spectral Density for Level 2, Location A, E-W Direction.

For Level 2 Location A, the acceleration response in the North-South direction is dominated by the second mode of vibration. Again, the first and second-mode natural frequencies can be identified as 4.7 Hz and 5.2 Hz, respectively (Figure 4.37).

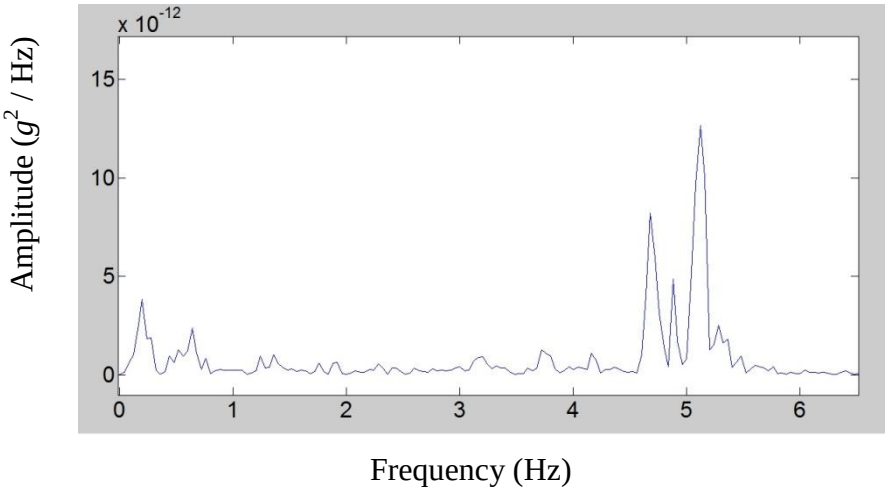


Figure 4.37. Power Spectral Density for Level 2, Location A, N-S Direction.

For Level 1 Location A, the acceleration response in the East-West direction is dominated by the first mode of vibration. The first-mode natural frequency can be identified as 4.7 Hz at this location (Figure 4.38).

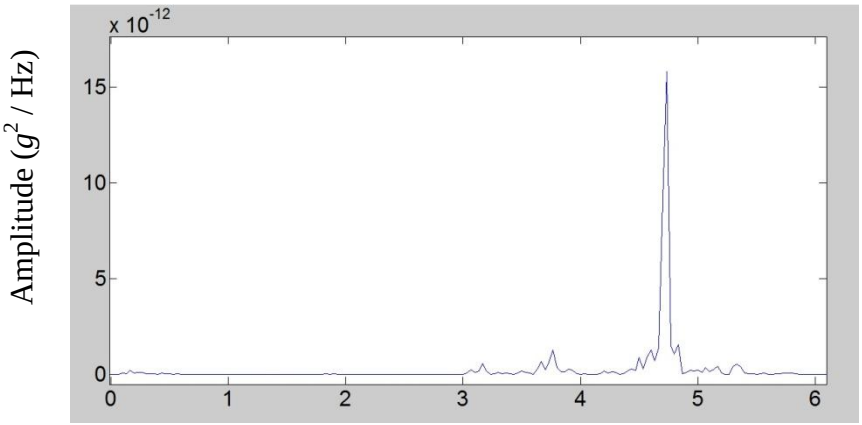


Figure 4.38. Power Spectral Density for Level 1, Location A, E-W Direction.

For Level 1 Location A, the acceleration response in the North-South direction is dominated by the second mode of vibration. The first and second-mode natural frequencies can be identified as 4.7 Hz and 5.2 Hz, respectively (Figure 4.39).

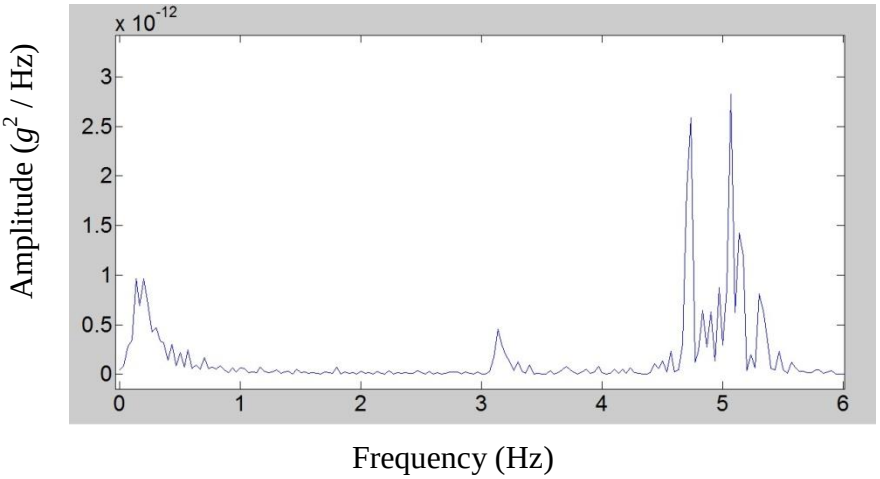


Figure 4.39. Power Spectral Density for Level 1, Location A, N-S Direction.

For Level 0 Location A, the acceleration response in the East-West direction is dominated by the first mode of vibration. The first-mode natural frequency can be identified as 4.7 Hz (Figure 4.40).

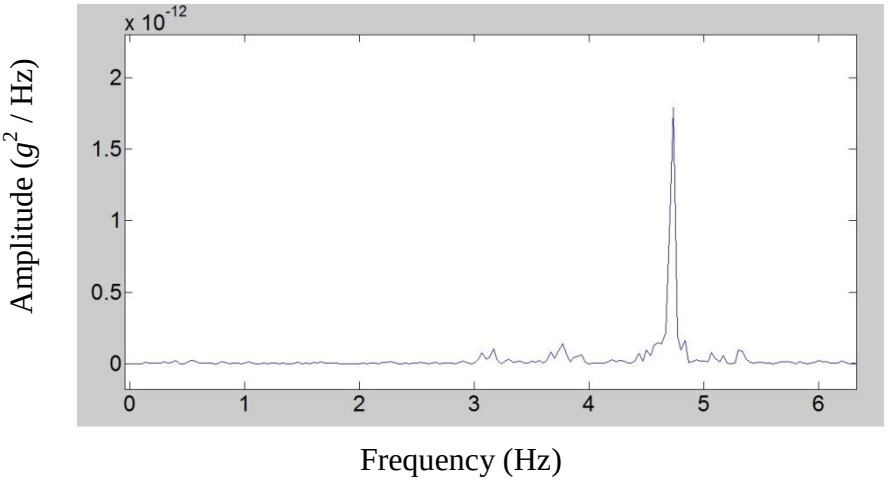


Figure 4.40. Power Spectral Density for Level 0, Location A, E-W Direction.

For Level 0 Location A, the acceleration response in the North-South direction is dominated by the second mode of vibration. The first and second-mode natural frequencies can be identified as 4.7 Hz and 5.2 Hz, respectively (Figure 4.41).

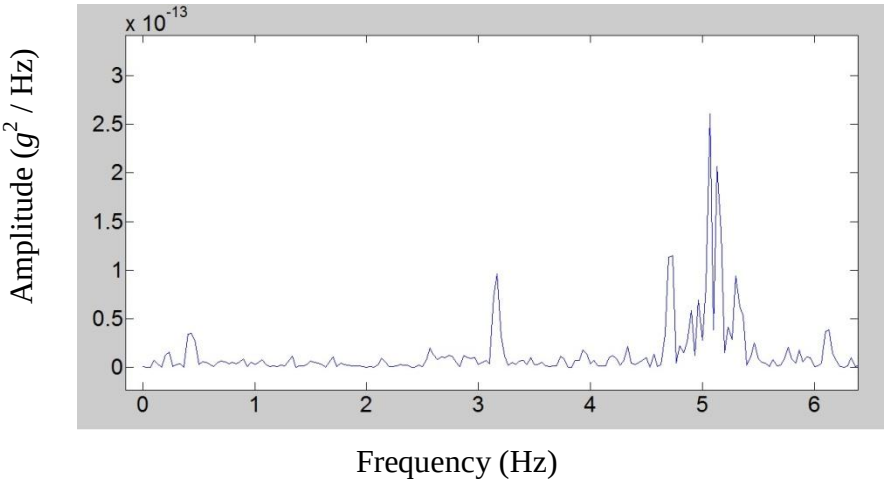


Figure 4.41. Power Spectral Density for Level 0, Location A, N-S Direction.

For Level 5 Location H, the acceleration response in the East-West direction is dominated by the first mode of vibration. Here, the first-mode natural frequency can be identified as 4.7 Hz (Figure 4.42).

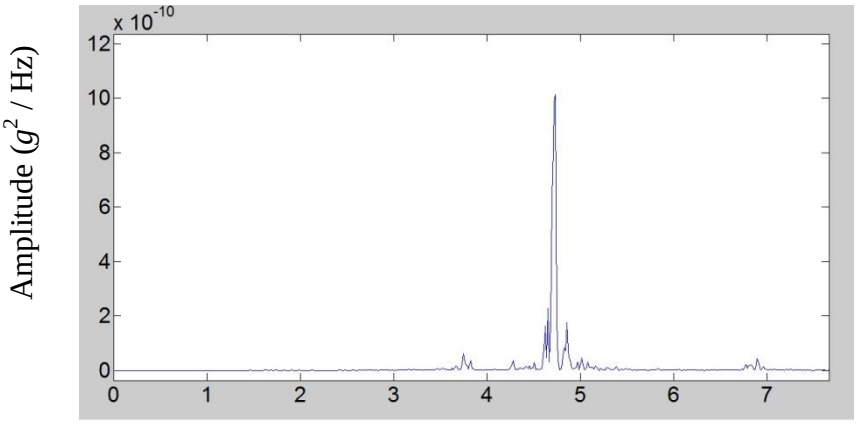


Figure 4.42. Power Spectral Density for Level 5, Location H, E-W Direction.

For Level 5 Location H, the acceleration response in the North-South direction is dominated by the second mode of vibration. At this location, the first, second and third-mode natural frequencies can all be identified, as 4.7 Hz, 5.2 Hz and 6.9 Hz, respectively (Figure 4.43).

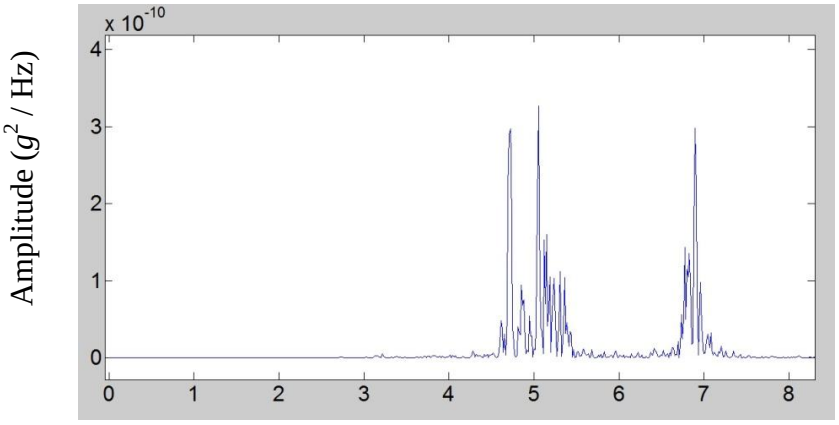


Figure 4.43. Power Spectral Density for Level 5, Location H, N-S Direction.

For Level 4 Location H, the acceleration response in the East-West direction is dominated by the first mode of vibration. Here, only the first natural frequency can be identified, as 4.7 Hz (Figure 4.44).

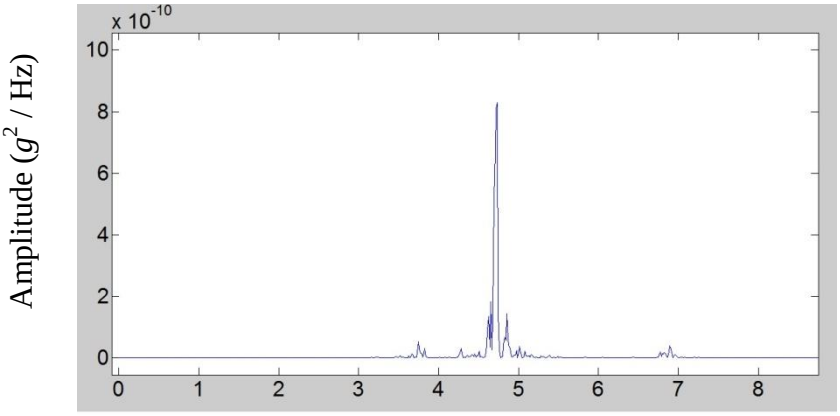


Figure 4.44. Power Spectral Density for Level 4, Location H, E-W Direction.

For Level 4 Location H, the acceleration response in the North-South direction is dominated by the second mode of vibration. Again, the first, second and third-mode natural frequencies can be identified at this location, as 4.7 Hz, 5.2 Hz and 6.9 Hz, respectively (Figure 4.45).

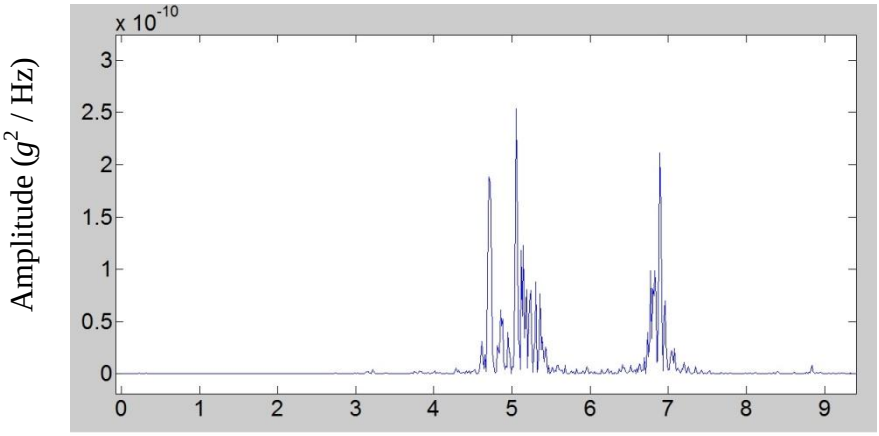


Figure 4.45. Power Spectral Density for Level 4, Location H, N-S Direction.

Results presented in Figure 4.30-45 show that the natural frequencies of the building for the first, second and third modes of vibration are 4.7 Hz, 5.2 Hz, and 6.9 Hz, respectively. The first mode of vibration is in the diagonal North-West – South-East direction of the building, the second mode is in the diagonal North-East – South-West direction, and the third mode is torsional. The East-West and North-South amplitudes of the first and second modes of vibration are very close to each other, indicating that these modes are in a diagonal direction. The phase signs of the locations A and H are different at the third mode; therefore, this mode of vibration is torsional. In order to determine the modal directions of vibration, the acceleration data at locations A and H on Levels 4 and 5 was processed (Figure 4.46, 4.47 and 4.48). The directions of vibrational motion were obtained from the phase signs of the modes of the spectra generated for the acceleration data (Table 4.2). The modal frequencies obtained from the data recorded at these locations are also 4.7 Hz, 5.2 Hz, and 6.9 Hz, and the phase signs of the data are listed in Table 4.2.

Table 4.2. The Natural Frequencies and Phase Signs of the Spectra Obtained from Sensors at Locations H and A on Level 4 and 5.

| Modal Freq. (Hz) | Locations | | | | | | | |
|---|---|---|---|---|---|---|---|---|
| | 5H | | 5A | | 4H | | 4A | |
| | X | Y | X | Y | X | Y | X | Y |
| 4.7 | - | + | - | + | - | + | - | + |
| 5.2 | + | + | + | + | + | + | + | + |
| 6.9 | + | - | - | + | + | - | - | + |

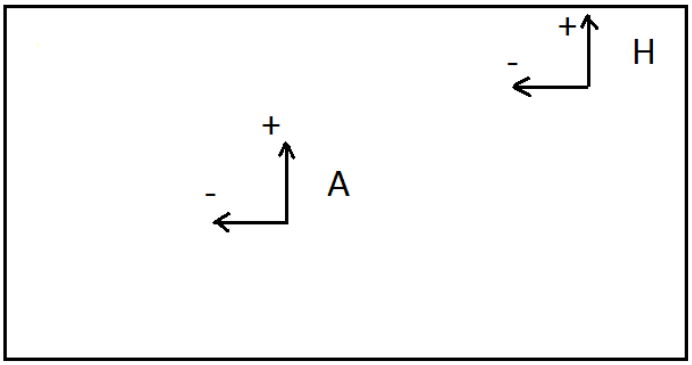


Figure 4.46. First Mode Phase Signs at Sensor Locations A and H on Level 4 and 5.

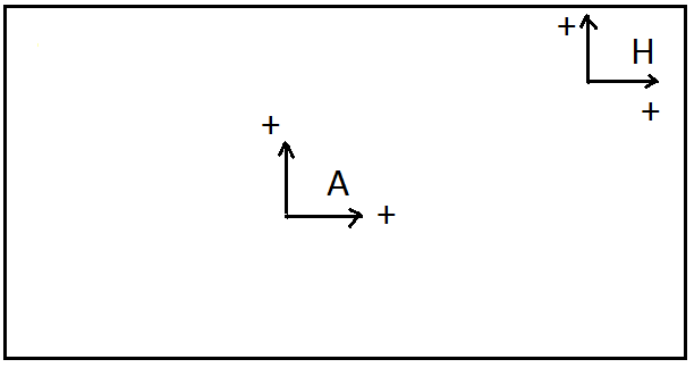


Figure 4.47. Second Mode Phase Signs at Sensor Locations A and H on Level 4 and 5.

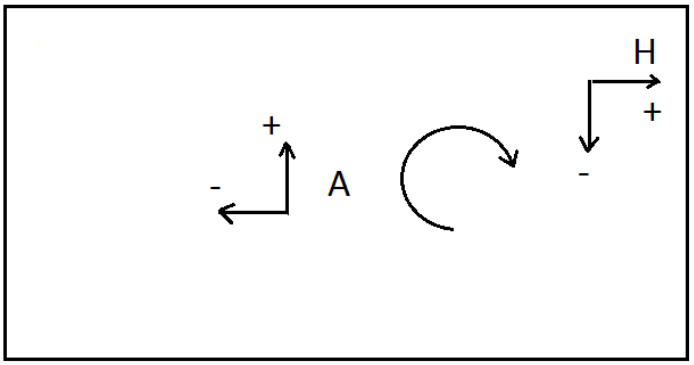


Figure 4.48. Third Mode Phase Signs at Sensor Locations A and H on Level 4 and 5.

Accordingly, the mode shapes obtained for the first two modes of vibration are shown in Figure 4.49 and 4.50. The mode shapes were obtained based on the relative amplitudes corresponding to the first three natural frequencies on the amplitude spectra of the acceleration records (Figure 4.30-45) at sensor location A, on all seven floors of the

building (Figure 4.1 and 4.2). The third mode shape could not be determined due to the fact that the amplitudes (power spectral densities) of the North-South and East-West acceleration records at location A of the levels were too small, since the third mode of vibration of the building was torsional, with rotations about the centroid of the building plan, which approximately coincides with sensor location A.

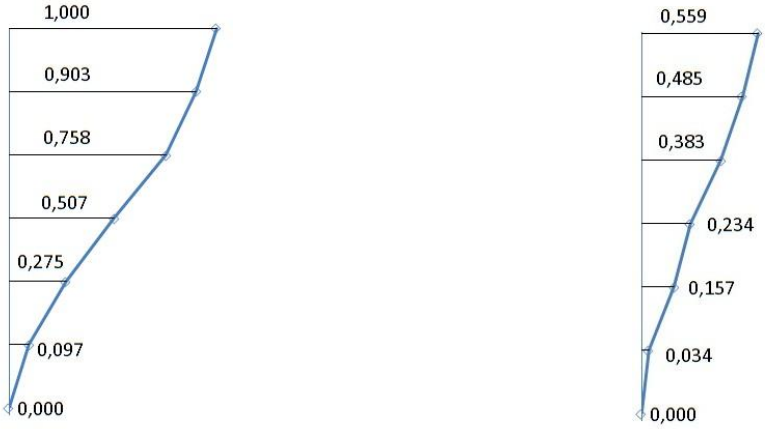


(a) (b)

Figure 4.49. First Mode Shape Amplitudes After Strengthening: (a) E-W Direction, (b) N-S Direction.

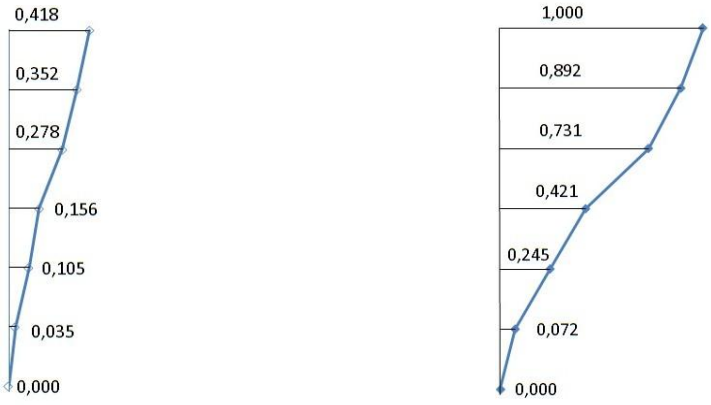


(a) (b)

Figure 4.50. Second Mode Shape Amplitudes After Strengthening: (a) E-W Direction, (b) N-S Direction.

## 4.3. Forced Vibration Test

A forced vibration test was conducted in December 2010 on the strengthened configuration of the building. An eccentric mass shaker (Figure 4.51) was used to excite the strengthened structure with harmonic forces. The shaker was anchored on the Level 2 slab, at location B on the floor plan (Figure 4.1 and 4.2). The eccentric mass shaker comprises a welded steel frame bolted to a steel-base, four main bearings, two main shafts, and six attached steel weights. The total weight is approximately 350 kg. The weights counter-rotate about the horizontal shafts to impart a unidirectional force in a horizontal or vertical plane to the test structure in proportion to its eccentricity and rotating speed squared. Eccentricity of the vibrator can be varied between zero and 100% in several increments. Maximum force output is limited to 88 kN. The shaker has an operating frequency range of 1-25 Hz with the eccentricity of 18.5 kg-m driven by a 7 HP motor. Table 4.3 lists the harmonic force amplitudes exerted by the shaker at various frequencies and eccentricities. During the forced vibration testing, the sensors were located on the 1st, 2nd, 3rd and 4th levels of the building (Figure 4.2), at locations B, D, F and H of the floor plan, as illustrated in Figure 4.52-54.

Figure 4.51. Eccentric Mass Shaker.

Table 4.3. Force Levels Exerted by the Shaker at Various Frequencies and Eccentricities.

| Eccentricity (%) | Frequency (Hz) | Force (kN) |
|---|---|---|
| 25 | 4.5 | 3.70 |
| 50 | 4.5 | 7.39 |
| 75 | 4.5 | 11.1 |
| 25 | 6.5 | 7.71 |
| 50 | 6.5 | 15.4 |
| 75 | 6.5 | 23.1 |

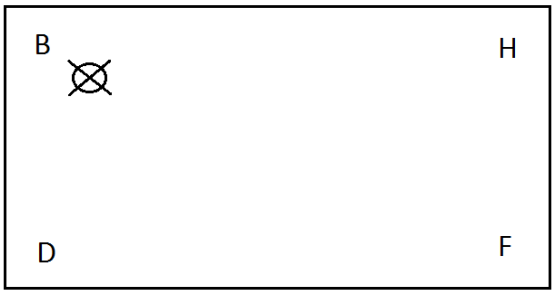


Figure 4.52. Sensor Locations on Levels 1 and 3.


Figure 4.53. Sensor Locations on Level 2.

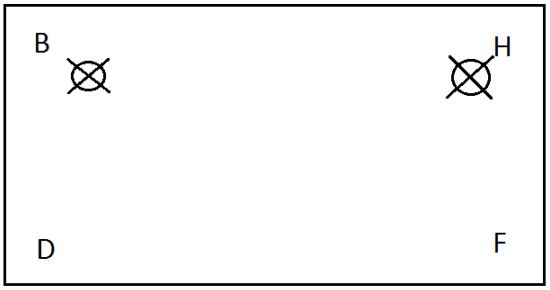


Figure 4.54. Sensor Locations on Level 4.

The shaker was operated at several frequencies and eccentricities, and acceleration data from the sensors were recorded. A frequency response function was defined, for which the amplitudes for each frequency were calculated using the recorded steady-state acceleration data obtained from the sensor at location B on Level 3 (Figure 4.52). For calculating the amplitudes, the recorded acceleration values were divided with the squared value of shaker operation frequencies. The frequency response functions generated in this manner are shown in Figure 4.55, 4.56, 4.57, and 4.58. The modal frequencies were obtained from these frequency response functions, using the peak-picking method.

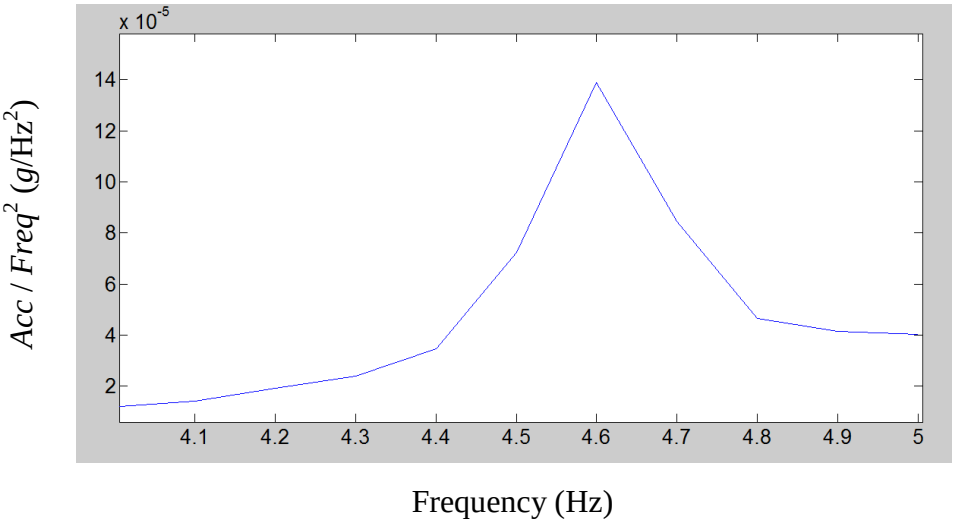


Figure 4.55. Frequency Response Function in East-West Direction for 25% Shaker Eccentricity.

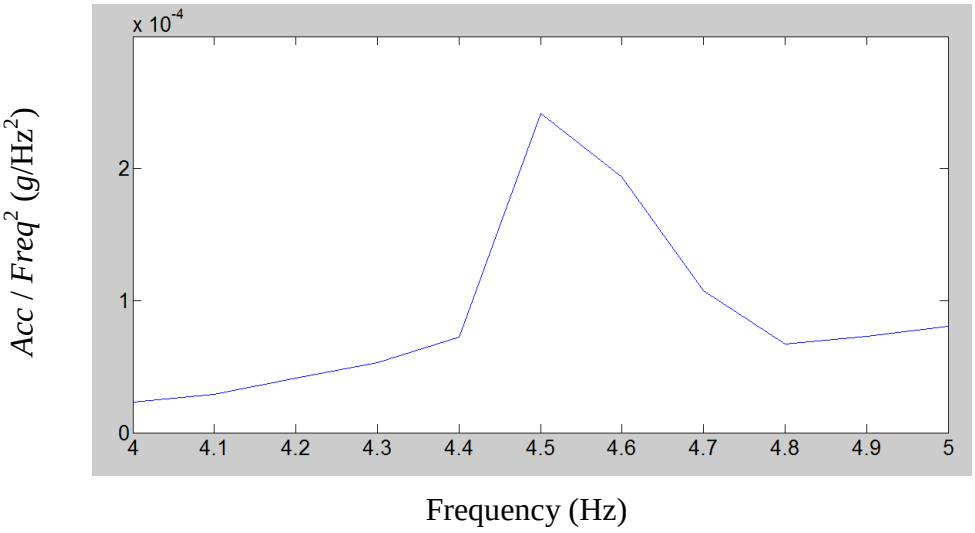


Figure 4.56. Frequency Response Function in East-West Direction for 50% Shaker Eccentricity.

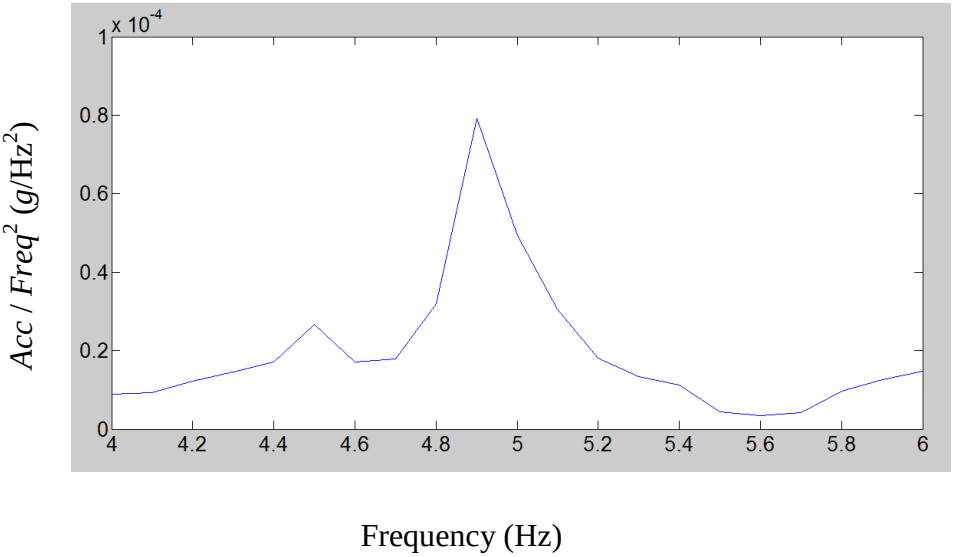


Figure 4.57. Frequency Response Function in North-South Direction for 25% Shaker Eccentricity.

To obtain the frequency response amplitudes presented in Figure 4.55, the shaker was operated at 25% eccentricity, with frequencies gradually increasing from 4 Hz to 5 Hz, applying harmonic forces in the East – West direction. The shaker was also operated in the East-West direction at 50% eccentricity (Figure 4.56). In order to excite the structure in the

North-South direction, the shaker was operated at 25% (Figure 4.57) and 75% (Figure 4.58) and eccentricities, with frequencies increasing gradually from 4 Hz to 6 Hz.

Modal frequencies were identified from these frequency response functions, using the peak-picking method. The first-mode natural frequency of the building (under excitation in the East-West direction) was obtained as 4.6 Hz when the shaker was operated at 25% eccentricity (Figure 4.55), and 4.5 Hz when the shaker was operated at 50% eccentricity (Figure 4.56). The building's second-mode natural frequency (under excitation in the North-South direction) was obtained as 4.9 Hz when the shaker was operated at 25% eccentricity (Figure 4.57), and 4.8 Hz when it was operated at 75% eccentricity (Figure 4.58). The slight differences between the identified natural frequencies demonstrate the sensitivity of the modal frequencies of the building, to the amplitude of the applied harmonic excitation force. Results presented in Figure 4.55-58 also confirm that the amplitudes of the frequency response functions (indicating the acceleration levels on the building) increase, with increasing shaker eccentricity (harmonic force amplitude), as expected.

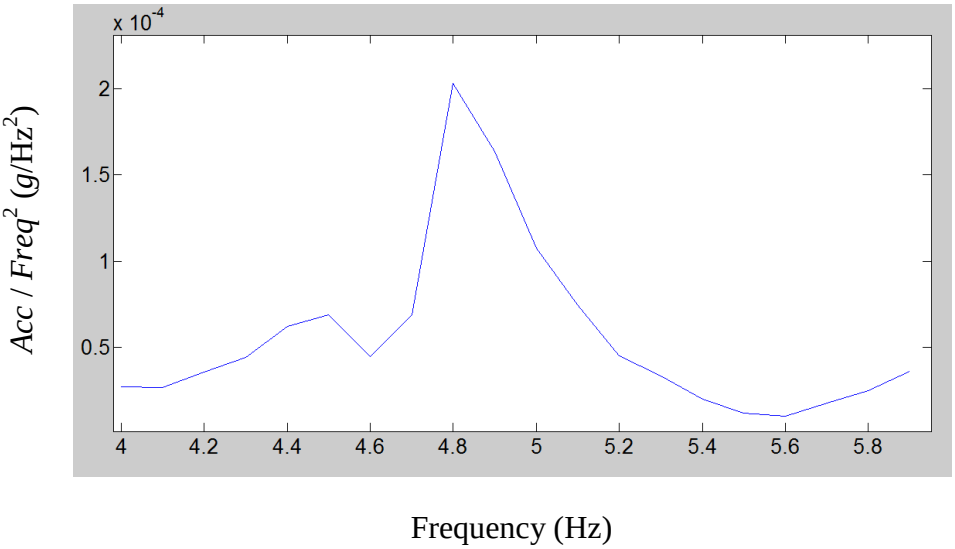


Figure 4.58. Frequency Response Function in North-South Direction for 75% Shaker Eccentricity.

# 5. FINITE ELEMENT MODEL OF THE BUILDING

The building was modeled using the structural analysis software SAP2000, in both the original and strengthened configurations (Figure 5.1 and 5.5). The purpose of creating a finite element model of the building was to demonstrate a simple model updating procedure, as well as to compare the vibration test results (natural frequencies and mode shapes) with those obtained using the finite element model. The Finite Element Models (FEM) of the building incorporated the dimensions of structural members before and after strengthening. Table 3.1 lists the cross-sectional dimensions of the columns and structural walls in the building before and after strengthening, whereas the locations of the jacketed columns and additional structural walls on the building floor plan are shown in Figure 3.6.

Structural walls and floor slabs in the FEM were modeled using shell elements, whereas line elements were used for the beams and columns. The primary motivation behind using shell elements for the floor slabs was to define the mass of the slabs in a distributed manner. In the FEM, a slab thickness of 120 mm was specified (Figure 5.1), representing the thickness of the reinforced concrete slab in the actual building. The contribution of the one-way and two-way joists on the mass and stiffness of the floor slabs were considered in the analysis, by assigning beam elements to model the joist members. The main beams spanning between the columns were modelled using line elements with rectangular cross-sections, with the dimensions obtained from the structural drawings of the building. 1100 mm wide and 400 mm deep shallow beams were assigned on levels 3, 4, and 5 of the building, whereas 300 mm wide and 700 mm deep beams were defined at levels 0, 1, and 2. The contribution of the slab on the flexural stiffness of the main beams were represented via a very simple model updating procedure, via assigning a multiplier on the moment of inertia of the beams, as described in the following section. The beams and columns of the building were rigidly connected. Rigid diaphragm constraints were also assigned to slab elements on all floor levels, in order to simplify the analysis. Walls and columns were assumed to be restrained at the foundation level with full fixity. This assumption neglects the effects of soil-structure interaction (SSI) on the vibration characteristics of the building. However, for low-amplitude vibrations, SSI effects are likely to be negligible.

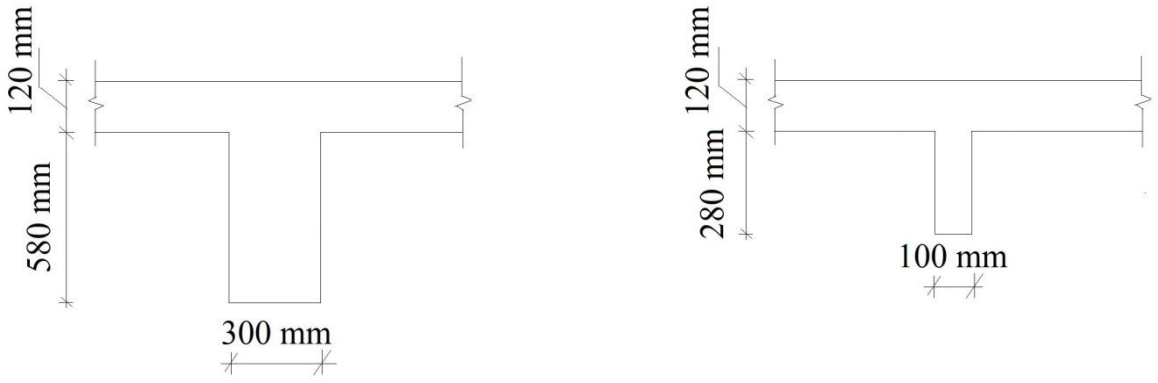


(a) (b)

Figure 5.1. Dimensions of Slab and Joists (a) One-Way Joist, (b) Two-Way Joist.

Peripheral walls at basement levels of the strengthened building were included in the FEM. Increase in the flexural stiffness of the beams due contribution of the floor slab was also considered in the model, using moment of inertia multipliers (effective stiffness multipliers) for the beams, during the process of model updating. Cracking of the structural members was ignored in the analysis, due to low-amplitude excitation. Two elastic modulus values of 28,000 MPa and 35,000 MPa was used for the structural members, during consecutive analyses, as described in the following section. For the jacketed columns, a single value of concrete elastic modulus was used in the FEM for simplicity, although the concrete grades for the original column and the column jacket were most likely, different.

The brick-infill partition walls in the building were conventionally modeled as diagonal elements (struts) connected to the structural frame at beam-column joints. The widths of the diagonal struts were calibrated using the well known empirical relationships developed by Mainstone [42]. Stiffness reduction factors by Asteris [43] were implemented to consider window and door openings in the partition walls.

The mass of the structural components of the building were taken into account in a distributed manner, via assigning unit weights for the materials. A unit weight of 25 kN/m$^3$ was used for the reinforced concrete structural members (beams, columns, walls, and floor slabs). The mass of infill walls, as well as plaster, floor covering, and roof superstructure were neglected in the analysis. It must be emphasized that the main objectives of the FEM were to verify the basic modeling assumptions, to demonstrate a simple model updating

procedure, and to illustrate the level of consistency among the test results and the results of a “baseline” FE model, which may be improved via further model updating. Detailed updating and evaluation of the FE model results are not within the scope of this study.

## 5.1. Finite Element Model Updating Procedure

In order to improve the correlation between the vibration test results and results of the FEM, a simple model updating procedure was adopted. For model updating, two fundamental parameters were selected, the first of which is the modulus of elasticity of concrete, and the second of which is the multiplier (amplification factor) to be applied on the moment of inertia of the beams, for considering the contribution of the floor slab of the beam flexural stiffness.

Two values were selected for concrete elastic modulus: 28000 MPa and 35000 MPa. The value of 35000 MPa was based on compression tests on concrete cylinder specimens from the strengthened building, which yielded an average compressive strength value of approximately 49 MPa. Sensitivity of the modal analysis results (modal frequencies obtained using the FEM) to the elasticity modulus value is shown in Table 5.1, 5.2, and 5.3. As explained in a later section, the analysis results were closer to the vibration test results when a value of 35000 MPa was used for all structural members of the building, in both the original and strengthened configurations.

For the multiplier (amplification factor) of the moment of inertia of the beams, two values were selected: 1.0 and 2.0. The value 1.0 approximately represents zero contribution from the floor slab to the flexural stiffness of the beams, whereas a value of 2.0 simply assumes that the slab stiffens the beams twofold, under flexure. Although in the FEM, shell elements were used for modeling of the floor slabs, the slabs do not significantly contribute to beam flexural stiffness, since they are connected to the beams at the beam geometric centroid; wheras in reality, the slabs are connected to the beams at the top of the beam cross-sections. Sensitivity of the modal analysis results (modal frequencies obtained using the FEM) to the beam stiffness multiplier is shown in Table 5.4, 5.5, and 5.6. As presented in the relevant section, the analysis results were closer to the vibration test results when a stiffness multiplier of 2.0 is used, in both the original and strengthened configurations of

the building. Therefore, in all future analysis results, the updated values of 35000 MPa and 2.0 were used for the modulus of elasticity and beam stiffness multiplier parameters, respectively.

Table 5.1. Variation in Modal Frequencies Depending on the Selected Elasticity Modulus of Concrete (After Strengthening).

| (Mpa) | (Hz) | | |
|---|---|---|---|
| Elasticity Modulus of Concrete | $f_1$ | $f_2$ | $f_3$ |
| 28000 | 4.0 | 4.2 | 6.3 |
| 35000 | 4.4 | 4.6 | 7.0 |
| | Increase Rate | | |
| | 10% | 10% | 11% |
| Multiplier on Moment Inertia of Beams = 2 | | | |

Table 5.2. Variation in Modal Frequencies Depending on the Selected Elasticity Modulus of Concrete (Before Strengthening, No Infill Walls).

| (Mpa) | (Hz) | | |
|---|---|---|---|
| Elasticity Modulus of Concrete | $f_1$ | $f_2$ | $f_3$ |
| 28000 | 1.8 | 2.3 | 3.7 |
| 35000 | 2.0 | 2.5 | 4.2 |
| | Increase Rate | | |
| | 11% | 9% | 14% |
| Multiplier on Moment Inertia of Beams = 2 | | | |

Table 5.3. Variation of Modal Frequencies Depending on the Selected Elasticity Modulus of Concrete (Before Strengthening, with Infill Walls).

| (Mpa) | (Hz) | | |
|---|---|---|---|
| Elasticity Modulus of Concrete | $f_1$ | $f_2$ | $f_3$ |
| 28000 | 2.2 | 2.6 | 4.2 |
| 35000 | 2.4 | 2.9 | 4.6 |
| | Increase Rate | | |
| | 9% | 12% | 10% |
| Multiplier on Moment Inertia of Beams = 2 | | | |

Table 5.4. Variation in Modal Frequencies Depending on the Selected Multiplier on the Moment of Inertia of Beams (After Strengthening).

| Multiplier on Moment Inertia of Beams | (Hz) | | |
|---|---|---|---|
| | $f_1$ | $f_2$ | $f_3$ |
| 1 | 4.1 | 4.4 | 6.9 |
| 2 | 4.4 | 4.6 | 7.0 |
| | Increase Rate | | |
| | 7% | 5% | 1% |
| $E_c$ = 35000 Mpa | | | |

Table 5.5. Variation in Modal Frequencies Depending on the Selected Multiplier on the Moment of Inertia of Beams (Before Strengthening, No Infill Walls).

| Multiplier on Moment Inertia of Beams | (Hz) | | |
|---|---|---|---|
| | $f_1$ | $f_2$ | $f_3$ |
| 1 | 1.7 | 2.3 | 4.0 |
| 2 | 2.0 | 2.5 | 4.2 |
| | Increase Rate | | |
| | 18% | 9% | 5% |
| $E_c$ = 35000 Mpa | | | |

Table 5.6. Variation in Modal Frequencies Depending on the Selected Multiplier on the Moment of Inertia of Beams (Before Strengthening, with Infill Walls).

| Multiplier on Moment Inertia of Beams | (Hz) | | |
|---|---|---|---|
| | $f_1$ | $f_2$ | $f_3$ |
| 1 | 2.1 | 2.7 | 4.4 |
| 2 | 2.4 | 2.9 | 4.6 |
| | Increase Rate | | |
| | 14% | 7% | 5% |
| $E_c$ = 35000 Mpa | | | |

## 5.2. FEM Results for the Unstrengthened Building

The FEM of the building in the unstrengthened configuration was created considering the original dimension of the structural members (Table 3.1). The additional structural walls, additional basement walls, and column jackets were not included in this model (Figure 5.2). Brick-infill walls were also not included, since these walls were already demolished during ambient vibration testing of the building. Modal analysis of the FEM provided values of 2.0 Hz, 2.5 Hz, and 4.2 Hz, respectively, for the first second, and third vibration modes of the building. The analysis results indicated that all three modes of vibration had modal displacement components in both the E-W and the N-S directions of the building.

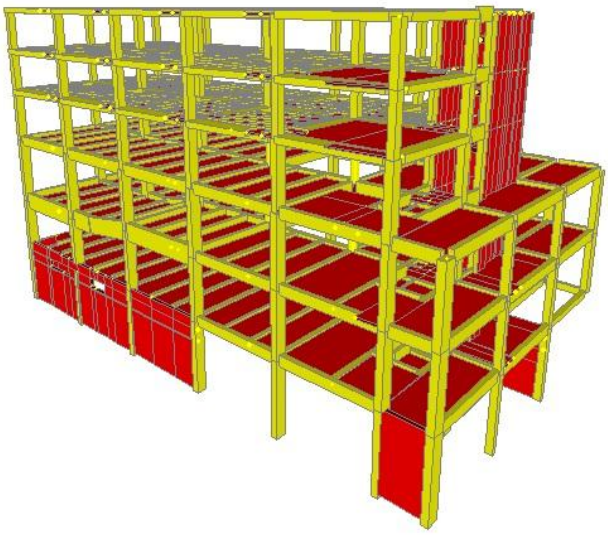

Figure 5.2. Finite Element Model of the Building before Strengthening.

The first three mode shapes obtained using the FEM of the building are as shown in Figure 5.3, 5.4 and 5.5. The mode shapes amplitudes were obtained from the modal displacement components at the geometric centroid of the floor plan, on Levels 0 to 5 of the building, normalized by the maximum amplitude (in either E-W or N-S direction) of modal displacement.

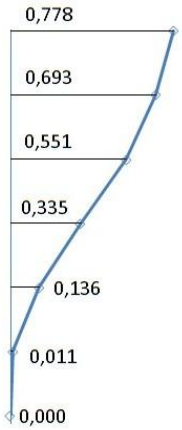


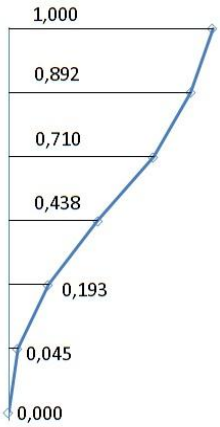


(a) (b)

Figure 5.3. 1. Mode Shapes Before Retrofit - (a) E-W Direction (b) N-S Direction.

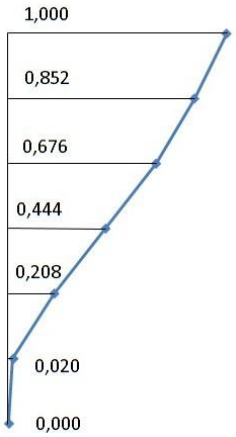


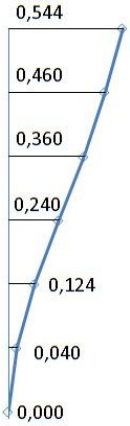


(a) (b)

Figure 5.4. 2. Mode Shapes Before Retrofit - (a) E-W Direction (b) N-S Direction.

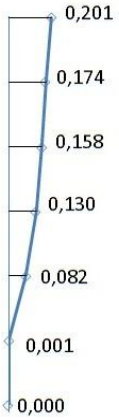


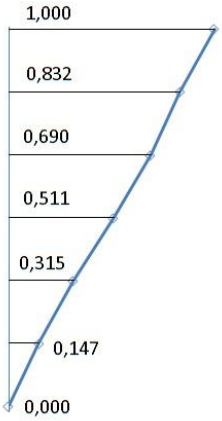


(a) (b)

Figure 5.5. 3. Mode Shapes Before Retrofit - (a) E-W Direction (b) N-S Direction.

## 5.3. FEM Results for the Strengthened Building

The FEM of the strengthened building was created considering the structural dimensions in the strengthened configuration (Table 3.1). The additional structural walls, additional basement walls, and column jackets were considered in this model (Figure 5.6). Brick-infill walls were also included, since these walls were present during the vibration tests conducted on the strengthened configuration of the building. Modal analysis of the FEM provided values of 4.4 Hz, 4.6 Hz, and 7.0 Hz, respectively, for the first second, and third vibration modes of the building. The analysis results indicated that the first mode of vibration was predominantly in the E-W direction, the second mode was predominantly in the N-S direction, and the third mode was a torsional mode about the geometric centroid of the floor plan.

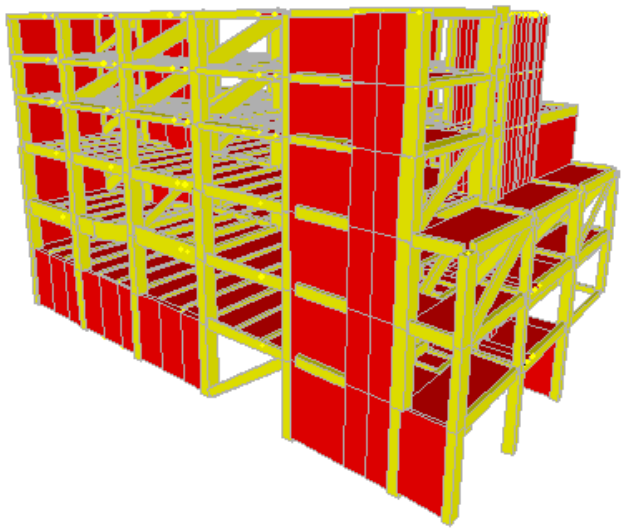

Figure 5.6. Finite Element Model of the Strengthened Building, with Brick Infill Walls.

The first three mode shapes obtained using the FEM of the building are as shown in Figure 5.7, 5.8 and 5.9. The mode shapes amplitudes were obtained from the modal displacement components at the geometric centroid of the floor plan, on Levels 0 to 5 of the building, normalized by the maximum amplitude (in either E-W or N-S direction) of modal displacement.

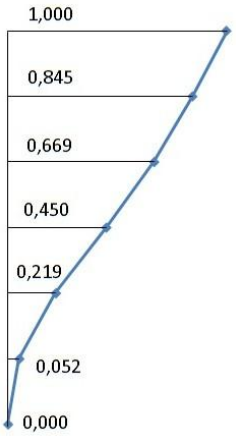



(a) (b)

Figure 5.7. 1. Mode Shapes After Retrofit - (a) E-W Direction (b) N-S Direction.


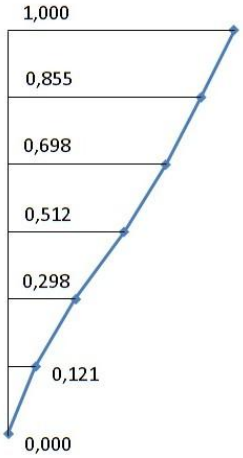


(a) (b)

Figure 5.8. 2. Mode Shapes After Retrofit - (a) E-W Direction (b) N-S Direction.

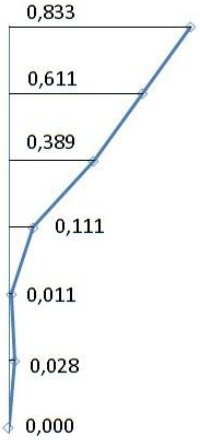


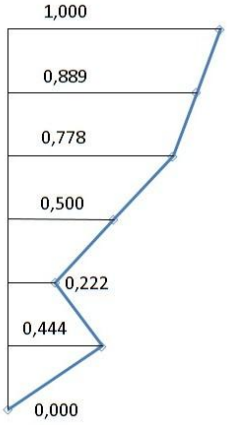


(a) (b)

Figure 5.9. 3. Mode Shapes After Retrofit - (a) E-W Direction (b) N-S Direction.

## 5.4. Modelling of Brick Infill Walls

The brick-infill partition walls in the building were conventionally modeled as diagonal elements (struts) connected to the structural frame at beam-column joints (Figure 5.10). The widths of the diagonal struts were calibrated using the well known empirical relationships developed by Mainstone [42]. Stiffness reduction factors by Asteris [43] were implemented to consider window and door openings in the infill walls. The diagonal struts were pin-connected to the beam-column joints with moment releases, and the material properties of the of the struts were calibrated to represent the stiffness of the brick infill material.

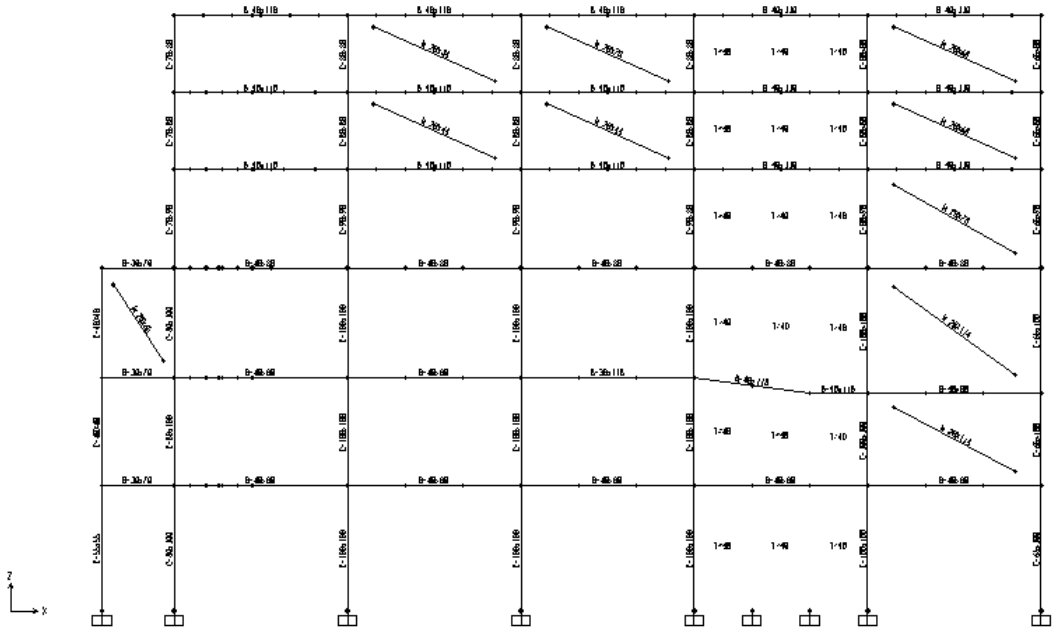

Figure 5.10. The One – Direction Diagonal Struts in the Finite Element Model.

For calculating the density of the plastered infill wall, the weight of one brick and the total number of 25 bricks per square meter was taken into account, together with estimated widths for mortar between the bricks and plaster on the wall. The dimensions of a single hollow clay tile brick was taken as 13.5 cm x 18 cm x 18.5 cm (25 bricks occupied a wall surface area of 95 cm x 97.5 cm); whereas the mass of a single brick was specified as 2.84 kg. The width of the mortar between the bricks was assumed to be 1.0 cm, and the total thickness of plaster was assumed to be 5.0 cm. By dividing the total mass of 25 bricks,

mortar, and plaster with their total volume, the average density of the infill wall was calculated as 1123 kg/m$^3$. The elasticity modulus for the infill wall material was selected as 5750 MPa [44-46].

The effective width of the infill wall, *w*, was calculated using the method recommended by Mainstone and Weeks [3] and Mainstone [42]. The thickness of the strut is equal to the thickness of the infill wall. Estimation of the effective width, *w*, of the strut follows Equation 5.1. The effective width depends on the parameter $\lambda_1$, defined in Equation 5.2, the effective height of the columns, and the diagonal length of the strut.

$$w = 0.175(\lambda_1 h_{col})^{-0.4} r_{inf} \tag{5.1}$$

$$\lambda_1 = \left[\frac{E_{me} t_{inf} sin2\theta}{4E_{fe} I_{col} h_{inf}}\right]^{\frac{1}{4}} \tag{5.2}$$

$$\theta = tan^{-1}\left(\frac{h_{inf}}{L_{inf}}\right) \tag{5.3}$$

In the equations above, $E_{me}$ is the elastic modulus of the infill wall, $E_{fe}$ is the elastic modulus of the concrete in the frame, $r_{inf}$ is the length of the strut, $h_{inf}$ is the clear height of the infill wall, $L_{inf}$ is the clear length of the infill wall, $I_{col}$ is the moment of inertia of the columns, $h_{col}$ is the height of the columns between the centerlines of the beams, *l* is the length of the beam between centrelines of columns, $t_{inf}$ is the thickness of infill wall, and $\theta$ is the sloping angle of the infill diagonal with respect to the horizontal (Figure 5.11).

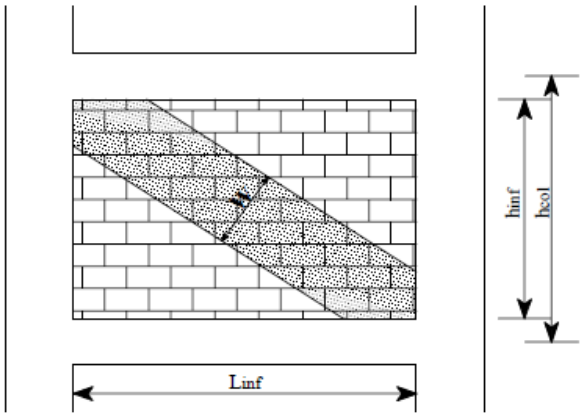


Figure 5.11. The Equivalent Diagonal Strut [47].

It must be mentioned that openings, such as door and window openings cause the stiffness of the infill walls to decrease. The empirical stiffness reduction factor proposed by Asteris [43] was implemented in the model to consider presence of window and door openings in the infill walls. The reduction factor ($\lambda_{graphical}$) is defined by Asteris in graphical form, as depicted in Figure 5.12. The reduction factor considers the opening area ratio, as well as the location of the opening on the infill wall. There are other studies available in the literature which also consider the aspect ratio of the openings on the infill wall stiffness; however, the relationships by Mainstone, together with the stiffness reduction factors by Asteris are well-known and widely used.

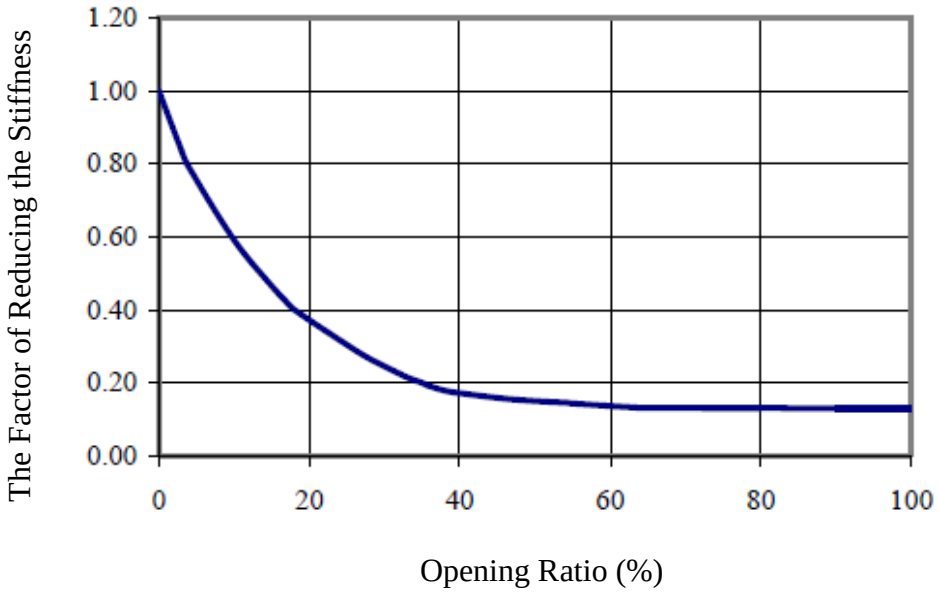


Figure 5.12. Opening Area Ratio versus Stiffness Reduction Factor ($\lambda_{graphical}$) [47].

The stiffness reduction factor ($\lambda_{graphical}$) is used in Equation 5.4, to obtain the effective width of the diagonal strut for infill walls with openings [47].

$$w = 0.175\lambda_{graphical}(\lambda_1 h_{col})^{-0.4} r_{inf} \tag{5.4}$$

Modal analysis results obtained using the FEM with and without brick infill walls, for the unstrengthened and strengthened configurations of the building, are presented in Table 5.7 and 5.8. The analysis results indicate that consideration of the brick infill walls in the FEM of the building can influence the prediction of the modal frequencies, by as much as 16%, for the building in the unstrengthened configuration. As presented in the following section, the analysis results are closer to the vibration test results when brick infill walls are included in the FEM of the strengthened building.

Table 5.7. Modal Frequencies Predicted by the Finite Element Model before Strengthening with and without Brick Infill Walls.

| Natural Frequencies | Without Infill Walls (Hz) | With Infill Walls (Hz) | Influence of Infill Walls (% Increase) |
|---|---|---|---|
| $f_1$ | 2.0 | 2.3 | 15% |
| $f_2$ | 2.5 | 2.9 | 16% |
| $f_3$ | 4.2 | 4.6 | 10% |

Table 5.8. Modal Frequencies Predicted by the Finite Element Model after Strengthening with and without Brick Infill Walls.

| Natural Frequencies | Without Infill Walls (Hz) | With Infill Walls (Hz) | Influence of Infill Walls (% Increase) |
|---|---|---|---|
| $f_1$ | 4.2 | 4.4 | 5% |
| $f_2$ | 4.5 | 4.6 | 2% |
| $f_3$ | 7.0 | 7.0 | 0% |

## 5.5. Comparison of the Test Results with the Finite Element Model

The modal frequencies obtained from the vibration tests, both before and after strengthening of the building, are compared with the frequencies predicted by the FEM of the building, in Table 5.9 and 5.10.

Table 5.9. Comparison of the Modal Frequencies Before and After Strengthening.

| | Vibration Tests | | | | | Finite Element Model (Hz) | | |
|---|---|---|---|---|---|---|---|---|
| | Ambient (Hz) | | | Forced (Hz) | | | | |
| | $f_1$ | $f_2$ | $f_3$ | $f_1$ | $f_2$ | $f_1$ | $f_2$ | $f_3$ |
| Before Strengthening | 2.6 | 3.1 | 3.4 | - | - | 2.0 | 2.5 | 4.2 |
| After Strengthening | 4.7 | 5.2 | 6.9 | 4.6/4.5* | 4.9/4.8** | 4.4 | 4.6 | 7.0 |
| Influence of Strengthening (% Increase) | 81% | 67% | 103% | - | - | 120% | 84% | 67% |

*values obtained for 25% and 50% shaker eccentricities, respectively, in E-W direction.

**values obtained for 25% and 75% shaker eccentricities, respectively, in N-S direction.

Results presented in Table 5.9 clearly indicate that seismic strengthening of the building has significantly influenced (increased) its modal frequencies. This can be observed in both the vibration test results and FEM analysis results, with a reasonable level of consistency. In the case of vibration test results, the largest frequency increase was found to be 103% for the third (torsional) vibration mode, with a corresponding increase of 120% in the FEM analysis results. As well, the vibration test results highlight the dependence of the identified frequency values on the amplitude of the excitation. Results of the ambient and forced vibration tests on the strengthened building indicate that the identified modal frequency values decrease when the structure is excited with an eccentric mass shaker (forced vibration frequencies are smaller than the ambient vibration frequencies), and the frequencies decrease further as the eccentricity of the shaker (therefore the amplitude of the harmonic excitation force) is increased.

Table 5.10. Comparison of Modal Frequencies Obtained from the Vibration Tests and the Finite Element Model.

| | Before Strengthening (Hz) | | | After Strengthening (Hz) | | |
|---|---|---|---|---|---|---|
| | $f_1$ | $f_2$ | $f_3$ | $f_1$ | $f_2$ | $f_3$ |
| Ambient Vibration Test | 2.6 | 3.1 | 3.4 | 4.7 | 5.2 | 6.9 |
| Forced Vibration Test | - | - | - | 4.6/4.5* | 4.9/4.8** | - |
| Finite Element Model | 2.0 | 2.5 | 4.2 | 4.4 | 4.6 | 7.0 |
| Difference between Model and Ambient Test Results (% Difference) | -23% | -19% | 23% | -6% | -11% | 1% |

* values obtained for 25% and 50% shaker eccentricities, respectively, in E-W direction.

**values obtained for 25% and 75% shaker eccentricities, respectively, in N-S direction.

Results presented in Table 5.10 point out that there is a more pronounced difference between the experimentally-identified and analytically-predicted modal frequencies of the building before strengthening, compared to that after strengthening. Before strengthening, the difference between test and analysis results can reach 23%, whereas the maximum difference after strengthening is 11%. The best correlation between the test and analysis results was obtained for the third (torsional) mode of the strengthened building.

The mode shapes identified from the vibration tests, both before and after strengthening of the building, are compared with the those predicted by the FEM of the building, in Figure 5.13 and 5.14. The mode shapes amplitudes were obtained from the modal displacement components at the geometric centroid of the floor plan (Location A), on Levels 0 to 5 of the building, normalized by the maximum amplitude (in either E-W or N-S direction) of modal displacement.

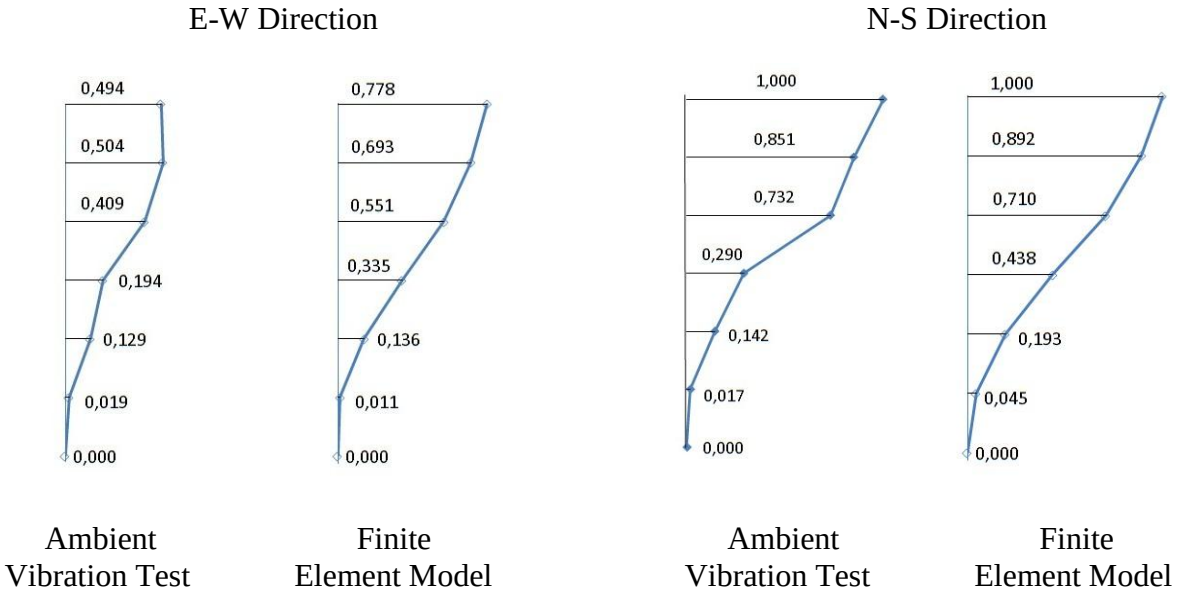


(a) 1. Mode

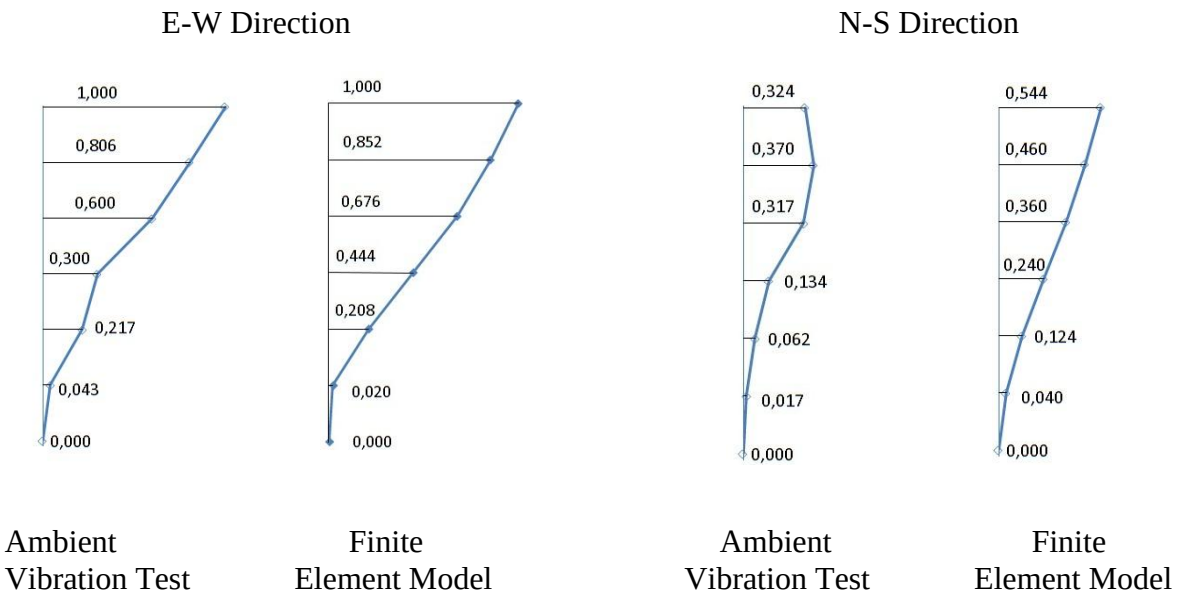


(b) 2. Mode

Figure 5.13. Comparison of Mode Shapes Before Strengthening.

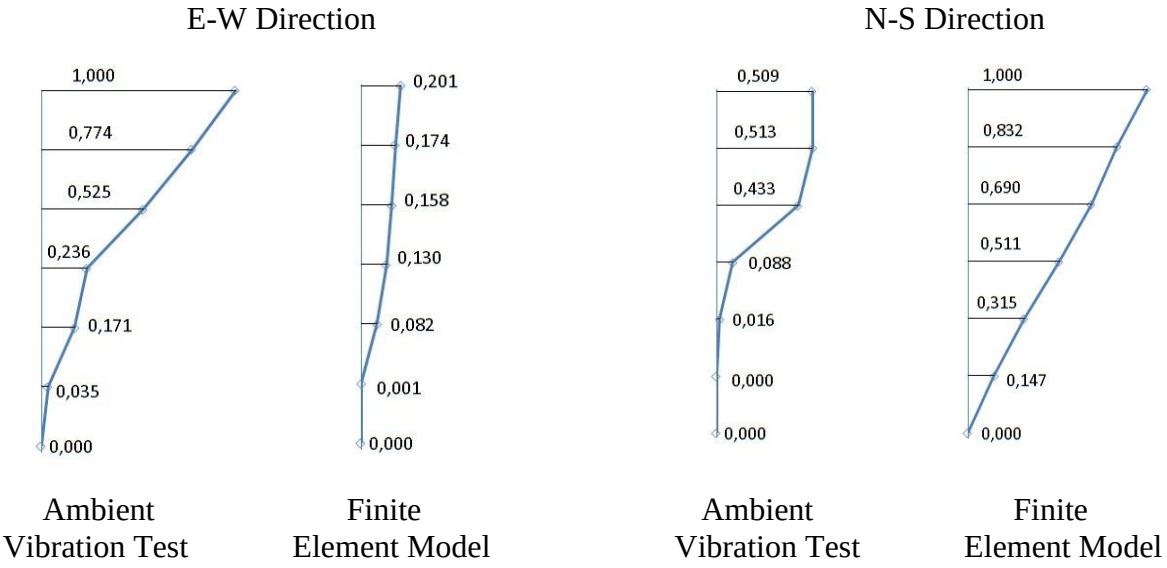


(c) 3. Mode

Figure 5.13. Comparison of Mode Shapes Before Strengthening (cont.).

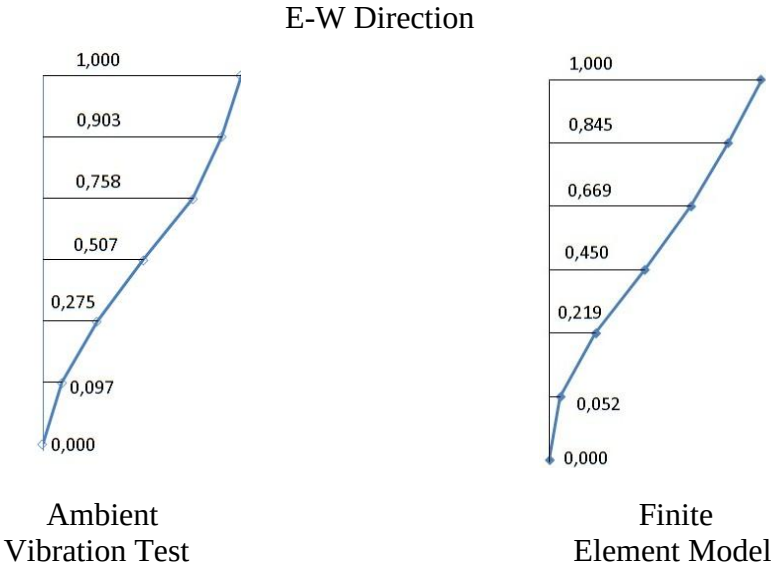


(a) 1. Mode

Figure 5.14. Comparison of Mode Shapes After Strengthening.

N-S Direction

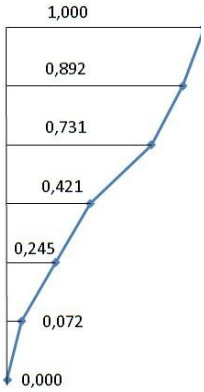


Ambient
Vibration Test

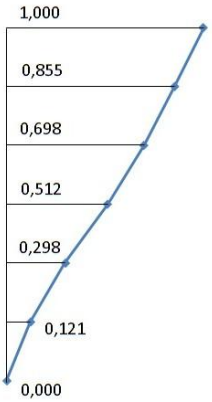


Finite
Element Model

(b) 2. Mode

Figure 5.14. Comparison of the Mode Shapes After Strengthening (cont.).

Overall, the level of agreement between the mode shapes identified from the vibration tests and those predicted by the FEM can be deemed acceptable, especially considering that the FEM of the building is a simple baseline model, on which a detailed model updating procedure has not been applied. In particular, there is significant inconsistency among the third mode shape amplitudes measured during the ambient vibration tests and those predicted by the FEM, for the building in its unstrengthened configuration (Figure 5.13(c)). The North and South facades of the building are in contact with adjacent buildings at levels 0, 1, and 2; where relatively low mode shape amplitudes were identified during the ambient vibration tests, especially in the N-S direction. Since the FEM neglects the contact between the building and adjacent buildings, it fails to reflect the irregular amplification in the identified mode shape amplitudes at levels 3, 4, and 5. However, the mode shapes identified during testing of the strengthened building are more regular (Figure 14), possibly since the increased lateral stiffness of the building diminishes the influence of the contact conditions on the mode shapes. In this case, the mode shape amplitudes predicted by the FEM are in better agreement with those identified for the strengthened building.

# 6. CONCLUSIONS

In this study, the effects of seismic strengthening on the modal characteristics of a six-story reinforced concrete building (the Educational Technologies Building Block B) located in Bogazici University North Campus in Istanbul, was investigated. The building was strenghthened via jacketing of columns, addition of structural walls, and construction of a mat foundation. Ambient vibration tests were conducted before and after the strengthening application. The ambient vibration test results were complemented with data from forced vibration tests, which were performed using an eccentric mass shaker, after strengthening was completed. As well, a linear elastic finite element model of the building was generated, for comparison of the modal parameters obtained from system identification with those predicted by the model. The finite element model results allowed investigating the influence of brick infills on the modal frequencies of the building. The following conclusions can be drawn from the study:

(i) Results of the ambient vibration tests on the conducted on the building before and after seismic strengthening indicated that strengthening of the building has significantly influenced its modal frequencies. Upon strengthening, an average of approximately 85% increase was observed in the modal frequencies of the building. Measurements such as these may be used to assess and verify the effectiveness of seismic strengthening; and to calibrate finite element models with which more accurate predictions of seismic demand on the retrofitted structure can be made.

(ii) Ambient and forced vibration test results pointed out the dependence of the identified frequency values on the amplitude of the excitation. Comparison of results of the ambient and forced vibration tests on the strengthened building highlighted that the identified modal frequency values decreased (by approximately 5%), when the structure was excited with an eccentric mass shaker (at harmonic force amplitudes of approximately 5 kN), and the modal frequencies decreased further (by approximately 2%) as the amplitude of the harmonic force applied by the shaker was doubled or tripled.

(iii) Upon a simple finite element model updating procedure (via calibration of the elasticity modulus for concrete and the flexural stiffness multiplier for the beams) an acceptable level of agreement was achieved between the modal frequencies identified from the vibration tests and those predicted by the finite element model of the building. The level of consistency between the identified and and predicted mode shapes of the building was also reasonable, especially for the strengthened configuration of the building. There was a more pronounced difference between the experimentally-identified and analytically-predicted modal frequencies of the building before strengthening, compared to that after strengthening. Before strengthening, the difference between test and analysis results reached 25%, whereas the maximum difference after strengthening did not exceed 11%. This is not unexpected, since there exists a higher level of uncertainty in the modeling parameters of the building, in its original configuration. The material properties and structural dimensions of the strengthened configuration of the building incorporates less uncertainty, due to better construction quality. More detailed model updating procedures can be applied on the Finite Element Model, for obtaining better estimates of modal characteristics of the building. In this process, the effective stiffness of structural elements may be systematically varied, soil springs may be added to the model to consider soil structure interaction effects, and alternative fixity (contact) conditions between the building and adjacent buildings may be considered.

(iv) Modal analysis results obtained using the finite element model of the building with and without brick infill walls, for both the unstrengthened and strengthened configurations of the building, indicated that consideration of the brick infill walls in the finite element model can influence the prediction of the modal frequencies, by as much as 16%. The analysis results were closer to the vibration test results when brick infill walls are included in the finite element model of the strengthened building.

# REFERENCES


1. Pintelon, R. and J. Schoukens, *System Identification: A Frequency Domain Approach,* The Institute of Electrical and Electronics Engineers, Inc., New York, 2001.

2. Polyakov, S. V., "On the Interaction between Masonry Filler Walls and Enclosing Frame When Loaded in the Plane of the Wall", *Earthquake Engineering Research Institute, Oakland*, pp. 36-42, 1960.

3. Mainstone, R. J. and G. A. Weeks, "The Influence of Bounding Frame on the Racking Stiffness and Strength of Brick Walls", *2nd International Brick Masonry Conference,* Watford, England, 1970.

4. Charles, R. F. And K. Worden, "An Introduction to Structural Health Monitoring", *Philosophical Transactions Royal Society A*, Vol. 365, No. 1851, pp. 303-315, 2006.

5. Nishimura, I., "The Application of Structural Health Monitoring for Improving the Performance of Building Structures", 2009, http://www.cncscs.org/wenjian/zrh/%C8%D5%B1%BE/The%20Application%20of%20Structural%20Health%20Monitoring%20for%20Improving%20the%20Performance%20of%20Buiding%20Structures.pdf, accessed at October 2009.

6. Picozzi, M., S. Parolai, C. Milkereit, D. Bindi, J. Zschau, R. Ditommaso, M. Mucciarelli, M. R. Gallipoli, M. Vona, and M. Bianca, "Structural Health Monitoring (SHM) by a Wireless Mesh Network of Accelerometers: The Example of L'Aquila (Italy) Seismic Sequence, 2009", *14th European Conference on Earthquake Engineering,* Ohrid, Republic of Macedonia, 2010.

7. Enckell, M., "Structural Health Monitoring of Bridges in Sweden", *The 3rd International Conference on Structural Health Monitoring of Intelligent Infrastructure Vancouver,* British Columbia, Canada, 2007.

8. Herminio, A. M., "Modal Identification from Ambient Vibration Measurement: A Technology for Optimization of the Performance of Civil Engineering Structures", http://external.adnu.edu.ph/Research/gibon4-v1n1.asp, accessed at August 2003.

9. Gentile, C. and A. Saisi, "Ambient Vibration Testing of Historic Masonry Towers for Structural Identification and Damage Assessment", *The Journal of Construction and Building Materials,* Vol. 21, pp. 1311-1321, 2007.

10. Brownjohn, J. M. W., "Ambient Vibration Studies for System Identification of Tall Buildings", *Earthquake Engineering and Structural Dynamics,* Vol. 32, No. 1, pp. 71-95, 2003.

11. Turek, M., K. Thibert, C. Ventura and S. Kuan, "Ambient Vibration Testing of Three Unreinforced Brick Masonry Buildings in Vancouver, Canada", *2006 IMAC-XXIV: Conference and Exposition on Structural Dynamics,* 2006.

12. Cantieni, R., "Experimental Methods Used in System Identification of Civil Engineering Structures", *Problems of Vibration in Civil Structures and Mechanical Engineering,* Vol. 2, pp. 10-11, June 2004.

13. Chen, C. K., R. M. Czarnecki, and R.E. Scholl, "Vibration Tests of a 4-Story Concrete Structure", *Special Publication,* Vol. 55, pp. 607-640, 1978.

14. Onouchi, A., A. Tachibana, A. Niousha, Y. Naito, M. Kan, and Y. Mihara, "Forced Vibration Test of an ABWR Nuclear Reactor Building – Data Analysis and System Identification", *18th International Conference on Structural Mechanics in Reactor Technology,* Beijing, China, 2005.

15. Karim, A. R. A., C. Oyarzo-Vera, N. M. Sa'don, and J. M. Ingham, "Forced Vibration Response of Small Scale URM House with Flexible Timber Diaphragm", *Australian Earthquake Engineering Conference AEES 2008,* Ballarat, Victoria, 2008.

16. Çelebi, M. and E. Şafak, "Seismic Response of Transamerica Building. I: Data and Preliminary Analysis", *The Journal of Structural Engineering,* ISSN 0733-9445, Vol. 117, No. 8, pp. 2389-2404, 1991.

17. Şafak, E. and M. Çelebi, "Seismic Response of Transamerica Building. II: System Identification", *The Journal of Structural Engineering,* ISSN 0733-9445, Vol. 117, No. 8, pp. 2405-2425, 1991.

18. Conte, J. P., B. Moaveni, X. He and A. R. Barbosa, "System and Damage Identification of a Seven-Story Reinforced Concrete Building Structure Tested on the UCSD-NEES Shake Table", *The Second Edition of the International Conference Experimental Vibration Analysis for Civil Engineering Structures,* Porto, Portugal, 2007.

19. Liu, He, R. Goel, F. Bai, W. Scott, and T. Kono, "System Identification, Modeling and Performance Prediction of a 20-Story Office Building", *4th International Conference on Earthquake Engineering,* Taipei, Taiwan, 2006.

20. Şafak, E., "Adaptive Modeling, Identification and Control of Dynamic Structural Systems. I: Theory", *Journal of Engineering Mechanics,* Vol. 115, No. 11, pp. 2386-405, 1989.

21. Şafak, E., "Identification of Linear Structures Using Discrete-Time Filters", *Journal of Structural Engineering,* Vol. 117, No. 10, pp. 3064-3085, 1991.

22. Ghanem, R. And M. Shinozuka, "Structural System Identification I: Theory", *Journal of Engineering Mechanics,* Vol. 121, No. 2, pp. 255-264, 1995.

23. Shinozuka, M. and R. Ghanem, "Structural System Identification II: Experimental Verification", *Journal of Engineering Mechanics,* Vol. 121, No. 2, pp. 265-273, 1995.

24. Doebling, S. W., C. R. Farrar, M. B. Prime, and D. W. Shevitz, *Damage Identification and Health Monitoring of Structural and Mechanical Systems from Changes in Their Vibration Characteristics: A Literature Review,* Los Alamos National Laboratory Report, LA-13070-MS, 1996.

25. Friswell, M. I. and J. E. Mottershead, *Finite Element Model Updating in Structural Dynamics*, Kluwer Academic Publishers, Dordrecht, the Netherlands, 1995.

26. Fang, S., R. Perera, and G. Roeck, "Damage Identification of a Reinforced Concrete Frame by Finite Element Model Updating Using Damage Parameterization", *Journal of Sound and Vibration,* Vol. 313, No. 3, pp. 544-559, 2008.

27. Ventura, C. E., R. Brincker, E. Dascotte, and P. Andersen, "FEM Updating of the Heritage Court Building Structure", *Proceedings of The 19th International Modal Analysis Conference (IMAC),* Kissimmee, Florida, 2001.

28. Skolnik, D., Y. Lei, and J. W. Wallace, "Identification and Model Updating of the UCLA Louis Factor Building", *The 2nd International Conference on Structural Health Monitoring of Intelligent Infrastructure: SHMII-2,* Shenzhen, P. R. of China, 2005.

29. Stafford Smith, B., "Behavior of the Square Infilled Frames", *Journal of Structural Engineering ASCE,* Vol. 92, No. 1, pp. 381-403, 1966.

30. Mainstone, R. J., *Supplementary Note on the Stiffness and Strengths of Infilled Frames,* B.R.E., UK, 1964.

31. Saneinejad, A. and B. Hobbs, “Inelastic Design of Infilled Frames”, *Journal of Structural Engineering ASCE,* Vol. 121, pp. 634-50, 1995.

32. Mehrabi, A. B. and P. B. Shing, “Finite Elements Modeling of Masonry-Infilled RC Frame”, *Journal of Structural Engineering,* Vol. 123, No. 5, pp. 604-13, 1997.

33. Dawe, J. L., C. K. Seah, and Y. Liu, “A Computer Model for Predicting Infilled Frame Behavior, NRC”, *Canadian Journal of Civil Engineering,* 28, pp. 133-41, 2001.

34. Shing, P. B. and A. Stavridis, “Seismic Performance of Non-Ductile RC Frames with Brick Infill”, *ATC/SEI Conference on Improving the Seismic Performance of Existing Buildings and Other Structures,* San Francisco, California, 2009.

35. Davis, R., P. Krishnan, D. Menon, and A. M. Prasad, “Effect of Infill Stiffness on Seismic Performance of Multi-Storey RC Framed Buildings in India”, *13th World Conference on Earthquake Engineering,* Vancouver, B. C., Canada, 2004.

36. Öztürk, M. S., *Effects of Masonry Infill Walls on the Seismic Performance of Buildings,* M.S. Thesis, Middle East Technical University, 2005.

37. Güler, K., E. Yuksel, and A. Koçak, “Estimation of the Fundamental Vibration Period of Existing RC Buildings in Turkey Utilizing Ambient Vibration Records”, *Journal of Earhquake Engineering,* Vol. 12, No. 2, pp. 140-150, 2008.

38. Morita, K. and J. Kanda, “Experimental Evaluation of Amplitude Dependent Natural Period and Damping Ratio of a Multi-Story Structure”, *Eleventh World Conference on Earthquake Engineering,* Acapulco, Mexico, 1996.

39. Motosaka, M., T. Sato, and Y. Yamamoto, “the Amplitude Dependent Dynamic Characteristics of an Existing Building before and after Seismic Retrofit”, *13th World Conference on Earthquake Engineering,* Vancouver, B. C. Canada, 2004.

40. Inman, D. J., *Engineering Vibrations*, Third Edition, Pearson Education, Inc., New Jersey, 2009.

41. *2007 Turkish Seismic Code,* Third Edition, Turkish Chamber of Civil Engineers İstanbul Branch, İstanbul, 2007.

42. Mainstone, R. J., "On the Stiffness and Strength of Infilled Frames", *Proceedings of the Institute of Civil Engineers,* Supplemental Vol. 4, pp. 57-90, London, England, 1971.

43. Asteris, P. G., "Lateral Stiffness of Brick Masonry Infilled Plane Frames", *Journal of Structural Engineering, ASCE,* Vol. 129, No. 8, pp. 1071-1079, 2003.

44. Kaltakçı, M. Y. and A. Köken, *Tuğla Dolgu Duvarlı Çelik Çerçevelerin Tersinir-Tekrarlanır Yükler Altındaki Davranışı*, İNTAG Araştırma Projesi, Proje No: 569 TÜBİTAK, Ankara 2003.

45. Kaltakçı, M. Y. and A. Köken, *Tersinir Yükleme Altındaki Çok Katlı ve Çok Açıklıklı Dolgu Duvarlı Çelik Çerçevelerin Davranışının Teorik ve Deneysel Olarak İncelenmesi*, Araştırma Projesi, Proje No: 99-030, S.Ü. BAP Koordinatörlüğü, Konya, 2003.

46. Köken, A., *Tersinir Yükleme Altındaki Çok Katlı ve Çok Açıklıklı Dolgu Duvarlı Çelik Çerçevelerin Davranışının Teorik ve Deneysel Olarak İncelenmesi*, Ph.D. Thesis, Selçuk Üniversitesi, 2003.

47. Köse, M. M. And Ö. Karslıoğlu, "Effects of Infill Walls on the Fundamental Periyod and Mode Shape of Buildings", *Sixth National Conference on Earthquake Engineering,* İstanbul, Turkey, 2007.